

This electronic thesis or dissertation has been downloaded from the King's Research Portal at <https://kclpure.kcl.ac.uk/portal/>



## **Mechanical Dyssynchrony in Heart Failure and Implications for Response and Guidance of Cardiac Resynchronisation Therapy**

Duckett, Simon

*Awarding institution:*  
King's College London

The copyright of this thesis rests with the author and no quotation from it or information derived from it may be published without proper acknowledgement.

### **END USER LICENCE AGREEMENT**



**Unless another licence is stated on the immediately following page** this work is licensed

under a Creative Commons Attribution-NonCommercial-NoDerivatives 4.0 International

licence. <https://creativecommons.org/licenses/by-nc-nd/4.0/>

You are free to copy, distribute and transmit the work

Under the following conditions:

- Attribution: You must attribute the work in the manner specified by the author (but not in any way that suggests that they endorse you or your use of the work).
- Non Commercial: You may not use this work for commercial purposes.
- No Derivative Works - You may not alter, transform, or build upon this work.

Any of these conditions can be waived if you receive permission from the author. Your fair dealings and other rights are in no way affected by the above.

### **Take down policy**

If you believe that this document breaches copyright please contact [librarypure@kcl.ac.uk](mailto:librarypure@kcl.ac.uk) providing details, and we will remove access to the work immediately and investigate your claim.

This electronic theses or dissertation has been downloaded from the King's Research Portal at <https://kclpure.kcl.ac.uk/portal/>



**Title:** Mechanical Dyssynchrony in Heart Failure and Implications for Response and Guidance of Cardiac Resynchronisation Therapy

**Author:** Simon Duckett

The copyright of this thesis rests with the author and no quotation from it or information derived from it may be published without proper acknowledgement.

#### END USER LICENSE AGREEMENT



This work is licensed under a Creative Commons Attribution-NonCommercial-NoDerivs 3.0 Unported License. <http://creativecommons.org/licenses/by-nc-nd/3.0/>

You are free to:

- Share: to copy, distribute and transmit the work

Under the following conditions:

- Attribution: You must attribute the work in the manner specified by the author (but not in any way that suggests that they endorse you or your use of the work).
- Non Commercial: You may not use this work for commercial purposes.
- No Derivative Works - You may not alter, transform, or build upon this work.

Any of these conditions can be waived if you receive permission from the author. Your fair dealings and other rights are in no way affected by the above.

#### Take down policy

If you believe that this document breaches copyright please contact [librarypure@kcl.ac.uk](mailto:librarypure@kcl.ac.uk) providing details, and we will remove access to the work immediately and investigate your claim.

**Mechanical Dyssynchrony in Heart Failure and  
Implications for Response and Guidance of Cardiac  
Resynchronisation Therapy**

Simon Graham Duckett

A dissertation submitted for

**Medical Doctorate**

of the

**University of London**

2012

Division of Imaging Sciences

Guy's and St Thomas Hospital

King's College London

## Table of Contents

<b>Mechanical Dyssynchrony in Heart Failure and Implications for Response and Guidance of Cardiac Resynchronisation Therapy .....</b>	<b>1</b>
<b>Table of Contents.....</b>	<b>2</b>
<b>Abstract .....</b>	<b>6</b>
<b>Acknowledgements .....</b>	<b>10</b>
<b>List of Figures .....</b>	<b>11</b>
<b>List of Tables.....</b>	<b>15</b>
<b>List of Abbreviations.....</b>	<b>17</b>
<b>Chapter 1.....</b>	<b>19</b>
<b>Summary of Thesis .....</b>	<b>19</b>
Introduction .....	19
Methods.....	20
Results .....	21
Conclusions.....	22
Key words.....	22
<b>Aims of Thesis .....</b>	<b>23</b>
Ethics .....	23
Contribution of Candidate and Colleagues .....	24
Setting up the Program.....	24
Clinical Data Acquisition.....	25
Data Analysis.....	25
Overview of Thesis .....	26
<b>Chapter 2 .....</b>	<b>28</b>
<b>Review of Current Practice and Concepts in CRT and Related Imaging and Physiology .....</b>	<b>28</b>
<b>Introduction.....</b>	<b>28</b>
Heart failure: The size of the problem .....	28
Pathophysiology .....	29
Medical Therapy for Heart Failure .....	32
Cardiac Resynchronisation Therapy .....	32
Current Guidelines .....	38
Measuring Response.....	40
Acute Response.....	40
Chronic Response .....	45
Understanding and Improving Patient Selection for CRT .....	48
Understanding Electrical Myocardial Activation in CRT .....	50
Understanding Myocardial Motion .....	53
Imaging in CRT and Techniques to Measure Dyssynchrony .....	62
Echocardiography in CRT .....	64
Cardiac Magnetic Resonance Imaging .....	73
Current Issues in CRT.....	83
<b>Chapter 3.....</b>	<b>85</b>



<b>Methods of Measuring Mechanical Dyssynchrony and Effectiveness in Predicting Acute and Chronic Response to CRT .....</b>	<b>85</b>
<b>Introduction.....</b>	<b>85</b>
<b>Methods.....</b>	<b>86</b>
Study population.....	86
Echocardiography Acquisition.....	89
Echocardiographic Assessment of Dyssynchrony.....	89
CMR Imaging Acquisition .....	89
Methods for CMR Processing.....	90
Myocardial Wall Thickening from Cine CMR.....	94
Myocardial Deformation from Cine and Tagged CMR .....	94
Systolic Dyssynchrony Index.....	95
Implant and Acute Haemodynamic Measurements.....	98
Classification of Acute Response.....	99
Classification of Reverse Remodelling and Responders .....	99
Comparison and Reproducibility of Methods.....	99
Statistical Analysis.....	100
<b>Results .....</b>	<b>101</b>
Acute Response.....	101
Measures of Dyssynchrony Predicting Acute Haemodynamic Response .....	101
Reverse Remodelling.....	107
Clinical Response .....	109
Aetiology: DCM vs ICM.....	110
Aetiology and Clinical Response.....	115
Agreement of Methods and Reproducibility .....	115
<b>Discussion.....</b>	<b>118</b>
Systolic Dyssynchrony Index Measurements .....	118
Aetiology.....	120
Comparing Imaging Techniques.....	121
Understanding Relationships Between SDI and LBBB .....	121
<b>Measurement Techniques.....</b>	<b>122</b>
<b>Limitations .....</b>	<b>123</b>
<b>Conclusions .....</b>	<b>124</b>
<b>Chapter 4.....</b>	<b>125</b>
<b>Relationship Between Acute and Chronic Response to CRT.....</b>	<b>125</b>
<b>Introduction.....</b>	<b>125</b>
Methods.....	125
Echocardiographic Assessment.....	126
Implant and Acute Haemodynamic Measurements.....	127
Haemodynamic Measurement Protocol and Data Analysis .....	129
Reverse Remodelling and Responders .....	129
Statistical Analysis.....	130
<b>Results .....</b>	<b>130</b>
Response and Reverse Remodelling.....	134
Aetiology and Reverse Remodelling.....	139
Lead Position .....	142
Clinical Response .....	142
<b>Discussion.....</b>	<b>144</b>
Aetiology and Reverse Remodelling.....	144
LV Pacing Site .....	145
Role of LV-dP/dt <sub>max</sub> .....	146
Clinical Implications .....	148

Study Limitations .....	148
<b>Conclusions .....</b>	<b>150</b>
<b>Chapter 5 .....</b>	<b>151</b>
<b>Relationship Between Myocardial Electrical Activation and Motion in Helping to Understand Response to CRT .....</b>	<b>151</b>
<b>Introduction.....</b>	<b>151</b>
<b>Methods.....</b>	<b>154</b>
Study Population.....	154
Echocardiographic Acquisition.....	154
Assessment of Dyssynchrony and Septal Flash .....	155
CMR Imaging.....	155
Non-contact Mapping Procedure .....	156
Statistical Analysis.....	159
<b>Results .....</b>	<b>159</b>
Baseline Analysis.....	162
Influence of BIV and RV Pacing.....	167
Acute Haemodynamic Response .....	168
Clinical Response and Reverse Remodelling (Table 24) .....	170
<b>Discussion.....</b>	<b>172</b>
LBBB: Measures of Dyssynchrony and the Septal Flash .....	175
Clinical Implications for CRT .....	176
<b>Study Limitations .....</b>	<b>176</b>
<b>Conclusions .....</b>	<b>177</b>
<b>Chapter 6.....</b>	<b>178</b>
<b>A Method for Imaging Coronary Veins and Myocardial Scar during a Single CMR Acquisition.....</b>	<b>178</b>
<b>Introduction.....</b>	<b>178</b>
<b>Methods.....</b>	<b>180</b>
Study Population.....	180
Data Acquisition .....	182
Data Analysis.....	183
Quantitative Analysis .....	186
<b>Results .....</b>	<b>187</b>
Anatomical Observations .....	188
Scar Imaging.....	192
Comparison of CMR Venous Anatomy and Venography at Implantation .....	195
Image Quality.....	195
<b>Discussion.....</b>	<b>195</b>
<b>Study Limitations .....</b>	<b>198</b>
<b>Conclusions .....</b>	<b>199</b>
<b>Chapter 7 .....</b>	<b>200</b>
<b>Image Guidance to Aid CRT Implantation.....</b>	<b>200</b>
<b>Introduction.....</b>	<b>200</b>
<b>Methods.....</b>	<b>201</b>
<b>Advanced Imaging Protocol.....</b>	<b>203</b>
Implantation.....	204
<b>Results .....</b>	<b>211</b>
<b>Discussion.....</b>	<b>214</b>
<b>Study Limitations .....</b>	<b>218</b>
<b>Conclusions .....</b>	<b>220</b>

<b>Chapter 8.....</b>	<b>221</b>
<b>Discussion and Personal Opinion.....</b>	<b>221</b>
<b>Limitations of this Work.....</b>	<b>225</b>
<b>The Future.....</b>	<b>225</b>
<b>Chapter 9.....</b>	<b>227</b>
<b>General Conclusions.....</b>	<b>227</b>
<b>References .....</b>	<b>229</b>
<b>Appendix 1.....</b>	<b>257</b>
<b>Publications from this Thesis .....</b>	<b>257</b>
<b>Appendix 2.....</b>	<b>264</b>
<b>Ethics sheets and patient information.....</b>	<b>264</b>

## **Abstract**

Cardiac Resynchronisation therapy (CRT) is an established treatment for heart failure patients with severe left ventricular (LV) dysfunction and widened QRS duration. Response to CRT remains variable. Up to 30% of patients do not gain symptomatic benefit with numbers that fail to reverse remodel (RR) even higher. Strategies to improve response rates have focused on pre-implant dyssynchrony following assumption that electrical dyssynchrony translates into mechanical dyssynchrony. Other factors that influence outcome are presence of myocardial scar and LV lead position.

Cardiac magnetic resonance (CMR) imaging can quantify global myocardial dyssynchrony in different modalities; volume change, muscle thickening and strain. Understanding how these measures of dyssynchrony relate to each other is important when considering how they can assist patient selection. In addition the role of CMR to assess cardiac anatomy and scar means that it is ideally placed as an imaging modality to provide comprehensive evaluation of heart failure patients prior to CRT.

This thesis aims to explore the feasibility of using CMR imaging as an inclusive imaging method to assess patients for CRT.

Forty-eight patients fulfilling the criteria for CRT were recruited (43 male,  $63.8 \pm 13.9$  years). 25 had dilated cardiomyopathy (DCM) and 23 ischaemic cardiomyopathy (ICM). All patients underwent a CMR and echocardiographic

assessment prior to CRT implantation and were followed up six months later to assess clinical response and RR (reduction of greater than 15% end systolic volume (ESV) on echocardiography). A sub group of the patients had invasive measurements during the CRT implant with a pressure wire in the LV measuring LV-dP/dt<sub>max</sub> and a further sub group had non-contact mapping (NCM) performed to assess the electrical activation patterns to different pacing modes.

A CMR examination framework allowing global assessment of dyssynchrony for volume change, muscle thickening and strain as well as coronary vein anatomy and myocardial scar was used. Developments in image segmentation tools and registration allowed the information from the CMR anatomy, scar and motion to be used during the implantation of the CRT devices.

I found volume derived systolic dyssynchrony index (SDI) predicted an acute haemodynamic response (AHR) ( $P=0.008$ ) and strongly predicted RR ( $P<0.0001$ ). Receiver operator characteristics (ROC) analysis showed a SDI of  $\geq 10\%$  was highly sensitive (0.94) and specific (0.87) for predicting which patients are likely to RR. SDI from volume dyssynchrony was superior to measures of myocardial strain and muscle thickening at predicting acute response to CRT and RR. Further more I found that  $\geq 10\%$  raise in LV-dP/dt<sub>max</sub> predicted RR for DDDL<sub>V</sub> pacing ( $p<0.001$ ). AHR predicted RR in both DCM and ICM ( $P=0.01$  &  $P=0.006$ ).

Thirteen patients underwent pre-implant NCM. Abnormal septal motion called the septal flash (SF) was defined from echo images both visually and with M-

mode and fused with NCM bull's eye plots of endocardial activation patterns. Five patients had a large SF, four small SF and four no SF. Patients with large SF had areas of conduction block in non-infarcted regions whereas those with small or no SF did not. Patients with large SF had greater acute response to LV and biventricular pacing versus those with small/no SF (% increase dP/dt  $28\pm14\%$  vs  $11\pm19\%$  for LV pacing and  $42\pm28\%$  vs  $22\pm21\%$  for BIV pacing). The lines of conduction block disappeared after LV and BIV pacing, while remaining present with RV pacing.

With the development of the CMR protocols I showed it is feasible to image coronary sinus (CS), coronary veins and scar in a single CMR examination. Using experimental image registration and segmentation software 12 patients had anatomical models of the cardiac chambers, CS and branches overlaid onto the live fluoroscopy using a prototype version of the Philips EP Navigator software to guide lead implantation. I achieved high fidelity segmentations of cardiac chambers, CS anatomy and accurate registration between the 3D anatomical models and the live fluoroscopy in all 12 patients confirmed by balloon occlusion angiography. The CS was cannulated successfully in every patient, and in all but one an LV lead was implanted successfully. (one patient had no acceptable lead values due to extensive myocardial scar).

This thesis shows it is feasible to use CMR as an inclusive imaging method to assess myocardial motion, coronary vein anatomy and scar, and thus has significant clinical benefits when assessing which patients will RR post CRT.

*To Jen my beautiful wife and Natalie my amazing new daughter the most important people in my life and without whose support this thesis would not have been written.*

## **Acknowledgements**

This work would not have been possible without the efforts of a large team of clinical and scientific colleagues. Their contributions are listed in the section on contributions of candidates and colleagues and I am very grateful for all their hard work and support. I would particularly like to thank Professor Reza Razavi, Dr Gerry Carr-White, Dr Aldo Rinaldi and Professor Tobias Schaeffter for their supervision and encouragement over the last two years. I would like to thank Dr Matthew Ginks and Dr Anoop Shetty for their help with patient recruitment. I would particularly like to thank Stephen Sinclair and John Totman for all their help with the CMR acquisitions, as without their patience and skills this research would have been very difficult. I would like to thank Benjamin Knowles, YingLiang Ma and Xiahai Zhung as without their image processing knowledge much of this work would not have been possible. I would also like to thank my father for his advice though out the period of my research as well as volunteering to have CMRs as a control. The most important person for all their help is my wife Jen who has shown immense patience and support during the long and stressful hours away from home in the last two years.



## List of Figures

- Figure 1** Incidence of heart failure by sex and age
- Figure 2** ECG of heart failure patient with LBBB
- Figure 3** Explanation of normal cardiac conduction and abnormal conduction in CRT
- Figure 4** Factors that affect response to CRT
- Figure 5** How response to CRT can be measured
- Figure 6** Measurement of  $LV-dP/dt_{max}$  from mitral regurgitation
- Figure 7** Pressure wire
- Figure 8** Real-time haemodynamic data from Physiomon software.
- Figure 9** Methods for measuring electrical and mechanical dyssynchrony
- Figure 10** Representations of how dyssynchrony can be defined.
- Figure 11** Dissection of heart showing muscle fiber orientation
- Figure 12** Shows the three main directions that ventricular myocardial mass move in during systole and diastole.
- Figure 13** Mitral valve filling patterns for two patients with heart failure
- Figure 14** Calculation of inter-ventricular mechanical delay.
- Figure 15** Overview of echocardiographic assessment of CRT patients
- Figure 16** Overview of analysis of echocardiographic imaging in CRT patients
- Figure 17** Workflow of how cine images are used to develop global motion and dyssynchrony assessment.
- Figure 18** Workflow of how tagged images are used to develop global motion and strain dyssynchrony assessment.

- Figure 19** Shows the graphs for SDI derived from different indices
- Figure 20** Shows the Anova plots for acute response and RR for QRS duration, volume and muscle thickening derived SDI.
- Figure 21** Shows the Anova plots for acute response (top row) and RR (bottom row) for SDI derived from various types of strain.
- Figure 22** Duration, volume and muscle thickening derived SDI in both DCM and ICM patients.
- Figure 23** Shows the Anova plots for acute response and RR for SDI derived from various types of strain for DCM and ICM patients.
- Figure 24** Bland and Altman plot showing the comparison between two different methods to measure volume SDI.
- Figure 25** Change in  $LV-dP/dt_{max}$  for various pacing modes and difference between best and worst  $LV-dP/dt_{max}$  for DDDL V pacing.
- Figure 26** Best and worst sites for each individual pacing position. Percentage of change in  $LV-dP/dt_{max}$  from AAI or RV baseline  $LV-dP/dt_{max}$  for each individual patient at best (blue bar) and worst (red bar) LV lead position.
- Figure 27** Shows the percentage change in  $LV-dP/dt_{max}$  from baseline for DDD-LV pacing plotted against the presence or absence of LV RR.
- Figure 28** Shows the relationship for echocardiographic parameters presence or absence of LV RR.
- Figure 29** Shows the percentage rise in  $LV-dP/dt_{max}$  from baseline with DDDL V pacing in patients with DCM and ICM.
- Figure 30** Comparison of  $LV-dP/dt_{max}$  for intrinsic, AAI, DDDL V pacing for the different final LV lead positions.

**Figure 31** **A** show the percentage of LV leads positioned in the branches of the coronary sinus. **B** shows the percentage of patients that RR.

**Figure 32** Breakdown of patients that RR that had  $\geq 10\%$  rise in  $LV-dP/dt_{max}$ .

**Figure 33** **1A** Grey scale M-mode image of a patient with a large SF. Septum is seen to have early and fast thickening and thinning. **1B** Patient with no SF.

**Figure 34** Patient with a large SF showing unipolar isochronal map with NCM

**Figure 35** Non contact mapping bulls of plots of patient with a large SF

**Figure 36** Non contact mapping bulls of plots of patient with no SF

**Figure 37** Activation maps for all patients with a large SF

**Figure 38** Activation maps for all the patients with a small SF

**Figure 39** Activation maps for all the patients with no SF

**Figure 40** Activation maps of patient with a large SF with different pacing modes.

**Figure 41** Electrical activation and associated mechanical events in patients with LBBB and a *Septal Flash*

**Figure 42** **A** Time difference for contrast to reach maximal signal intensity within the LV in a patient with normal and impaired LV function. **B** Correlation between cardiac output and time for contrast to reach maximum signal intensity in the left

**Figure 43** Whole heart 3D reconstruction with the coronary sinus and tributaries

**Figure 44** Multiplanar reformatted images of the coronary sinus and great cardiac vein and myocardial scar

**Figure 45** Multiplanar reformatted images of the coronary sinus and great cardiac vein and myocardial scar

**Figure 46** Shows a patient with a dilated cardiomyopathy and anterior scar.

**Figure 47** 3D reconstruction of the heart with the coronary venous system

**Figure 48** The workflow of how the CMR images are used to form a 3D road map and then registered during the implant.

**Figure 49** Registration of venous anatomy and registration error

**Figure 50** Images from a patient with a left sided SVC draining directly into the coronary sinus

**Figure 51** CMR 3D whole heart images with scar registered as an overlay to the real time fluoroscopy

**Figure 52** 16 segment regional volume map superimposed on the LV volume

## List of Tables

<b>Table 1</b>	Aetiology of heart failure
<b>Table 2</b>	Summary of the studies showing benefit from CRT
<b>Table 3</b>	Methods of assessing chronic response to CRT
<b>Table 4</b>	Comparisons of pros and cons of echocardiography and CMR
<b>Table 5</b>	Patient characteristic
<b>Table 6</b>	Implant details
<b>Table 7</b>	Characteristics of patients in whom acute haemodynamics were measured at the time of CRT implant
<b>Table 8</b>	Shows the P values for each SDI derived from the various methods to predict a $\geq 10\%$ rise in $LV-dP/dt_{max}$ .
<b>Table 9</b>	Shows the P values for each SDI derived from the various methods to predict a $\geq 15\%$ reduction in end systolic volume.
<b>Table 10</b>	Sensitivity, specificity and area under the curve for 15% reduction in ESV for standard echocardiographic measures of dyssynchrony
<b>Table 11</b>	Difference between DCM and ICM patients' pre and post CRT
<b>Table 12</b>	P values for echocardiographic measures of dyssynchrony for predicting RR in DCM and ICM patients
<b>Table 13</b>	Patient characteristics in acute hemodynamics study
<b>Table 14</b>	Implant details in acute hemodynamics study
<b>Table 15</b>	Responders and hemodynamic response depending on LV lead position

- Table 16** Sensitivity and specificity for 10% rise in LV-dP/dt<sub>max</sub> for LV pacing as well as standard echocardiographic measures of dyssynchrony predicting 15% reduction in ESV
- Table 17** Sensitivity, specificity and area under the curve for 15% reduction in ESV.
- Table 18** Differences in hemodynamic and chronic response between DCM and ICM
- Table 19** Comparison of patients with varying size of septal flash
- Table 20** Acute haemodynamic response with different pacing modes
- Table 21** NYHA class and echocardiographic parameters pre and post CRT
- Table 22** Demographics of heart failure patients in coronary vein imaging study
- Table 23** Anatomical observations and the correlation with vein anatomy during occlusive venography
- Table 24** Ostial diameter of the identified vein and the distance from the ostium of the coronary sinus to the identified vein and measurable vessel length
- Table 25** Position, transmuralty of scar and number of veins associated with scar
- Table 26** Patient demographics for image registration study
- Table 27** Implant information for image registration study
- Table 28** Shows the recorded pacing thresholds and R wave for pacing in and out of areas of myocardial scar as depicted on the overlay

## List of Abbreviations

2D	Two Dimensional
3D	Three Dimensional
AHR	Acute Hemodynamic Response
AIV	Anterior Inter-ventricular Vein
AV	Atrio-ventricular
CMR	Cardiac Magnetic Resonance
CRT	Cardiac Resynchronization Therapy
CS	Coronary Sinus
CT	Computer Tomography
GCV	Great Cardiac Vein
ECG	Electro Cardiogram
ESV	End Systolic Volume
DCM	Dilated Cardiomyopathy
ICM	Ischaemic Cardiomyopathy
IVMD	Inter Ventricular Mechanical Delay
LA	Left Atrium
LBBS	Left Bundle Branch Block
LMV	Left Marginal Vein
LV	Left Ventricle
LVPE	Left Ventricular Pre-Ejection Time
NCM	Non-Contact Mapping
NYHA	New York Heart Association
PEP	Pre-Ejection Period

PIV	Posterior Inter-Ventricular
PVLV	Posterior Vein of the Left Ventricle
QOL	Quality of Life
RR	LV Reverse Remodelling
RA	Right Atrium
RV	Right Ventricle
SDI	Systolic Dyssynchrony Index
SF	Septal Flash
SVC	Superior Vena Cava
TDI	Tissue Doppler Imaging
TTE	Trans Thoracic Echocardiography



## **Chapter 1**

### **Summary of Thesis**

#### **Introduction**

Cardiac resynchronisation therapy offers reduction in morbidity and mortality for patients with significant LV dysfunction, advanced symptomatic heart failure and conduction delay on the surface ECG. Under current selection criteria there unfortunately remain a significant proportion of patients that do not derive clinical benefit, and the numbers that do not RR are even higher.

This has led to a large amount of research to develop strategies that improve patient selection. Much of this work has focused on measures of dyssynchrony derived from echocardiography. Although single centre trials have been positive these findings have not been reproduced in large multicentre trials. The reasons that echocardiographic measures of dyssynchrony do not aid patient selection include poor reproducibility of techniques as well as over simplifying assessment of myocardial motion.

Furthermore the relationship between electrical and mechanical dyssynchrony is not fully understood, along with the relationship between dyssynchrony and cardiac motion. In addition echocardiography does not take into account cardiac anatomy, in particular that of the coronary veins, myocardial scar and their relationship with each other.

Developments in CMR imaging have led to it becoming an increasingly integral imaging modality in the assessment of heart failure. The superior image quality means that CMR has the potential to answer many of the questions left unanswered by echocardiographic studies. With this comes the potential to improve patient selection and improve response rates to CRT.

## **Methods**

Patients with heart failure fulfilling the criteria for CRT were recruited (NYHA class III or IV, EF < 35%, QRS duration > 120ms). All patients were assessed pre CRT implantation using the Minnesota living with heart failure questionnaire and six-minute walk. A full echo study was performed including TDI, speckle tracking and 3D SDI. Patients were then followed up at six months with the same assessments.

All patients underwent a CMR on a 1.5T MR-scanner (Achieva, Philips Healthcare, Best, Netherlands) with a 32-element cardiac coil or a 5-element cardiac coil (large or claustrophobia patients). An all-inclusive CMR examination was developed for this project that included anatomical (coronary veins), functional, motion and scar assessment.

During implantation acute response to CRT was determined using a pressure wire within the LV, and long-term response was measured by improvement in clinical indices and RR governed by reduction in ESV at six months.

CMR images were post-processed with respect to anatomical assessment of coronary veins and relationship to late gadolinium enhancement. Motion and dyssynchrony assessment was performed semi automatically using both cine and tagged imaging. Various indices of myocardial motion were measured and compared including endocardial volume change, muscle thickening, and strain (longitudinal, circumferential, radial and combined). These indices were then used to understand the relationship with each other and how they may aid in improving patient selection to CRT.

In order to study the relationship between electrical and mechanical dyssynchrony a small group of patients underwent non-contact mapping which was compared to the echocardiographic mechanical motion.

## **Results**

A protocol was developed that allowed assessment of myocardial motion/dyssynchrony and cardiac anatomy (including scar and coronary veins) in a single CMR examination.

Relating non-contact mapping to echocardiography and CMR images allowed a relationship between the electrical activation patterns of the left ventricle and septal motion to be demonstrated.

I demonstrated volume-derived measures of dyssynchrony. The systolic dyssynchrony index strongly predicted both an acute response to LV pacing, and

RR at six months ( $\geq 10\%$  rise in LV-dP/dt<sub>max</sub> from baseline pacing with LV pacing was highly predictive of RR at six months).

Using novel image segmentation and registration tools I showed it is feasible to incorporate the information from CMR with regards to myocardial motion, scar and vein anatomy during the CRT implantation procedure to aid LV lead position.

### **Conclusions**

The work in this thesis shows how CMR can be used as an all-inclusive imaging technique to improve patient selection for CRT. By developing new image processing techniques it is possible to explain the relationship between various indices of dyssynchrony and which are likely to be helpful in assessing and improving patient selection pre CRT. It is also feasible to use the information about anatomy and motion to aid in the CRT implantation with novel image segmentation and registration tools.

### **Key words**

Cardiac resynchronisation therapy, Heart failure, Dyssynchrony, Left ventricle, Myocardial scar.

## **Aims of Thesis**

The aim of the work in this thesis is to demonstrate the feasibility of using cardiac magnetic resonance imaging as comprehensive imaging method to assess patients for cardiac resynchronisation therapy.

The thesis focuses on a number of key areas;

1. Using CMR to measure myocardial motion/dyssynchrony and explain how these measures related to each other, and the potential of using them to predict which patients are likely to respond to CRT.
2. The relationship between electrical and mechanical dyssynchrony.
3. The relationship between acute and chronic response to CRT.
4. The development of a comprehensive CMR examination to image cardiac anatomy of the coronary veins and myocardial scar as well as mechanical motion in a single examination.
5. The potential to register CMR information on coronary vein anatomy, scar position and mechanical motion during a real time implant to improve procedure success rates and overall long-term response.

## **Ethics**

All studies in this thesis complied with the local ethics committees and informed consent was obtained from each patient. See appendix 2.

**Contribution of Candidate and Colleagues**

By its nature, this work could not have been done without the involvement of a large number of basic scientists and clinical colleagues. This section describes my contribution and the contribution of my many colleagues who were involved. I had a key scientific contribution in all of the work in this thesis and none of the work would have happened without my input.

**Setting up the Program**

The Imaging Sciences department is a multidisciplinary collaboration between basic and clinical scientists. This work would not have been possible without the contributions from all of these skill bases. Professor Razavi proposed and acquired the grant that funded this work. I wrote and submitted the ethics. With the help of Professor Razavi, Professor Schaeffter and Dr Carr-White we developed an all-inclusive imaging protocol and CRT assessment for patients recruited into the research. I was instrumental in setting up an assessment clinic for patients pre and post CRT to enable appropriate assessment and follow up of all patients with CRT implants.

Dr Aldo Rinaldi was instrumental in development of some of the methodology, particularly with respect to acute haemodynamic response and overlay studies where he was the main implanter.

### **Clinical Data Acquisition**

Several researchers working in this group contributed to the work described. I was involved in all parts of this work from patient recruitment to data acquisition and analysis.

Dr Matthew Ginks and Dr Anoop Shetty, clinical research fellows working in imaging sciences, helped with patient recruitment and data acquisition.

Eliane Cuncliffe and Hollie Butler, echocardiography technicians, helped in the acquisition of the echo data. Stephen Sinclair and John Totman, CMR technicians, helped in the acquisition of the MRI data. Julian Bostock, electrophysiologist, helped in the acquisition of pressure wire and Ensite mapping data.

### **Data Analysis**

Dr Amedeo Chiribiri, a clinical research fellow, helped with CMR analysis, particularly of the coronary veins.

Benjamin Knowles, YingLiang Ma and Xiahai Zhung, post-doctoral research fellows, helped with the segmentation and registration of CMR images. Dr Kawal Rhodes, lecturer in Rayne Institute, helped with image registration. Dr Phani Chinchapatnam, post-doctoral research fellow, helped with analysis of the Ensite data. Dr Oscar Camara, post-doctoral research fellow, aided with the registration of Ensite data to motion maps. Dr Stam Kapetanakis, consultant cardiologist, helped with 3D echocardiographic acquisition, analysis of the echo dyssynchrony and advice on statistical analysis.

## **Overview of Thesis**

### ***Description of chapters***

Chapter 2: Review of Current Practice and Concepts in CRT and Related Imaging and Physiology

This is an overview of major issues surrounding CRT and an in-depth description of the place of CMR in heart failure assessment and the potential of this imaging technique to aid in our understanding.

Chapter 3: Methods of Measuring Mechanical Dyssynchrony and Effectiveness in Predicting Acute and Chronic Response in CRT

This chapter describes the methods we used to measure myocardial motion and the relationship between the different measurements, and the use of different indices of dyssynchrony to predict acute and chronic response to CRT

Chapter 4: Relationship Between Acute and Chronic Response to CRT

This chapter explains how acute response to CRT was measured and how this relates to reverse remodelling.

Chapter 5: Relationship Between Myocardial Electrical Activation and Motion in Helping to Understand Response to CRT

This chapter explains a method used to show the relationship between mechanical myocardial motion and electrical activation of the ventricle.



## Chapter 6: A Method for Imaging Coronary Veins and Myocardial Scar during Single CMR Acquisition

This chapter explains a method used to image coronary veins and myocardial scar in a single CMR examination, and the ability to show the relationship between myocardial scar and position of coronary veins.

## Chapter 7: Image Guidance to Aid CRT Implantation

This chapter describes how anatomical information about coronary veins and scar as well as motion information can be used to aid CRT implantation with the use of novel overlay techniques and its implementation into the clinical arena

## Chapter 8: Discussion and Personal Opinion

This chapter is a discussion of the author's views of the pros and cons of the techniques presented in the thesis, and their likely roles in the future.

## Chapter 9: General Conclusions

Short conclusions of this thesis and future works

## **Chapter 2**

# **Review of Current Practice and Concepts in CRT and Related Imaging and Physiology**

### **Introduction**

There follows an introduction and review of the key issues around heart failure and cardiac resynchronisation therapy as well as the current techniques used to assess patients prior to CRT.

### **Heart failure: The size of the problem**

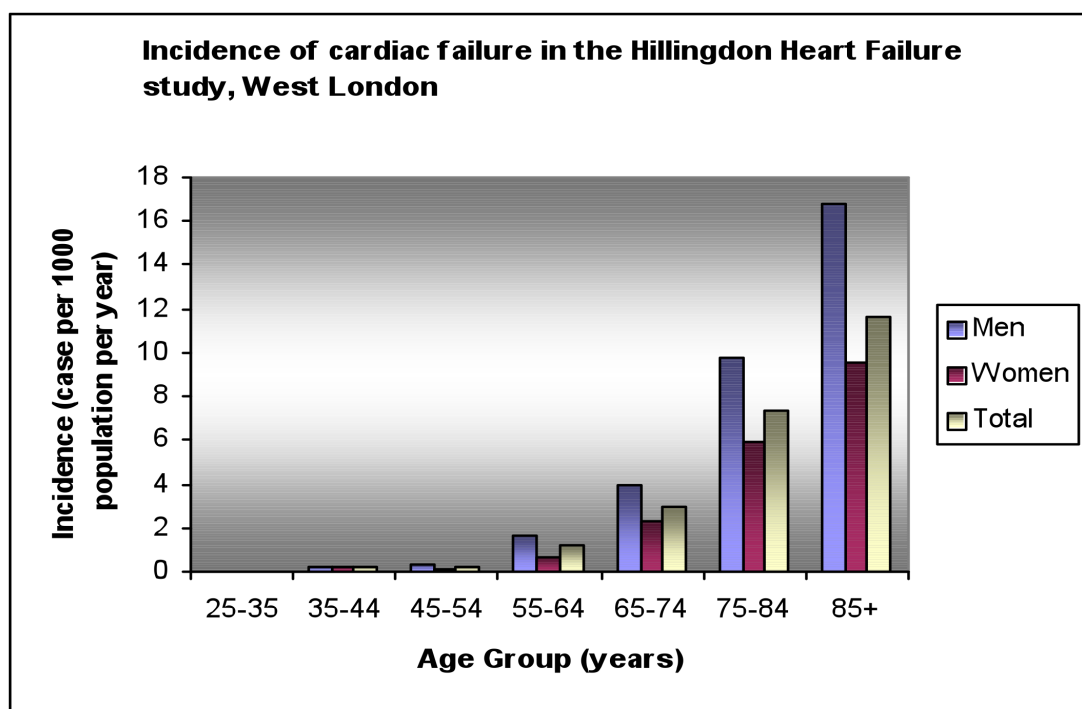
Diseases of the heart and circulatory system are the main cause of death worldwide, accounting for an estimated 17.5 million deaths in 2005. Nearly half of all deaths from cardiovascular disease are attributed to coronary heart disease. The global prevalence of heart failure is approximately 22.5 million. In 2004 the incidence of heart failure worldwide was 5.7 million. With improvements in survival from coronary heart disease the prevalence of heart failure is likely to increase.

In the UK alone, 700,000 people are living with heart failure. There are approximately 63,500 new cases of heart failure each year, and heart failure causes approximately 4% of all deaths. <sup>1</sup> The in-hospital mortality for heart failure admissions is 15% <sup>2</sup> and the one-year survival is 62%. <sup>3</sup> The five-year survival reported in the Framingham study has improved only slightly from 30%

to 41% from the middle to the end of the 20<sup>th</sup> century. <sup>4</sup> The incidence of heart failure increases with age (Figure 1), with the consequence that heart failure patients are placing increasing demands on the NHS and represent a huge burden, with a cost of over £600 million per year.

**Figure 1**

Incidence of heart failure by sex and age <sup>5</sup>



### Pathophysiology

Patients are typically divided into ischaemic (ICM) or dilated cardiomyopathy (DCM) on the basis of the clinical history, examination, and subsequent investigations including 12 lead ECG, echocardiogram, coronary angiography and increasingly CMR. (Table 1)

Left ventricular (LV) systolic dysfunction causes a fall in cardiac output, leading to activation of neurohormonal mechanisms aimed at improving tissue and organ perfusion. Activation of the sympathetic nervous system leads to increased circulating catecholamines, causing peripheral vasoconstriction, increased heart rate and increased myocardial contractility. Activation of the renin-angiotensin-aldosterone system also leads to increase in vascular tone as well as an increase in circulating blood volume resulting from salt and water retention. The physiological countering effect to this is the release predominantly of atrial natriuretic peptides and brain natriuretic peptides in response to myocardial stretch. These peptides lead to vasodilatation and promote renal sodium and water excretion.

In the short term, these physiological responses act to increase cardiac output. However, the increases in pre and after load that result from fluid retention and increased vascular tone have adverse effects in the long term. In conjunction with chronic increases in sympathetic activation, they lead to adverse remodelling and deterioration in cardiac function.

**Table 1** Causes of heart failure

<b>Anatomical category</b>	<b>Aetiology</b>	<b>Examples</b>	<b>Approximate UK prevalence (%)</b>
<b>Pericardial</b>		Constrictive pericarditis	<1
<b>Myocardial</b>	ICM	Myocardial infarction	50-60
	DCM		10-20
	Idiopathic		
	Infective	Viral, Bacterial	
	Metabolic	Thyroid disease	
	Toxin	Alcohol	
	Deficiency	Thiamine	
	Genetic	Mitochondrial myopathy	
	Peripartum		
	Hypertrophy		5
	Hypertensive		
	Genetic defect		
	Restrictive	Amyloidosis	<1
		Haemochromatosis	
<b>Endocardial</b>	Valvular disease	Aortic stenosis	10
<b>Arrhythmia</b>		Atrial fibrillation	
<b>High-output states</b>		Paget's disease	5
		Ateriovenous fistula	
<b>Congenital</b>		Ventricular septal defect	<1

## **Medical Therapy for Heart Failure**

Advances in pharmacological treatment of heart failure have demonstrated prognostic benefits of cardio-selective beta blockers, <sup>6</sup> angiotensin converting enzyme inhibitors, <sup>7</sup> angiotensin receptor antagonists <sup>8, 9</sup> and spironolactone. <sup>10</sup> These drugs act by counteracting the pathophysiological mechanisms described earlier. Although advances in medical therapy have improved prognosis the long-term survival from heart failure remains poor. <sup>4</sup>

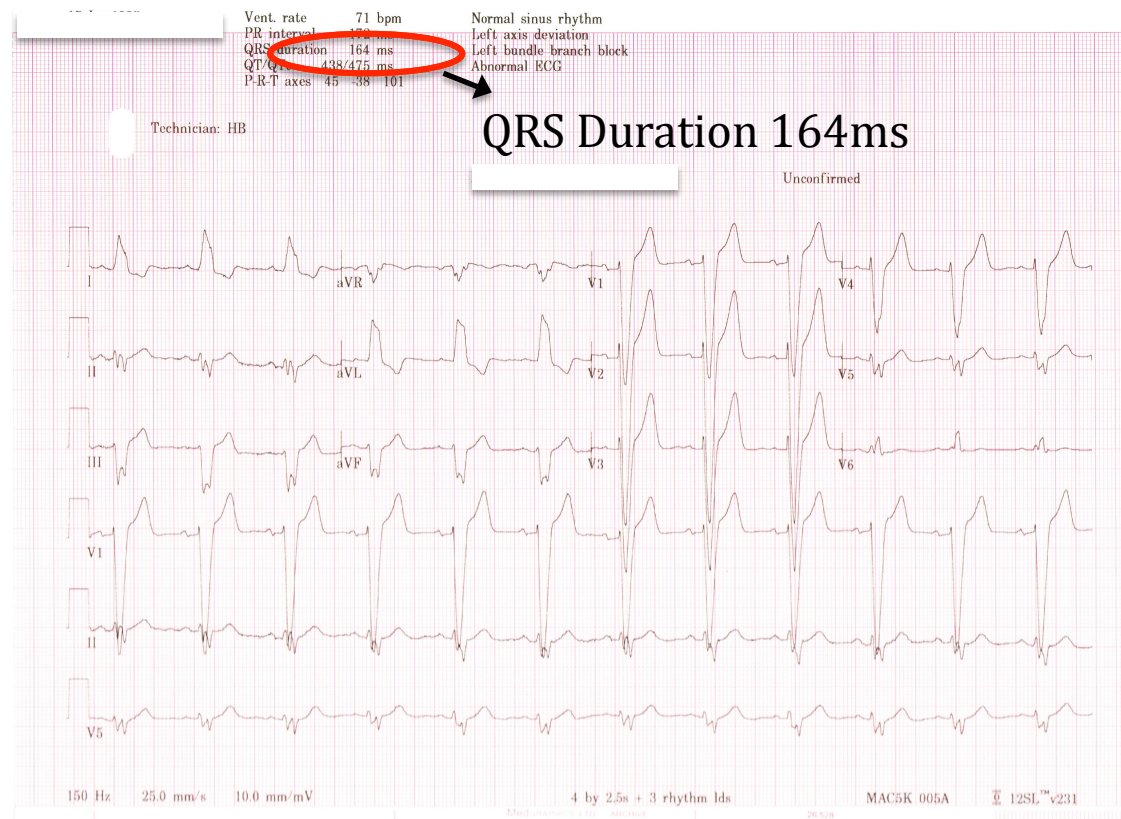
## **Cardiac Resynchronisation Therapy**

### ***Rationale***

Heart failure patients frequently have abnormal ventricular conduction manifested on the surface ECG with broad QRS complexes often seen as left bundle branch block (LBBB) <sup>11</sup> (Figure 2). This gives rise to delayed electrical stimulation and thus delayed mechanical activation of the lateral LV free wall, which contracts late relative to the inter ventricular septum. This loss of synchronous contraction disrupts mechanical efficiency, causing further impairment of the cardiac output. Furthermore QRS duration tends to increase with time and is associated with an adverse outcome.<sup>12</sup>

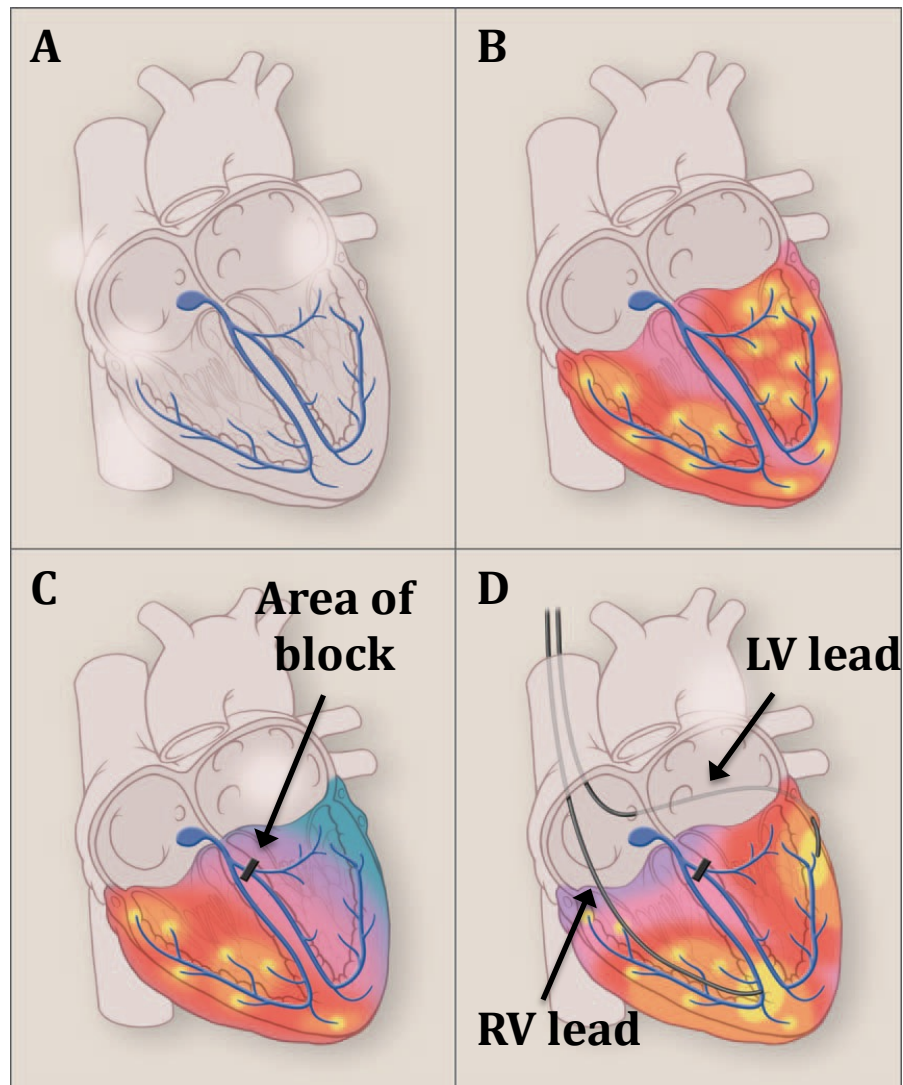
**Figure 2**

ECG of heart failure patient with LBBB



The aim of CRT is to re-coordinate the heart by artificially correcting the timing of electrical stimulation. This is achieved by pacing both the LV and right ventricles (RV) in conjunction with the right atrium (Figure 3). The LV lead is generally empirically implanted in a lateral or posteriolateral vein, which appears to confer greater benefit than an anterior or anterolateral branch<sup>13</sup> although a recent study showed that LV lead placement is patient specific.<sup>14</sup> The correction of dyssynchrony with CRT is associated with improvements in LV systolic function<sup>15</sup>, myocardial oxygen consumption<sup>16</sup>, and reduction in mitral regurgitation<sup>17</sup>.

**Figure 3** Explanation of normal cardiac conduction and abnormal conduction in CRT



**A** and **B** show the normal conduction system within the heart with conduction down the Purkinje fibers leading to depolarization of the LV and RV simultaneously. **C** shows an area of block and therefore abnormal activation of the LV, this is typical of the process that occurs in LBBB. **D** shows the presence of a LV lead within the coronary sinus, which overcomes the area of block leading to synchronous RV and LV depolarization.



***Evidence for CRT***

CRT has changed the management of patients in New York Heart Association (NYHA) class III and IV heart failure on maximum drug therapy. There are numerous multi-centre trials (Table 2) that have shown the benefits of CRT. Clinical studies have demonstrated acute haemodynamic benefit<sup>18, 19</sup>, LV reverse remodeling (RR)<sup>20, 21</sup> and improvements in symptoms incorporating exercise capacity, quality of life score (QOL) and NYHA class<sup>22-24</sup>. In addition, large prospective randomized clinical trials have shown reductions in hospital admissions and mortality<sup>25, 26</sup>.

**Table 2** Summary of studies showing benefit from CRT

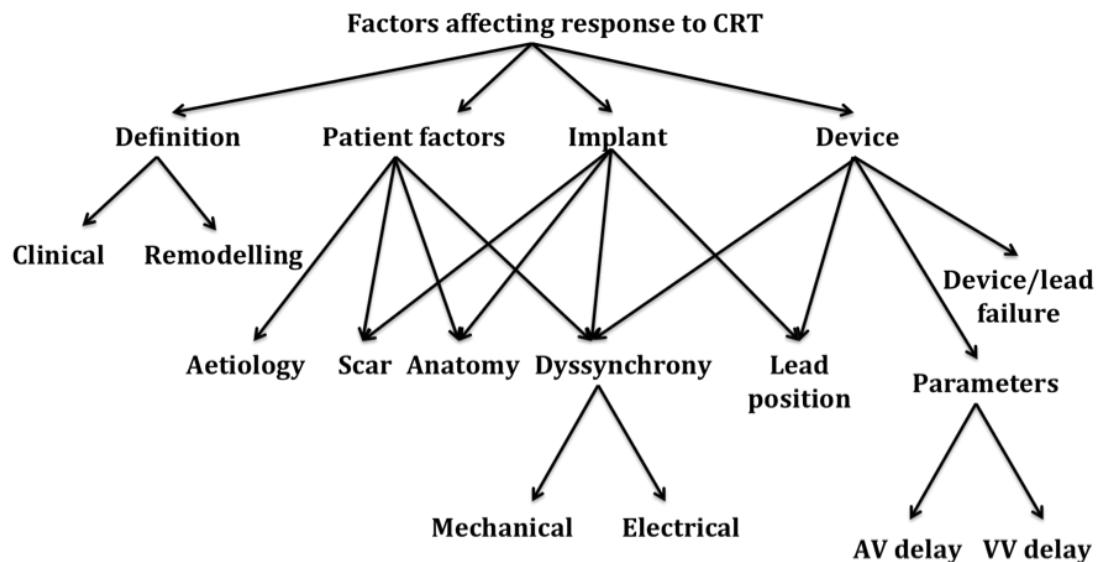
<b>Trial</b>	<b>Design</b>	<b>Patient (no.)</b>	<b>Primary end point</b>	<b>Secondary end point</b>	<b>Results summary</b>
<b>PATH-CHF<sup>27</sup></b>	Crossover	41	6MWT Peak V02	NYHA class QOL Hospitalizations	Improvement in 6MWT NYHA class QOL Less hospitalizations
<b>MUSTIC-SR<sup>22</sup></b>	Crossover	58	6MWT	NYHA class QOL Peak V02 LV volumes MR Hospitalizations Total mortality	Improvement in 6MWT NYHA class QOL Peak V02 LV volumes MR Less hospitalizations
<b>MIRACLE<sup>28</sup></b>	Parallel arms	453	6MWT NYHA class QOL	Peak V02 LV EF LVEDD MR Clinical composite response	Improvements in 6MWT NYHA class QOL LVEF LVEDD MR
<b>MIRACLE- ICD<sup>24</sup></b>	Parallel arms	555	6MWT NYHA class QOL	Peak V02 LV EF LVEDD MR Clinical composite response	Improvements in NYHA class QOL
<b>COMPANION<sup>25</sup></b>	Parallel arms	1,520	All-cause mortality or hospitalizations	All-cause mortality and cardiac morbidity	Reduced all-cause mortality/hospitalization

Trial	Design	Patient (no.)	Primary end point	Secondary end point	Results summary
CARE-HF <sup>29</sup>	Open label, randomized	814	All-cause mortality	NYHA class QOL LVEF LVESV Hospitalization for heart failure	Reduced mortality/morbidity Improvement in NYHA class QOL LVEF LVESV
PATH-CHF II <sup>30</sup>	Crossover (no pacing vs LV pacing)	86	6MWT Peak O2	NYHA class QOL	Improvement in 6MWT QOL Peak V02
CONTAK- CD <sup>20</sup>	Crossover, parallel controlled	490	6MWT NYHA class QOL	LVEF LV volumes Composite of mortality, Hospitalizations, VT/VF	Improvement in 6MWT NYHA class QOL LVEF LV volumes

### Current Guidelines

Current European Society of Cardiology guidelines recommend that CRT is indicated in patients in sinus rhythm with symptomatic severe heart failure despite optimal drug therapy, with evidence of dyssynchrony as defined by prolongation of the QRS complex on the surface ECG >120ms. However up to 30% of patients do not derive significant clinical benefit from CRT and a higher percentage do not RR.<sup>29</sup> The reasons for this are multi factorial (Figure 4).

**Figure 4** Factors that affect response to CRT



### ***“Non-response” to CRT***

The terms “responder” and “non responder” are frequently used although there is no clear consensus on what should be considered as response.<sup>31</sup> Some authors use clinical end point such as improvement in NYHA class whereas others use composite measures, such as freedom from hospitalisation or RR. Patients that do not derive clear benefit from CRT are labeled “non-responders”, although this is a poor term as the response to treatment may be a lack of deterioration rather than clear improvement. In addition most clinical studies have not incorporated a placebo arm for comparison.

There are various reasons for patients not improving with CRT (figure 4). Not only does it depend on the definition of response, but also on the heterogeneity of the heart failure population. Patient specific factors include; aetiology, degree of dyssynchrony, burden and location of scar<sup>32</sup>, ischaemia, coronary vein anatomy<sup>33</sup>, arrhythmias, co-morbidity, and baseline level of function.

### ***Areas where further work is required***

- Defining and measuring response
- Improving patient selection
- Determining the optimal site and method to stimulate the left and right ventricle in order to maximise electromechanical recruitment
- Optimising device settings

Improving our understanding of these key areas may enable us to improve patient selection, maximise the number of patients who are likely to derive benefit from CRT, and avoid potentially harmful procedures in those that will not.

### **Measuring Response**

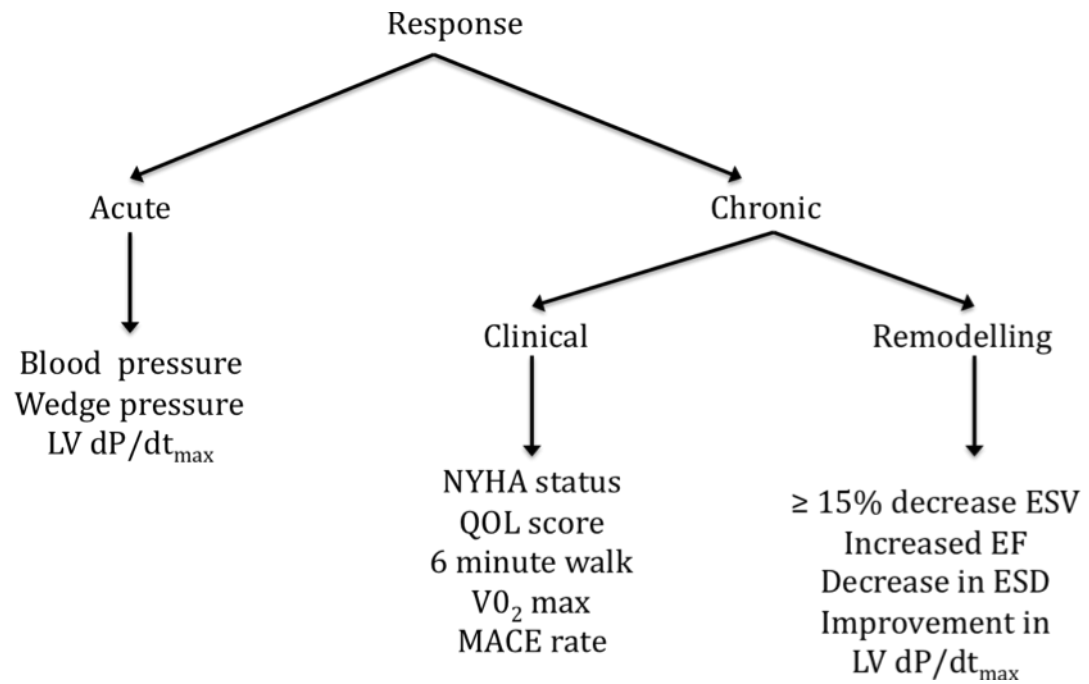
Response to CRT can be measured in the acute setting by measuring haemodynamic parameters at the time of implant, and in the long-term by looking at clinical or echocardiographic parameters (Figure 5).

### **Acute Response**

#### ***Evidence for $LV-dP/dt_{max}$ and response to CRT***

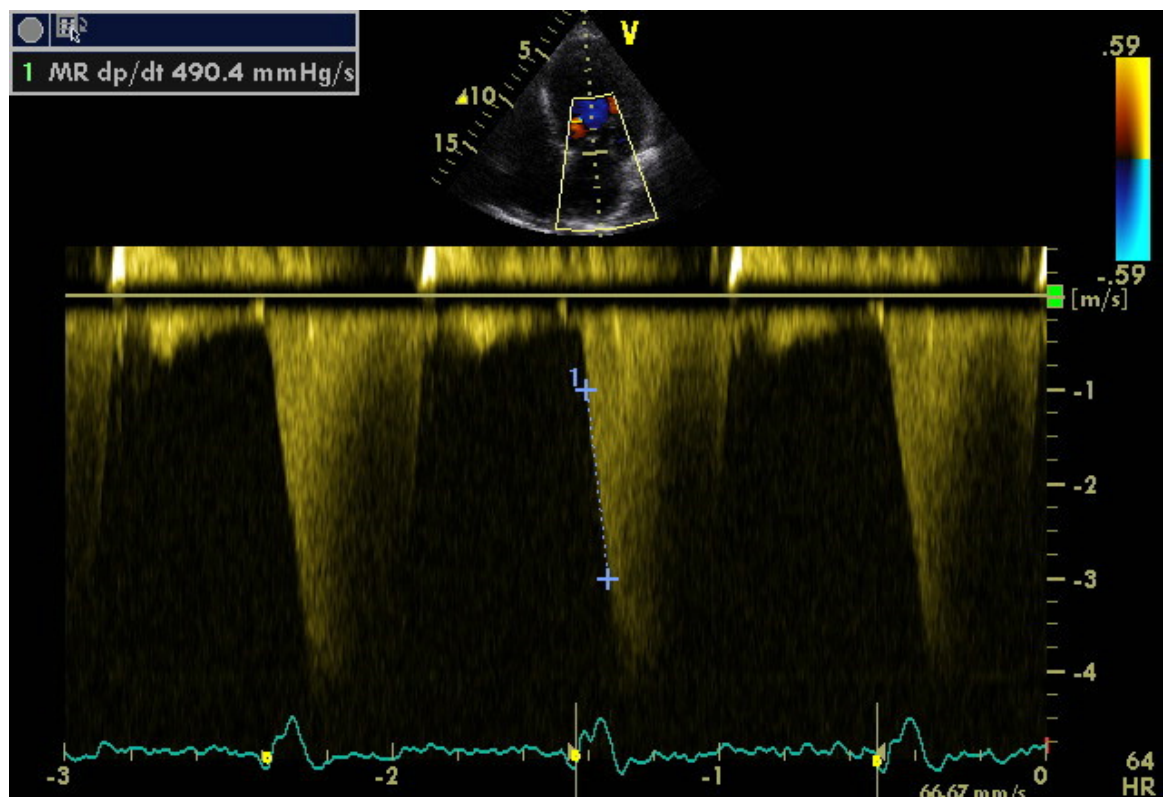
Several studies have used acute haemodynamic response (AHR) to determine lead position <sup>34, 35</sup> and to optimise pacing settings <sup>36, 37</sup>. Studies have evaluated the effect of LV pacing in the context of CRT using  $LV-dP/dt_{max}$  as an end-point <sup>34, 37-39</sup>.  $LV-dP/dt_{max}$  is a reproducible marker of LV contractility. The implication is that acute improvement in contractility translates into beneficial effects from CRT in the longer term. Whilst it is logical that energy, which is wasted as a result of LV dyssynchrony, may be “harnessed” by LV pacing in order to improve cardiac function, it is likely that there are more complex mechanisms involved in RR. Echocardiographic based assessments of AHR to CRT have shown it is a useful predictor of long-term clinical outcome <sup>40, 41</sup> (Figure 6).

**Figure 5** Shows how response to CRT can be measured



MACE=Major adverse cardiac event

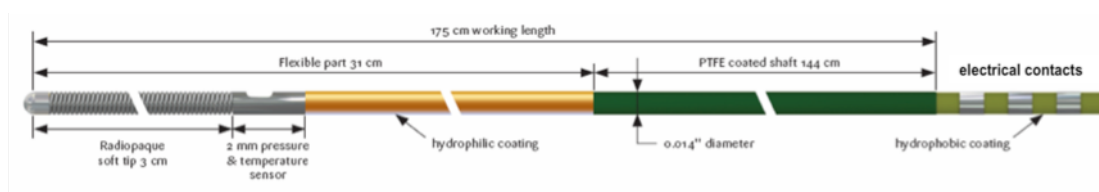
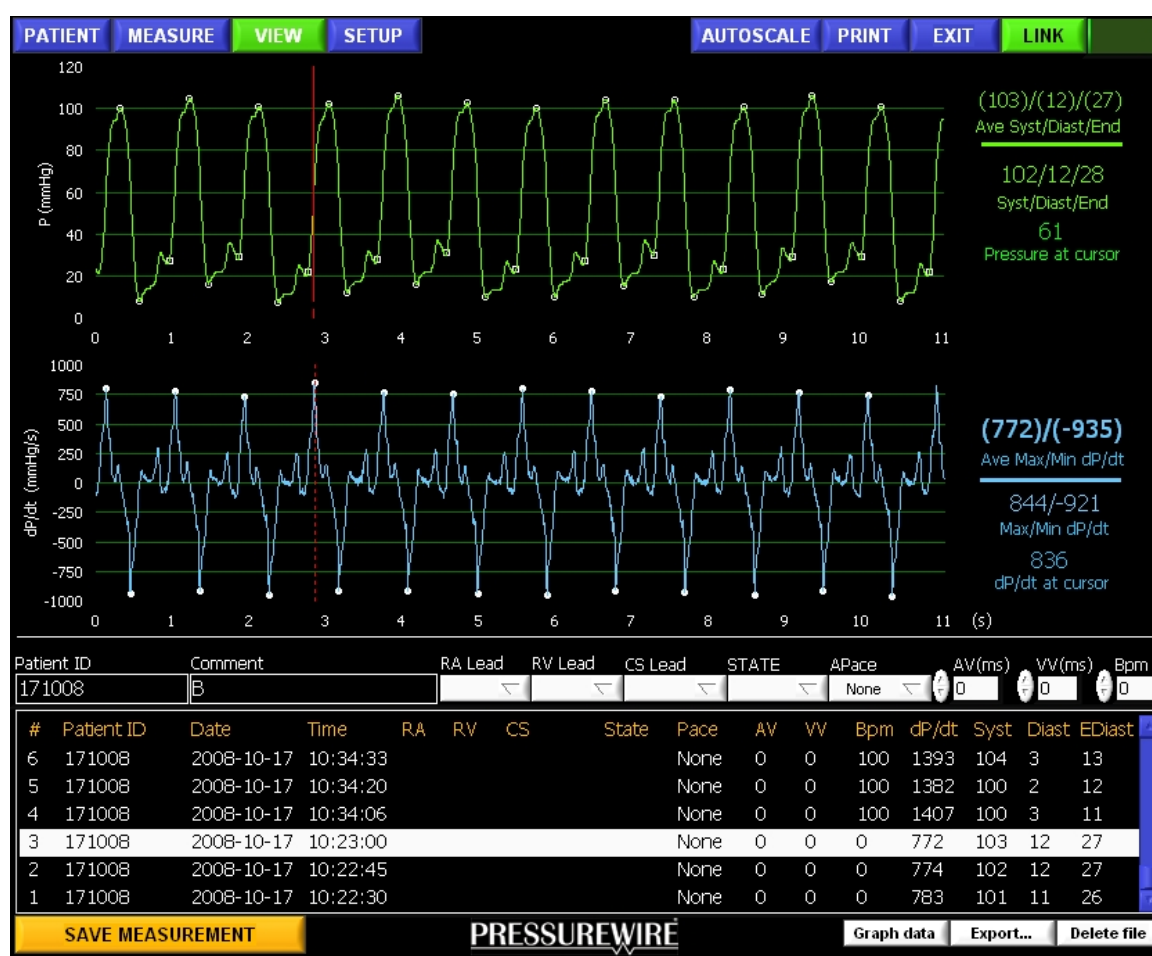
**Figure 6** Measurement of  $LV-dP/dt_{max}$  as an indicator of LV performance derived from mitral regurgitation.





However use of echocardiographic derived  $LV-dP/dt_{max}$  is confined to patients with enough mitral regurgitation to obtain a clear signal and is difficult to measure during CRT implant.  $LV-dP/dt_{max}$  can be measured invasively with a pressure wire in the LV (figure 7 and 8). Although it has been shown with invasive measurement that AHR improves with CRT <sup>39</sup> it remains unclear if an AHR at the time of CRT equates to RR and improvement of clinical parameters. Furthermore, many of the studies have only used patients with non-ischaemic cardiomyopathy<sup>34</sup>.

There are many potential benefits to using AHR at the time of CRT implant. The current consensus to position the LV lead in a lateral or posterolateral branch of the coronary sinus (CS) <sup>15, 42</sup> has recently been challenged by a study showing marked variation in haemodynamic response depending on LV pacing position. <sup>34</sup>

**Figure 7** Pressure wire**Figure 8** Real-time haemodynamic data from Physiomon software. Green trace:blood pressure; Blue trace:  $LV-dP/dt_{max}$ 

### ***Issues with $LV-dP/dt_{max}$***

Methods to assess acute response are not without problems and it is unclear how acute response equates to long-term outcomes. During implants there are multiple factors that will affect the measurements, for example patient anxiety leading to elevated sympathetic drive, use of fluids and analgesia throughout the procedure, and cessation of medication prior to the implant. All of these factors affect the accuracy and relevance of measures of AHR in determining how a patient will respond in the long-term.

### **Chronic Response**

#### ***Defining chronic response to CRT***

The best measure for defining chronic response to CRT has not been established (table 3). There is no universally accepted definition of response to CRT, although improvements in clinical criteria (NYHA class, peak oxygen consumption, exercise capacity, quality of life scores), echocardiographic parameters (ejection fraction, end-systolic volume and severity of mitral regurgitation) and hard end-points (hospitalisation due to heart failure or death) have been used. The measurement of brain natriuretic peptide (BNP) is becoming more widely available and changes in levels are now being used.<sup>43</sup>

**Table 3** Methods of assessing chronic response to CRT

<b>Clinical parameters</b>	<b>Echocardiographic parameters</b>	<b>Biochemical markers</b>
NYHA class	LV ejection fraction	Decrease in BNP
Quality of life score	LV dimensions/volume	
6 minute walk distance	Mitral regurgitation	
Exercise capacity	Inter ventricular synchronization	
Peak V <sub>O</sub> <sub>2</sub> max	Intra ventricular synchronization	
Hospitalisations (heart Failure)		
Mortality (cardiac)		
Psychological status		

## ***Methods Used to Assess Chronic Response to CRT***

### ***Measuring clinical response***

There are many clinical measures that are considered for assessment of patient response post CRT. A major limitation with many of these methods is that they are subjective and can vary on a daily basis. What one doctor considers NYHA class 3 another would consider NYHA class 2. Also patients' functional status can vary throughout the day.

### ***Measuring reverse remodelling***

Echocardiographic measurements of LV dimensions and volume are normally used to define RR.<sup>44, 45</sup> However a recent study comparing clinical and echocardiographic response to CRT demonstrated clinical improvement in 70% of cases, but RR (defined as reduction in LV ESV  $\geq 15\%$ ) in only 56%.<sup>46</sup> When change in LV ESV was subdivided into quantiles of response, a clear relationship was seen between the percentage of clinical responders and degree of RR suggesting a spectrum rather than an absolute response/non-response to CRT.<sup>47</sup>

### ***Definition of reverse remodelling and clinical response in this work***

In this thesis patients were deemed to have RR if there was a  $\geq 15\%$  reduction in LV ESV as measured using Simpson's modified biplane method on 2D echo images.<sup>48, 49</sup> Evaluation of symptomatic response was made using NYHA class and Minnesota living with heart failure questionnaire.<sup>50</sup> To assess sensitivity and specificity for LV-dP/dt<sub>max</sub> to predict RR, response was deemed acute if the

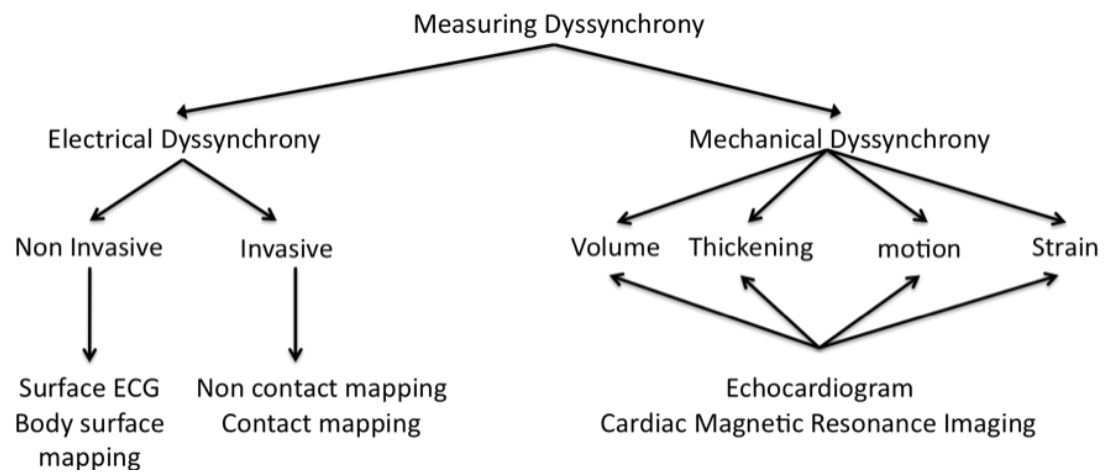
percentage improvement in  $LV-dP/dt_{max}$  was  $\geq 10\%$  compared with fixed rate atrial / RV pacing (baseline). This cut-off value has been used in previous studies<sup>37, 51</sup>. Patients were labeled clinical responders if the NYHA class fell by  $\geq 1$ , if there was a  $\geq 10\%$  reduction in heart failure questionnaire score, or  $\geq 10\%$  improvement in six minute walk distance.

### **Understanding and Improving Patient Selection for CRT**

The significant number of patients failing to either RR or derive clinical benefit from CRT has led to extensive research into trying to understand why some groups of patients respond and others do not.

Work has generally focused on two broad lines of investigation; either understanding the electrical activation, or mechanical myocardial motion/dyssynchrony (Figure 9). The general concept is that CRT works by correcting electrical dyssynchrony within the heart that in turn leads to correction of mechanical dyssynchrony and improved myocardial performance. Therefore investigation of either the electrical activation or myocardial motion may give insight into likely patient response to CRT. It is important to recognise that the assumption that electrical dyssynchrony translates into mechanical dyssynchrony is not necessarily true. The most widely used marker of electrical dyssynchrony in CRT is the surface ECG. The QRS duration is used as an electrical surrogate measurement for LV dyssynchrony. However, this inadequately identifies mechanical dyssynchrony.<sup>52</sup> This, therefore, raises a further question: What is the relationship between electrical activation and mechanical motion?

**Figure 9** Methods for measuring electrical and mechanical dyssynchrony



## **Understanding Electrical Myocardial Activation in CRT**

### ***Surface ECG***

The surface ECG is the most basic assessment of electrical activation. Patients for CRT are selected on the basis of QRS duration  $\geq 120\text{ms}$  normally with LBBB morphology. It is assumed that the broader the QRS complex the more electrical dyssynchrony there is. However LBBB is a complex electrical disease resulting from conduction delay located at several anatomical levels of the activation sequence<sup>53</sup> and the surface ECG recordings are unable to characterise the location and extent of specific ventricular delays.<sup>54</sup>

This inability of the surface ECG to adequately characterise the activation patterns of the myocardium has led to the use of more accurate but invasive methods such as non-contact mapping (NCM).

### ***Non-contact mapping and heart failure***

NCM has been used in several studies of human patients with heart failure to characterise the LV endocardial activation pattern in patients with intra-ventricular conduction delay. The concept of reconstructing intra-cavity potentials mathematically without the need for contact with the walls of the chamber was introduced by Taccardi et al.<sup>55</sup> This technology has been refined, culminating in the development of the EnSite 3000 non-contact mapping system. This consists of a multi-electrode array (MEA): 64 laser-etched electrodes mounted on a wire braid on a 8mm balloon. This is seated on a 9F catheter,



which allows introduction of the balloon to the chamber of interest (with the balloon deflated).

The geometry of the chamber of interest can be reconstructed using a low current locator signal emitted from the tip of the MEA, at 5.68Hz. This is sensed by two ring electrodes mounted on either side of the MEA balloon. With this system, other catheters can be localised in 3D. A roving electro physiological (EP) catheter is moved around the chamber to define the location of the chamber walls in 3D.

The array then records intra-cavity far-field potentials that are sampled at 1.2kHz and digitally filtered at 0.1-300Hz. The resulting signals are resolved using the inverse solution to Laplace's equation by the boundary element method. This allows mathematical reconstruction of over 3000 virtual unipolar electrograms, which are superimposed on the chamber geometry. Both isopotential and isochronal maps can be generated, with colour coding to allow the endocardial activation pattern to be visualised. Data can be analysed off-line in any orientation.

Auricchio et al demonstrated the high prevalence of functional lines of block in patients with LBBB, often with the pattern of activation taking a "U-shape" around the area of slow conduction.<sup>53</sup> Furthermore, areas of slow conduction could be defined by low voltage or fragmented electrograms. Conduction boundaries can be defined formally based on voltage distribution within the chamber, using an algorithm called dynamic substrate mapping.

Lambiase et al demonstrated that positioning of the LV lead in an area of slow conduction was associated with a significantly reduced haemodynamic benefit from CRT, when compared with pacing outside these areas.<sup>56</sup> Moreover, pacing in areas of slow conduction was associated with longer LV endocardial activation times, suggesting that correcting electrical delay was the underlying mechanism of haemodynamic benefit. Characterisation of the myocardial substrate was further advanced by Fung et al<sup>57</sup> who described two distinct types of activation pattern in patients with intra-ventricular conduction delay. This work suggested that CRT response was higher in the patients with functional block as compared with a more homogeneous activation pattern.<sup>57</sup>

Whilst non-contact mapping can characterise areas of slow conduction and lines of block, it is important to realise that it remains unclear how the electrical activation corresponds to the myocardial motion/dyssynchrony.

## **Understanding Myocardial Motion**

Prior to looking at how imaging techniques can be used to study myocardial motion and measure dyssynchrony it is important to understand the mechanisms behind ventricular systole and diastole and also the different ways these mechanisms can be investigated with various imaging modalities.

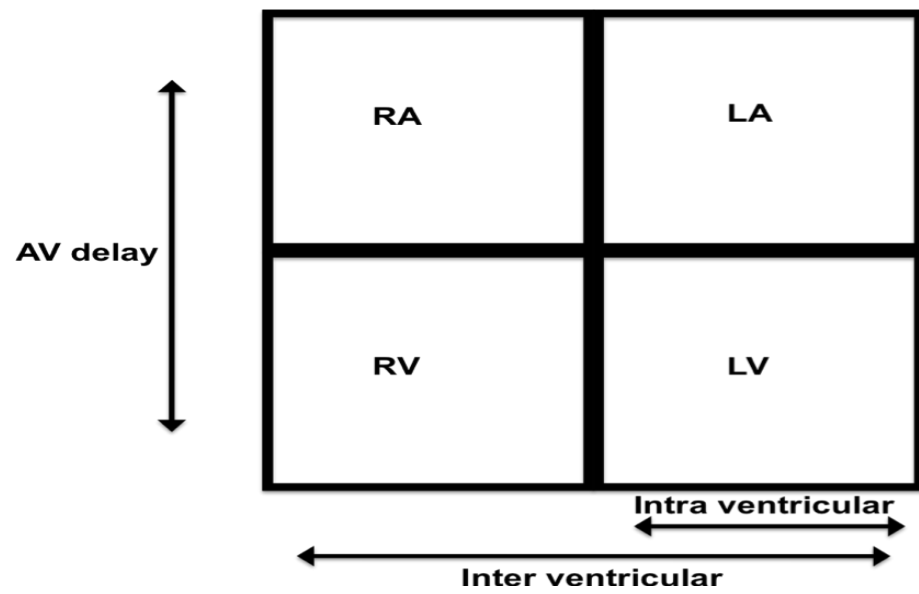
### ***Defining myocardial dyssynchrony***

Myocardial dyssynchrony can be divided into three basic categories (figure 10).

1. Atrio-Ventricular dyssynchrony (delay between the atria and the ventricles)
2. Inter-ventricular dyssynchrony (delay between the right and left ventricle)
3. Intra-ventricular dyssynchrony (delay between the walls of the left ventricle)

**Figure 10**

Representations of how dyssynchrony can be defined.



Atrio-ventricular (AV) dyssynchrony is common in patients with heart failure and first-degree heart block and was the first objective of CRT in the bicameral pacemaker in the early 1990s.<sup>58</sup> AV dyssynchrony reduces the duration of filling, thus inducing diastolic and mitral regurgitation and reduced stroke volume. Heart failure patients often have abnormal filling patterns with either prolonged or shortened transmitral filling.<sup>59</sup>

Inter-ventricular dyssynchrony represents the discordance between the times for RV and LV contraction.

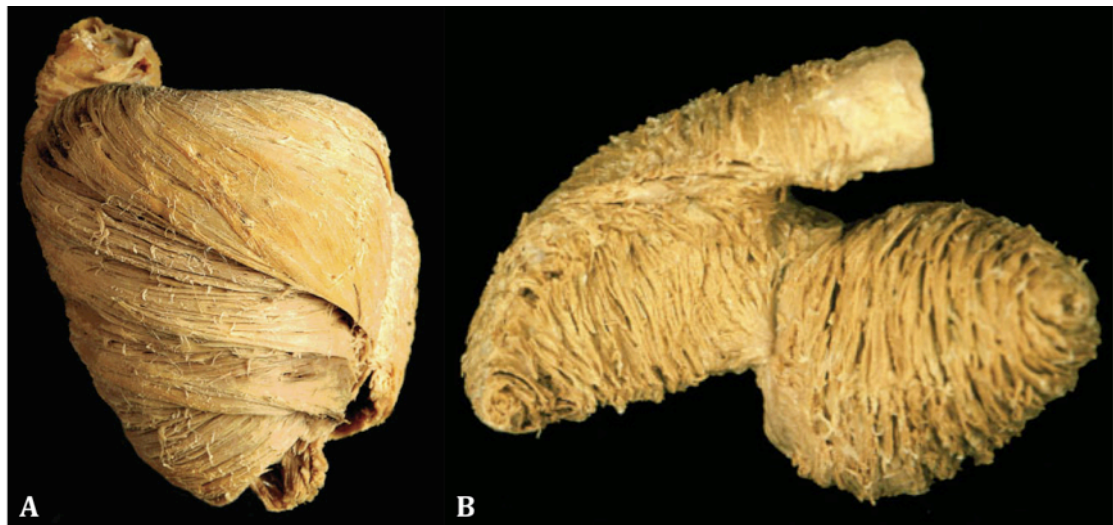
Intra-ventricular dyssynchrony is characterized by either the premature or late contraction of LV wall segments. Much of this thesis concentrates on ways to measure intra-ventricular dyssynchrony.

Patients with heart failure can have problems with any or all of these indices. CRT can affect all three of these, therefore it is important to understand how they are measured.

### ***Myocardial myocyte anatomy***

Anatomical studies are important in explaining the complex structure of the myocardium and understanding how to measure myocardial motion. Anderson et al<sup>60</sup> showed that myocytes aggregate together in a 3D mesh within a supporting matrix of fibrous tissue. Within this mesh of aggregated myocytes, it is possible to recognise two populations depending on the orientation of their

long axis. The first population is aligned with the long axis of the aggregated myocytes tangential to the epicardial and endocardial borders, albeit with marked variation in the angulations relative to the ventricular equator. The second population is aligned at angles of up to 40 degrees from the epicardium toward the endocardium (figure 11).

**Figure 11** <sup>60</sup>

**A** Porcine heart prepared by removing increasing layers from the wall of the LV, increasing the depth of dissection from base to apex. The overall alignment of the chains of myocytes can readily be distinguished, and their angulations relative to the equator can be seen to change with increasing depth within the wall. **B** Dissection of a human heart, viewed from the apex having separated and moved the left away from the RV, which is seen to the left hand supporting the pulmonary trunk on its infundibulum. The mass of myocytes aligned in circular fashion to make up the middle layers of the LV wall.

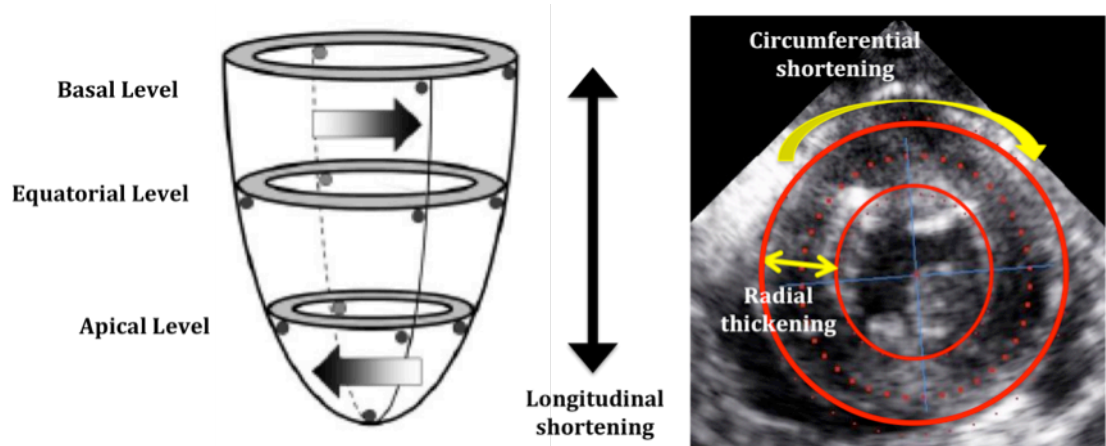
When considering the mechanics of LV motion it is important to realise that the heart is made up of complex 3D meshwork of myocytes formed into sheets set in a supporting fibrous matrix. Biomechanical studies have shown the pattern of wall thickening appears to be a function of the orientation of the laminar sheets, which vary regionally and transmurally. <sup>61</sup> Within the meshwork of sheets are to be found populations of myocytes aligned, on the one hand, with their long axis tangential to the epicardial and endocardial surfaces, and on the other hand with

angles of intrusion across the ventricular wall. Only by recognising the antagonistic roles of the two populations are we able to understand the forces involved during ventricular systolic emptying and diastolic filling. Understanding this allows better insight in to how imaging techniques can be used to investigate and quantify myocardial motion. These features, including changes in the fibrous matrix rather than the myocytes themselves, should be taken into account to fully understand the workings of the ventricular myocardium (figure 12).



**Figure 12**

Shows the three main directions that ventricular myocardial mass move in during systole and diastole.



### ***Techniques for measuring and assessing myocardial motion***

The measurement of myocardial motion can be undertaken in various ways with increasing complexity.

#### **Volume change**

The simplest method is to assess the change in LV cavity volume. Measuring the LV cavity volume over the course of the cardiac cycle gives an indication of how coordinated the ventricular contraction is. However, this does not provide information on how the myocardial mass is working to bring about ventricular contraction.

Methods using volume change over the cardiac cycle do not take into account the difference between active and passive motion and the magnitude of change within specific areas in the ventricle. Scarred and akinetic myocardial segments can be pulled or stretched by adjacent areas that can lead to change in volume.

The importance of knowing these areas are working actively or moving passively is unclear and needs further investigation.

#### Muscle thickening/shortening

To gain better understanding of the active processes involved in ventricular contraction, muscle thickening can be measured over the cardiac cycle. The assumption is that for the cardiac muscle fibers to contract they must thicken and shorten. This in turn must be an active process and would exclude areas of passive motion. During ventricular contraction there is radial thickening, longitudinal shortening and twisting of the ventricle (figure 12). Simple measurement of the radial thickening and longitudinal shortening over the cardiac cycle may allow a better understanding of the mechanism that leads to active myocardial contraction and of active dyssynchrony.

#### Motion and deformation

Assessing the change in position of particular anatomical points or structures allows the motion to be investigated during the cardiac cycle. More information can be gleaned by looking at the change from the normal size or shape of an anatomic structure due to mechanical forces that distort an otherwise normal structure, known as deformation. Myocardial deformation can be described in different ways. Mirsky et al <sup>62</sup> initially introduced the concept of *strain* to facilitate the understanding of elastic stiffness in heart muscle. They defined “strain” as a dimensionless quantity that represented the percentage change in dimension from a resting state to one achieved following application of force (stress). Therefore, strain is the relative deformation of tissue from an applied force, whereas *strain rate* is the rate of this deformation. Thus, negative strain

would indicate compression or shortening and conversely positive strain would imply lengthening or expansion.<sup>63</sup>

### ***Relationship Between Strain and Dyssynchrony***

The use of longitudinal and circumferential strain dyssynchrony measurements that align with the orientation of the helical cardiac microstructure<sup>64</sup> as sole metrics of cardiac function is fraught with physiological limitations. The intrinsic variation in the time taken for different regions of the heart to contract and reach their peak strain in the healthy heart obscures any changes in synchrony that may occur with heart failure. The timing of peak contraction in the heart varies transmurally<sup>65</sup>, circumferentially<sup>66</sup> and in the apex to base<sup>67</sup> directions. This variation is significant with an 83ms<sup>65</sup> dispersion in time to peak strain across the heart wall in canines compared with a QRS duration of approximately 60ms<sup>68</sup>, and the time to peak circumferential strain varies by 121ms<sup>66</sup> in human LV, where the QRS duration is approximately 80ms.<sup>69</sup> The distribution of timing of peak deformation is consistent with the distribution of electrical activation<sup>70-72</sup> only amplified.<sup>68</sup> This increased heterogeneity in the spatial variation in deformation is potentially facilitated by multiple factors including the non-uniformity of fibre and sheet orientation<sup>73-75</sup>, activation times<sup>72</sup>, regional cavity curvature<sup>76</sup>, contractile function<sup>77-79</sup>, electrophysiology<sup>71</sup> and passive material properties.<sup>78,79</sup>

The correlation between types of strain and predicting which patients are likely to respond to CRT is variable with some studies showing no correlation<sup>80</sup>

whereas others do.<sup>81</sup> The apparent separation of radial from circumferential and axial strain seen in some studies correlates with the different mechanisms underpinning ejection due to wall thickening and apical-basal shortening. In a normal subject, wall thickening contributes 25-48% of stroke volume<sup>82-84</sup> and is the result of a combination of shearing and elongation along the laminar sheets that make up the myocardium<sup>85-88</sup> and has a limited correlation with fibre shortening.<sup>89</sup> Furthermore, wall thickening is sensitive to both local perfusion<sup>90</sup> and metabolism<sup>91</sup> providing a potential indicator of metabolic heterogeneities and inefficiencies that are rectified in the case of CRT responders.<sup>92</sup>

### **Imaging in CRT and Techniques to Measure Dyssynchrony**

Imaging techniques in CRT are integral in determining function as well as response to therapy. The pursuit of improving patient selection has concentrated extensively on use of imaging methods, particularly transthoracic echocardiography (TTE), to develop measures of dyssynchrony that have the potential to improve CRT response rates. Although much of the work has concentrated on the use of echocardiography, similar comparable measures are being developed with CMR. Table 4 shows the comparison of echocardiography and CMR.

**Table 4** Comparisons of pros and cons of echocardiography and CMR

	<b>Echocardiography</b>	<b>CMR</b>
<b>Functional assessment</b>	++	+++
<b>Dyssynchrony</b>	+++	+++
<b>Myocardial anatomy</b>	++	+++
<b>Coronary vein anatomy</b>		+++
<b>Myocardial scar</b>		+++
<b>Inter procedural imaging</b>	++	+
<b>Post procedural imaging</b>	+++	

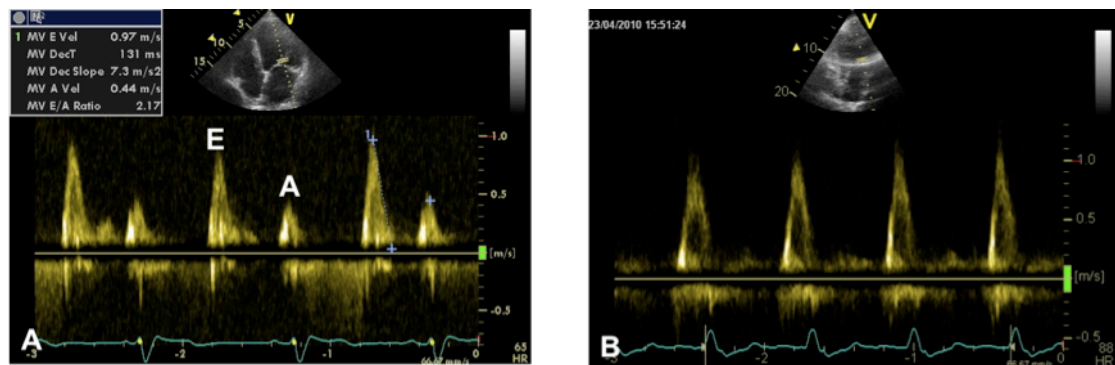
**Echocardiography in CRT**

TTE has a role in the routine evaluation of patients pre and post CRT for assessment of LV function, chamber dimensions and EF as well as exclusion of significant valvular disease and other cardiac pathology. Furthermore, TTE is required for the quantification of dyssynchrony as UK NICE guidelines stipulate that there must be echocardiographic evidence of dyssynchrony in patients with QRS duration between 120 and 150ms in order for patients to qualify for CRT. There is worldwide interest in the potential of TTE to distinguish between responders and non-responders to CRT due to the premise that electrical surrogate measurements for dyssynchrony (such as the QRS duration) inadequately identify mechanical dyssynchrony.

***Assessment of Atrio-Ventricular Dyssynchrony***

AV dyssynchrony is typically measured using pulsed wave Doppler recording of the transmitral inflow (figure 13), which requires the sample volume placed at the tips of the mitral leaflets.<sup>93</sup>

**Figure 13** Mitral valve filling patterns for two patients with heart failure.

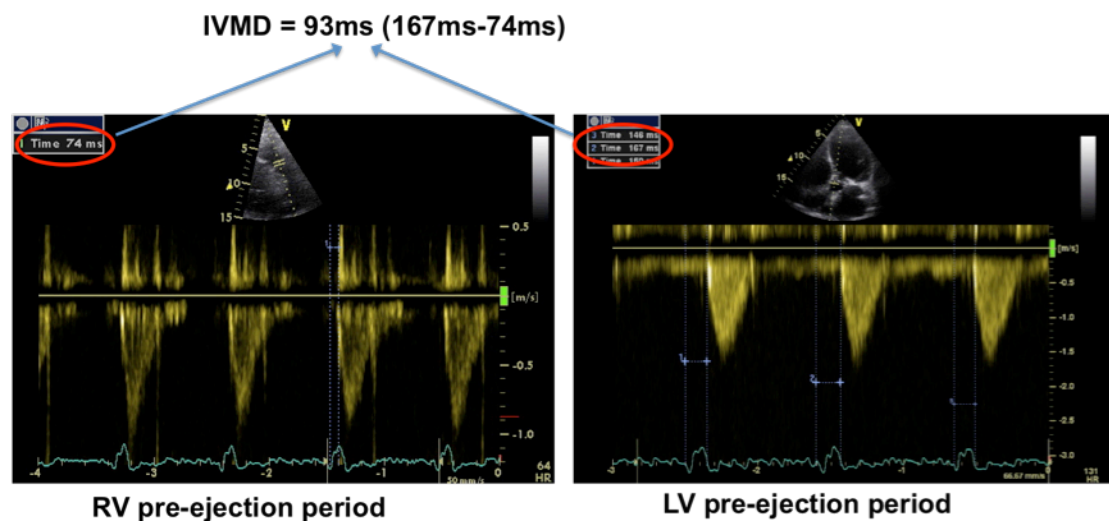


**A** Shows clearly defined E/A waves whereas **B** there is clearly very abnormal filling with fused E/A waves.

### ***Assessment of Inter-ventricular Dyssynchrony***

Inter-ventricular dyssynchrony is commonly assessed by using pulsed wave Doppler in the aorta and pulmonary artery, with the pre-ejection periods (PEP) defined as time from the Q wave on the ECG to onset of flow on Doppler (figure 15). Aortic pre-ejection period  $\geq 140$ ms and inter-ventricular delay (IVMD)  $\geq 40$ ms are considered to be pathological <sup>94</sup> and were two of the three criteria in the CARE-HF study to define echocardiographic evidence of dyssynchrony. Alternatively, pulsed tissue Doppler can be used to determine IVMD by measuring the time from QRS onset to the peak myocardial systolic velocity ( $S_m$ ) of the RV free wall versus the same time of the LV lateral wall in the apical four-chamber view. <sup>44</sup>

**Figure 14** Calculation of inter-ventricular mechanical delay.



### ***Assessment of intra-ventricular Dyssynchrony***

The best TTE method for measuring intra-ventricular dyssynchrony is not known. This has led to the development of multiple methods to assess intra-ventricular dyssynchrony of varying complexity which are described below:

#### **M-mode echocardiography**

The septal to posterior wall motion delay (the time difference between peak inward motion of the ventricular septum and the posterior wall) in the parasternal long axis view was described by Pitzalis et al.<sup>95</sup> A delay of >130ms was thought to predict reduction in ESV and improvement in LVEF as well as prognosis at six months. Limitations to this technique include the lack of wall thickening in infarcted regions as well as difficulty in aligning the ultrasound beam perpendicular to the ventricle in the case of off-axis views. Subsequent studies did not confirm the initial findings.<sup>96, 97</sup>



### Tissue velocity imaging

This is performed using TDI in the apical views to identify peak systolic velocity in the longitudinal direction. Studies have varied in;

1. Number of segments sampled
2. Whether velocity peaks were measured during systole alone or also during the post-ejection period
3. Use of either time to peak velocity or time to onset of systolic velocity
4. Whether the dyssynchrony index is derived from the maximum difference of timing intervals or the standard deviation of individual times
5. Use of pulsed wave versus colour-coded TDI.

The latter is more robust as it allows simultaneous processing of multiple sample points on the same image. A basal septal-lateral delay in time to peak systolic velocity of >60ms using this technique was reported by Bax et al to predict improvements in LVEF <sup>98</sup> and RR. <sup>49</sup> Yu, the other principal proponent of TDI, proposed a dyssynchrony index of standard deviation in time to peak systolic velocity between 12 basal and mid segments, which predicted RR after CRT. <sup>99</sup> Furthermore, this group demonstrated that RR rather than symptomatic improvement predicts long-term survival after CRT. <sup>45</sup>

There are several limitations to these techniques. Two distinct peaks of tissue velocity may be seen during systole, leading to difficulties in interval measurement. Peak velocities may occur after the end of systole, giving rise to uncertainty as to whether these should be included in analysis. In heart failure patients with LBBB, a rocking motion is frequently seen, but this may not

represent dyssynchronous contraction and may be difficult to interpret with TDI. Therefore, differences in the timing and magnitude of regional contraction may be better evaluated in radial or circumferential planes.

### Strain imaging

Strain can be measured using TDI or 2D speckle tracking. Results using TDI-derived strain have been mixed. Yu et al found that tissue Doppler longitudinal velocity, but not longitudinal strain, predicted RR after CRT.<sup>100</sup> 2D speckle tracking has the advantage that it is angle independent, but at the cost of lower temporal resolution. Suffoletto et al demonstrated that radial strain assessed by speckle tracking was predictive of acute and chronic improvements in LVEF after CRT<sup>101</sup> with incremental benefit seen when the LV lead position was concordant with the site of latest mechanical activation. Ypenburg et al demonstrated a reduction in a combined endpoint of hospitalisation and death in cases where the LV lead was positioned in the site of latest mechanical activation corroborated these findings.<sup>14</sup>

### Three-dimensional echocardiography

A single breath-hold acquisition over several heartbeats gives the entire ventricular volume, which is subdivided into 16 pyramidal sub-volumes. It is then possible to derive time-volume data for the entire cardiac cycle and assess the time taken to reach the minimum systolic volume. The standard deviation of these values across 16 segments is expressed as a percentage of the cardiac cycle to give the systolic dyssynchrony index (SDI), which is a marker of the global dyssynchrony of the LV, first described by Kapetanakis et al.<sup>102</sup> Real-time 3DE

(RT3DE) has been shown to predict acute response to CRT <sup>17</sup> although follow-up data are limited. The large volume of acquisition of RT3DE gives rise to relatively poor temporal resolution compared with 2D echo. This technique also relies on a regular RR interval thereby limiting its utility in patients with atrial fibrillation or frequent ectopy.

### ***Current role of echocardiography***

Echocardiography is an essential tool for assessment of LV function, chamber dimensions and LV EF to identifying candidates for CRT. In light of the negative results of the PROSPECT study, which did not find any individual echocardiography criterion superior to QRS duration at predicting CRT response <sup>103</sup> the assessment of dyssynchrony remains unclear when used to help determine which patients will do well from CRT. A major limitation to TTE is significant intra- and inter-observer variability, which was particularly marked in the PROSPECT trial. Reasons for the significant observer variability are multifactorial.

1. Patients with heart failure often have poor acoustic windows.
2. Difficulty breath holding leading to reduced image quality.
3. Arrhythmias such as atrial fibrillation or ventricular ectopics affect measurement accuracy.

Furthermore, there remains no clear consensus on which measure to use when assessing dyssynchrony. It therefore, remains unclear which TTE parameters of dyssynchrony should be used to determine which patients are likely to respond to CRT. However, the role of echocardiography in patients with intermediate QRS

prolongation is currently mandated in the UK by the NICE guidelines. It is important to realise that newer techniques such as speckle tracking and 3DE were not assessed in the PROSPECT study. The clinical usefulness of an imaging modality capable of predicting CRT response continues to drive forward research in this area. Overview of current echo acquisition and analysis methods is shown in figures 15 and 16.

**Figure 15** Overview of echocardiography assessment of CRT patients

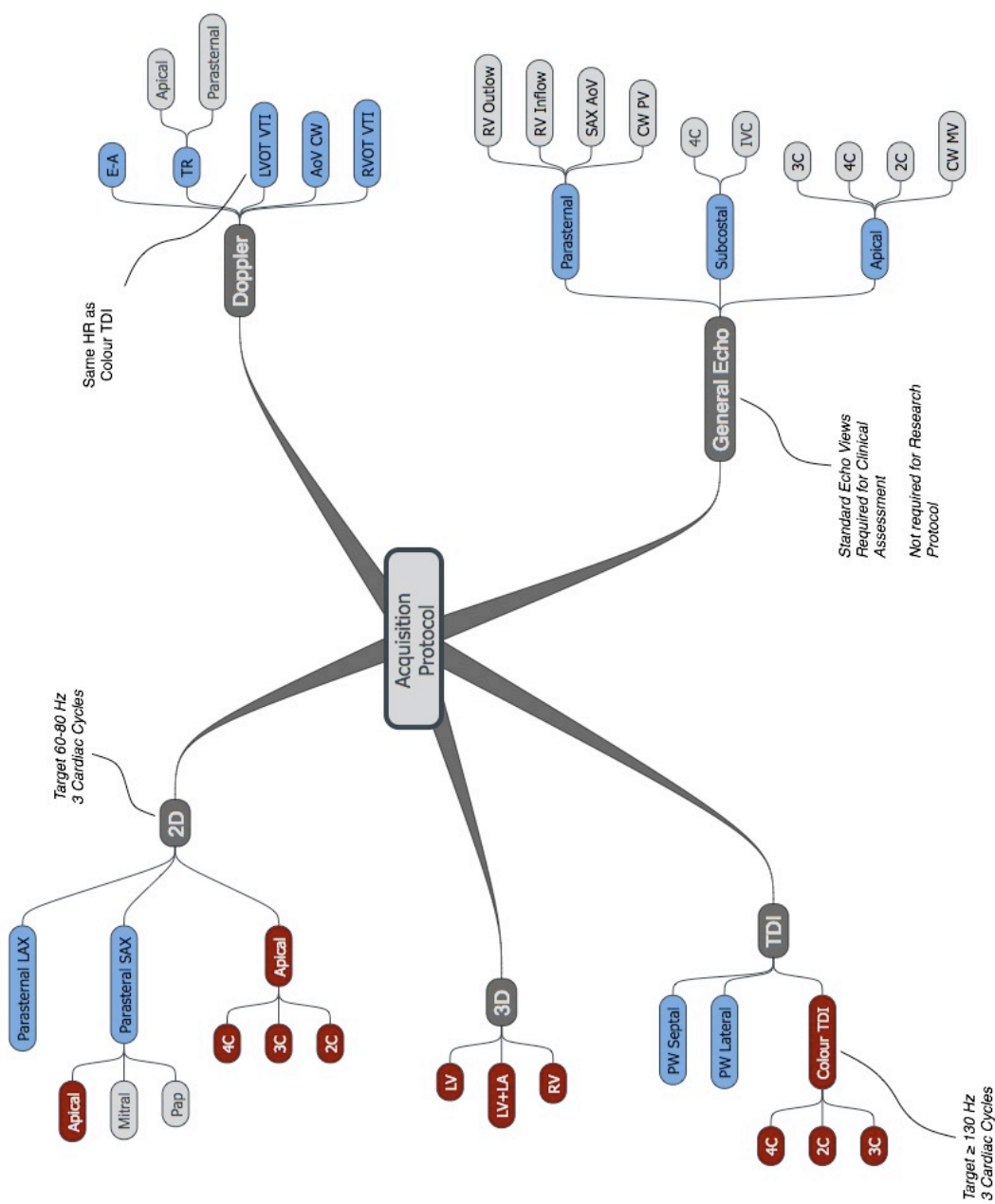
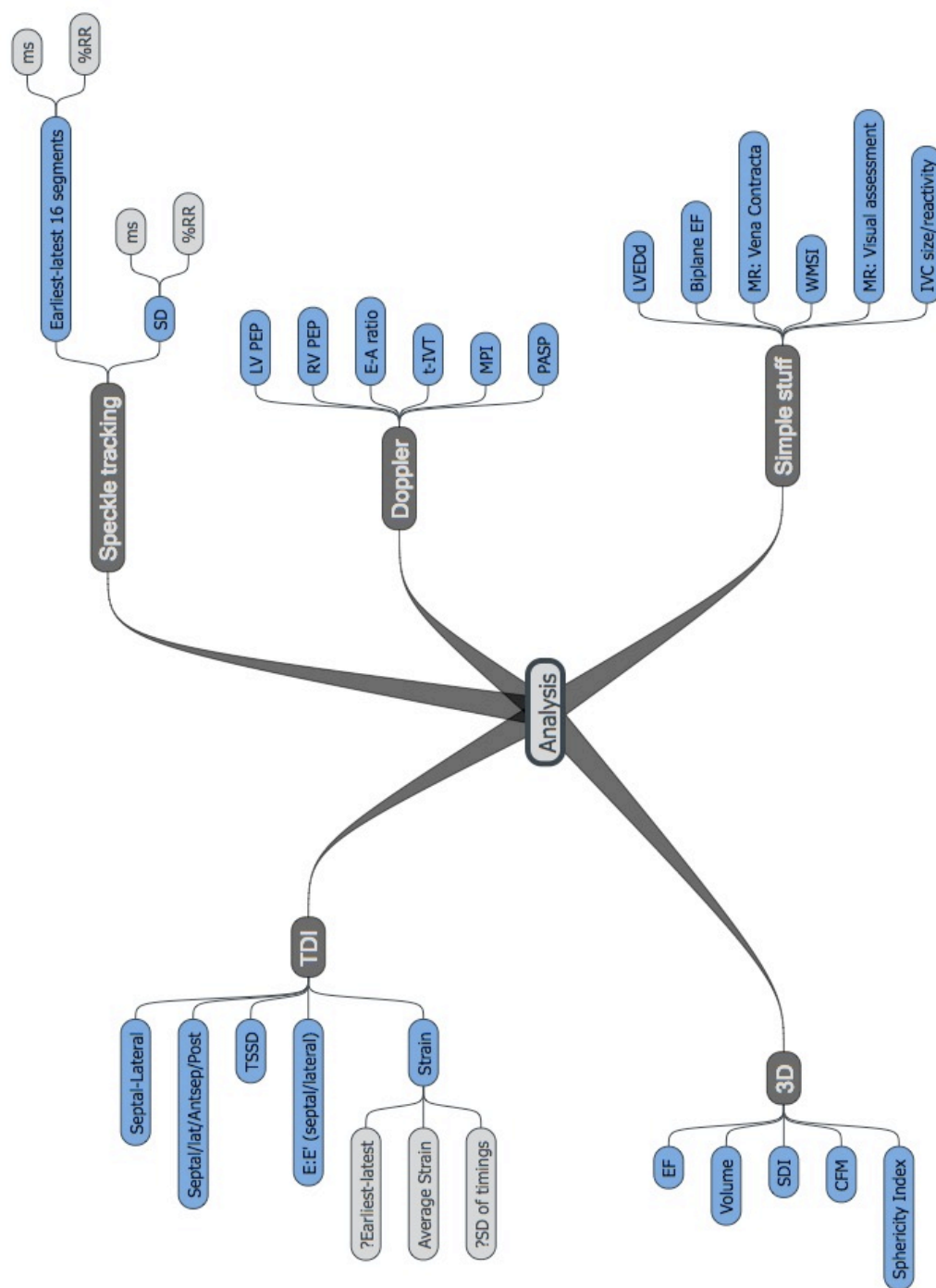


**Figure 16** Overview of analysis of echocardiography imaging in CRT patients



## **Cardiac Magnetic Resonance Imaging**

### ***A brief history of magnetic resonance imaging***

Felix Bloch and Edward Purcell both described the phenomenon of nuclear magnetic resonance in the 1940s independently. During the 1950s and 1960s this was widely used for the analysis of chemical compounds. Not until the 1970s when Damadian applied MRI for tissue characterisation did the technique break into the clinical medicine arena. The application of imaging was developed when Lauterbur applied the idea of magnetic field gradients in 3D to derive spatial orientation using MRI. Ernst developed the basis of modern MRI techniques with the introduction of phase and frequency encoding, and the Fourier transform. Mansfield developed echo-planar imaging, with improvements in the use of gradients and signal analysis.

### ***Basic principles of CMR***

The hydrogen atom consists of a positively charged proton and electrons and is abundant in the human body. This forms the basis for the use of MRI in medical imaging. The proton has an inherent nuclear spin, which creates a tiny magnetic field. In the tissues of the body, the magnetic fields resulting from each proton are randomly distributed. When the body is placed in a large and powerful magnet, these tiny magnetic fields align with the large external magnetic field and reach equilibrium. This equilibrium can be disturbed by applying energy to the body's tissues ("excitation"). This is achieved using a radio-frequency (RF) pulse, if the pulse is of the same resonance frequency as that of the protons. The result of the excitation with the RF pulse is a rotational movement of the total

magnetisation, called precession. The frequency of precession for protons is proportional to the magnetic field strength and the strength of the magnetisation is dependent on the proton density in the tissue. The angle of magnetisation is moved to an angle away from the main magnetic field depending on the amplitude and duration of the RF pulse. The magnetisation rotates around the main axis of the magnetic field, resulting in a high frequency alternating magnetic field. This gives rise to a signal, which is a voltage that can be measured in a receiver coil.

However, the signal is only transient, as the nuclei give off the energy they have acquired back to the surrounding tissues and the magnetisation becomes realigned in the longitudinal plane with the main magnetic field, at an exponential rate. This is known as longitudinal relaxation. The rate at which this happens depends on characteristics of the tissue and if the equilibrium is restored more quickly, the tissue has a short T1 (longitudinal) relaxation time. The second aspect of restoring equilibrium is loss of the transverse component of the magnetisation, i.e. that which is in the plane perpendicular to the main axis of the magnetic field. This happens because of interaction between different protons causing inhomogeneities in the magnetic field. The rotating vectors of magnetisation are fanned out ("dephased") such that they are not all pointing in the same direction, although they remain within the plane perpendicular to the main magnetic field. As a result, the sum of these rotating vectors is reduced and so is the signal. This is known as transverse relaxation. Again, the speed at which this occurs is dependent on tissue properties, which govern the T2 (transverse) relaxation time.



Spatial orientation is necessary in order to create an image. This is made possible using gradient fields. In contrast to the static field of the magnet, gradient fields can be altered over time in all three dimensions. In this way, a 2-D slice can be selected by applying a gradient in the direction perpendicular to it, while the excitation RF pulse is transmitted. The pulse will only have an effect on the slice of tissue in which the protons have the same resonance frequency as the pulse itself. The signal induced in the detector coil is described by a sine function. The frequency and phase of this function are used to define spatial orientation. Phase differences result from the use of a gradient field in one direction ("phase encoding") and frequency differences in the signal result from a gradient field applied in the other direction of the field of view ("frequency encoding"). This sampling process is repeated multiple times (this is the number of phase encoding steps) in order to acquire all of the spatial frequency components needed to make the image. The time between consecutive measurements is called the repetition time ("TR"). The image can then be calculated using these individual spatial frequency components using Fourier transformation. This gives a representation of the signals in the frequency domain. The digitized representations of these signals are converted into a data matrix called k-space, which is derived on one axis from frequency encoding information and on the other from phase encoding information. Data in the centre of k-space encodes contrast information as it has low spatial frequency but high amplitude, whereas data in the periphery of k-space provides image sharpness, as it has high spatial frequency but low amplitude.

### ***Cardiac magnetic resonance imaging in CRT***

CMR has huge potential in the assessment and selection of patients for CRT. Although echocardiography remains the primary imaging modality in CRT, CMR has a number of advantages. The following can all be assessed with CMR.

1. Cardiac function
2. Myocardial scar
3. Cardiac vein anatomy
4. Ventricular motion/dyssynchrony

CMR is the only imaging modality that is able to address all of these factors that have the potential to influence patient selection and thus improve the response to CRT.

#### **Functional assessment**

The combination of an excellent spatial, contrast and temporal resolution, providing high-quality morphological images of the heart throughout the cardiac cycle enables truly volumetric quantification and regional functional analysis. Velocity-encoded CMR techniques allow assessment of flow profiles through cardiac valves and analysis of myocardial motion patterns. CMR myocardial tagging techniques offer unique information about myocardial wall deformation and the mechanisms of myocardial contraction.

#### **Myocardial scar imaging**

Late gadolinium enhancement imaging is used to visualise myocardial damage, such as scar, fibrosis or oedema. Assessment of scar tissue not only helps with

determining the aetiology of heart failure, but also can help in determining which patients are likely to respond to CRT.

An intravenous contrast agent is administered, most frequently a chelate of gadolinium. This agent is extracellular, therefore is distributed into the intravascular and interstitial space, but does not penetrate healthy myocardial cells. Therefore, areas of acute or chronic infarction or oedema show higher signal than normal tissue. The inversion recovery technique <sup>104</sup> is used to null the healthy myocardium by suppressing the magnetisation, the tissue appears dark. The contrast agent accumulates in areas of damaged myocardium, and appears bright due to faster T1 relaxation. The distribution and transmural extent of late gadolinium enhancement can be used to assess myocardial viability. <sup>105</sup>

#### Cardiac vein anatomy

Knowledge of the cardiac anatomy particularly of the coronary veins is becoming increasingly important in CRT. In the vast majority of CRT procedures the LV lead is implanted transvenously through the coronary sinus into a lateral or posterior branch of the coronary sinus. There is marked individual variation in coronary venous anatomy, which can make it difficult to find a suitable position for the LV lead. <sup>106</sup>

CMR can be used to assess coronary veins using an intravascular contrast <sup>107, 108</sup> or without a contrast agent by employing an MTC-prepulse. <sup>109</sup> The use of an intravascular contrast agent has been shown to give excellent CV anatomy. <sup>108</sup>

The use of intravascular contrast agents means that limited information with respect to myocardial scar can be obtained.

A recent retrospective study <sup>110</sup> evaluated CMR angiograms of 31 patients for the ability to visualize coronary venous anatomy using conventional extravascular contrast agent. This was part of a comprehensive research protocol for patients with suspected coronary disease. This study demonstrated the feasibility of using CMR for assessment of scar and venous anatomy. However the scans were not optimized for visualization of the venous system. Furthermore, the average ejection fraction in the patient group was over 50%. The clinical relevance of this study is therefore limited as heart failure patients requiring CRT have ejection fractions of less than 35% and often have fast irregular heart rhythms and irregular breathing patterns leading to technical challenges with respect to CMR image acquisition.

Further work is required to enable visualization of coronary veins and myocardial scar in heart failure patients in a single CMR.

#### Assessing cardiac motion and dyssynchrony with CMR

Using cine wall motion, myocardial tagging, tissue velocity mapping, or displacement imaging can quantify mechanical motion/dyssynchrony. However, no guidelines exist for the use of CMR derived measures of dyssynchrony for selection of patients for CRT. Therefore, the question remains how useful these

measures of mechanical dyssynchrony are for indicating which patients will benefit from CRT.

*Cine imaging and myocardial motion and dyssynchrony*

Cine anatomical images of the myocardium provide excellent information about both endocardial and epicardial borders. The images are normally acquired in the four-chamber, three-chamber, two-chamber and short axis stack. Often mechanical dyssynchrony is apparent visually on these images. More quantitative methods of identifying mechanical dyssynchrony have been developed.<sup>111-113</sup> These methods utilize semi automated or automated border detection to compute myocardial wall motion, wall thickening or deformation. A method for quantification of myocardial dyssynchrony based on the amount of internal flow within the LV blood pool derived from the cine short-axis images has also been proposed.<sup>114</sup> Issues with these techniques are that multiple breath holds are required, which lead to alignment errors between separate slices. The use of 3D SSFP techniques either as breath holds or novel respiratory navigators<sup>115</sup> has the potential to overcome these problems. However, these techniques suffer from reduced blood pool contrast.

The benefit of these techniques for predicting response to CRT is not clear. Studies have shown differences in systolic timings,<sup>112</sup> regional myocardial thickening,<sup>113</sup> maximal radial motion,<sup>116</sup> and internal flow fraction between normal volunteers and heart failure patients with QRS durations greater than 120ms selected for CRT. A dyssynchrony index based on maximal radial wall

motion deemed the “*cardiovascular magnetic resonance tissue synchronization index*” (CMR-TSI) was shown to be a predictor of all-cause mortality and the hospitalizations related to heart failure after CRT.<sup>116</sup>

### *CMR tagging*

Myocardial tagging imposes a series of dark bands or grids across the image. This technique was devised to assess regional myocardial deformation.<sup>117</sup> Radiofrequency and gradient pulses are used to saturate lines in the myocardium in which the signal is destroyed, and the lines therefore appear black. This process is called spatial modulation of magnetization (“SPAMM”). The “tag” lines formed in this way produce a stripe or grid pattern. These are used as non-invasive markers on the myocardium. The changes in these lines through multiple phases of the cardiac cycle can be used to derive regional changes in deformation (or strain). The tag lines do not persist indefinitely, as the magnetization recovers towards equilibrium. Complementary SPAMM (“CSPAMM”) improves the persistence of the tag lines in order to assess strain through the whole cardiac cycle.<sup>118</sup>

Tagged images are usually analysed by tracking the location of the tag lines over time. This information is used to quantify regional deformation or compute regional strain. A variety of techniques are used for the analysis of tagged imaging.<sup>119 120</sup> Most dyssynchrony measures reflect the temporal dispersion of cardiac events measured in terms of the absolute difference delay or the

standard deviation of the time to onset or peak wall motion, deformation, strain or strain rate.

The clinical usefulness of CMR tagging has been limited by the time-consuming nature of the data analysis. Tagging has been used to quantify strain in animal models of ventricular pacing <sup>121</sup> and subsequently in humans with heart failure. <sup>16</sup> Circumferential assessment of strain using CMR appears to be more sensitive to dyssynchrony when compared to longitudinal strain. <sup>81</sup>

Harmonic phase (HARP) is a method of more rapid analysis of tagged MRI data, which measures motion by filtering out regions in the frequency domain of the images (harmonic peaks). <sup>122</sup> The harmonic magnitude and harmonic phase correspond to the anatomy and tag deformation of the resulting images, with the frequency of the tag lines reflecting local myocardial strain. This technique has been validated and applied in human studies to characterise regional function. <sup>123</sup> More recently this approach has been used to characterise regional strain in the assessment of patients for CRT using an index of circumferential strain (the CURE index).<sup>81</sup> The methodology used to derive the CURE index involves generating time plots of strain for each segment in each short axis slice. Each plot of strain versus myocardial location is submitted to Fourier analysis to yield zero to first order terms. Bichick et al showed that a CURE cut-off of <0.75 (0 denotes pure dyssynchrony and 1 denotes perfect synchrony) predicted improvement in NYHA class post CRT with 90% accuracy. <sup>124</sup>

The various methods to analysis tagged data still suffer from the similar problems to TTE strain assessments in that motion analysis is limited to 2D. As stated earlier the LV wall is a complex structure and a dyssynchrony assessment based on only one plane of motion is unlikely to reflect the extent of LV dyssynchrony.

There have been developments in the 3D CMR tagging.<sup>125</sup> This technique allows quantification of strain as well as direction of myocardial deformation and although it has only been applied to animals it may prove useful in the assessment of patients for CRT.



### **Current Issues in CRT**

A lot of the research within CRT has been driven by the high non-responder rate. There has been extensive work focusing on dyssynchrony measures to determine which patients are likely to respond. However, recent multi-centre trials have shown echocardiography measures are no better than the QRS duration for predicting response. The reasons for this are multi factorial and need resolving. To fully understand this problem the measures of dyssynchrony need to be understood, in particular how they relate to the coordinated contraction of the ventricle and how these indices change within the failing heart. Echocardiography remains the key imaging modality in CRT. With CMR becoming widely available and the improvements in image processing there is huge potential to improve our understanding of how measures of dyssynchrony may aid patient selection for CRT.

Currently QRS duration as a measure of electrical dyssynchrony is used as a surrogate for mechanical dyssynchrony. The relationship between electrical and mechanical activation remains unclear. Methods such as NCM allow accurate assessment of the activation patterns of the LV and image registration techniques allow these patterns to be compared to the ventricular motion.

It is important to realise that although the aim of CRT is to synchronise ventricular contraction there are anatomical limitations particularly with respect to the coronary veins and position and extent of myocardial scar. It is known that the position and the extent of scar affect response to CRT. Most CRT devices are implanted using the coronary sinus. The relationship between scar and veins has

the potential to aid implantation and improve response rates. Improvement in image registration tools within the interventional cardiac catheter laboratory has the potential to allow information about dyssynchrony, scar and veins to be registered real time and aid implantation.

The concept of response to CRT remains unclear. There are no clear guidelines to determine what is acute or chronic response. Furthermore, the relationship between acute and chronic response is unclear as is the relationship between myocardial dyssynchrony and acute and chronic response. This remains an important issue that needs resolving.

## **Chapter 3**

# **Methods of Measuring Mechanical Dyssynchrony and Effectiveness in Predicting Acute and Chronic Response to CRT**

### **Introduction**

What follows is the methodology, results and discussion for a study investigating global LV dyssynchrony with CMR. Using CMR cine and tagged images a method for assessing global myocardial muscle thickening and radial, circumferential and longitudinal strain was developed. Using this information a systolic dyssynchrony index (SDI) was derived for all parameters that is comparable to the previously described SDI for volume change. By developing comparable measures of myocardial dyssynchrony, which take into account both active and passive motion I aimed to evaluate how these techniques can aid in our understanding of myocardial dyssynchrony and in predicting which patients are likely to respond to CRT.

## **Methods**

### **Study population**

Patients with severe heart failure fulfilling standard criteria for CRT (NYHA class III-IV drug refractory heart failure, LVEF  $\leq 35\%$ , LV end-diastolic diameter  $\geq 55\text{mm}$  and prolonged QRS  $> 120\text{ms}$ , or were going to be RV pacing dependent) were recruited. Clinical characteristics of the patients are presented in Table 5. Patients had a quality-of-life questionnaire and six-minute walk as well as standard 2D and 3D echocardiogram to assess LV volumes and dyssynchrony pre and six months post CRT. Acute haemodynamic response was evaluated in 27 patients using a pressure wire passed to the LV cavity at the time of CRT. Patients had a standard BIV pacemaker inserted (table 6).

**Table 5** Patient characteristics

	All Patients	DCM	ICM	P value
	N=48	N=25	N=23	
Age (years)	63.8±13.9	63.3±16.3	64.3±11.0	0.4
Sex (male/female)	43/5	21/4	22/1	0.2
NYHA status	2.9±0.5	2.9±0.6	2.8±0.4	0.4
QOL score pre CRT	51±24	51±22	51±27	0.5
QRS duration (ms)	154±24	159±27	149±19	0.07
Rhythm	42 SR 6 AF	20 SR 5AF	22SR 1AF	
6 minute walk distance (m)	255±112	260±109	248±118	0.4
Ejection fraction (%)	25±9	25±10	26±8	0.6
End diastolic volume (ml)	230±70	234±75	226±66	0.4
End systolic volume (ml)	175±67	180±73	170±61	0.3
B Blockers (%)	91	95	87	
ACE/ARB (%)	98	100	96	
Diuretics (%)	62	76	50	
Aldosterone antagonists (%)	38	35	40	

ACE=Angiotensin II converting enzyme inhibitors, ARB=Angiotensin receptor blockers

**Table 6** Implant details

	<b>Implant</b>
<b>Device</b>	13 St Jude Promote Q CD3221 14 St Jude Promote RF 3213-36 7 St Jude Pacesetter Atlas II HF v-367 4 St Jude Frontier II 5596 2 Medtronic-maximo II DR D284DRG 1 Medtronic-syncra CRT-P C2TR01 2 Medtronic concerto C174AWK 3 Medtronic-Insync III 8042 1 Biotronik-Lumax 340 HF-T 1 no device implanted
<b>LV lead position</b>	2 Posterior vein 21 Posteriolateral vein 19 Lateral vein 2 Middle cardiac vein 3 Anteriolateral vein 1 patient no implant
<b>RV lead position</b>	28 Septum 19 Apical
<b>LV lead threshold</b>	1.3±0.7
<b>RV lead threshold</b>	0.7±0.3

### **Echocardiography Acquisition**

Prior to CRT, standard echocardiograms, with TDI, were acquired on a GE vivid 7 scanner (General Electric-Vingmed, Milwaukee, Wisconsin). Analysis was performed using EchoPac version 6.0.1 (General Electric-Vingmed). Ejection fractions and LV dimensions were measured using 2D biplane Simpson's method. Transmitral flow velocities were obtained from the apical-4-chamber view with pulsed-wave Doppler positioned at the tip of the leaflets. End diastole (onset of isovolumic contraction) and end systole (aortic valve closure) were determined using transmitral and aortic Doppler profiles.

### **Echocardiographic Assessment of Dyssynchrony**

The IVMD was calculated as the difference between the LV and RV pre-ejection periods measured from the QRS to the onset of pulmonary and aortic flows respectively.<sup>126</sup> Intra-ventricular dyssynchrony was assessed with TDI by measuring the difference between septal to lateral peak velocity within the aortic valve opening and closing times<sup>4,127</sup> Real-time transthoracic 3D echocardiography<sup>102</sup> was performed on all patients and volumes analysed with TomTec 4D LV-Analysis software (TomTec Imaging systems Inc, Munich, Germany).

### **CMR Imaging Acquisition**

The patients were scanned using 1.5T MR-scanner (Achieva, Philips Healthcare, Best, Netherlands) with a 32-element cardiac coil or a 5-element cardiac coil. Cardiac synchronisation was performed with vector electrocardiography (VECG).

After localisation and a coil sensitivity reference scan an interactive real-time scan was performed to determine the geometry of the short axis, four, three and two chamber. A multiple slice cine steady state free precession scan was performed in SA orientation to assess the ventricular function (FA=60°, TR/TE=2.9/1.5ms, resolution 2.2x2.2x10mm, 30 heart phases). The 4CH, 3CH and 2CH views were used to assess LV function for regional wall motion abnormalities. A short axis and longitudinal stack of breath hold ECG-gated 2D CSPAMM or 3D CSPAMM <sup>128</sup> images were acquired of the whole LV. The change in acquisition was because of the availability of 3D CSPAMM half way through the study which allowed a reduction in scan time and better alignment of slices. Delayed enhancement (DE-MR) imaging was performed to assess myocardial scar. DE-MR was performed 15-20mins following the administration of 0.1-0.2mmol/kg gadopentetate dimeglumine (Magnevist®, Bayer Healthcare, Dublin, Ireland) using conventional inversion recovery techniques. <sup>129</sup>

### **Methods for CMR Processing**

The SDI for change in LV cavity volume over the cardiac cycle was determined by using commercially available TomTec 4D LV-Analysis software (TomTec Imaging systems Inc, Munich, Germany). For myocardial strain and wall thickening, a framework<sup>130</sup> was developed (Figure 17 and 18) which semi-automatically computed these values at each phase across the cardiac cycle. The framework included three steps: (1) Manual slice by slice segmentation of the endo and epicardial borders of the LV in the stack of SA and three long-axis SSFP images in the first end diastolic (ED) cardiac phase; (2) detection of endo and epi-cardial



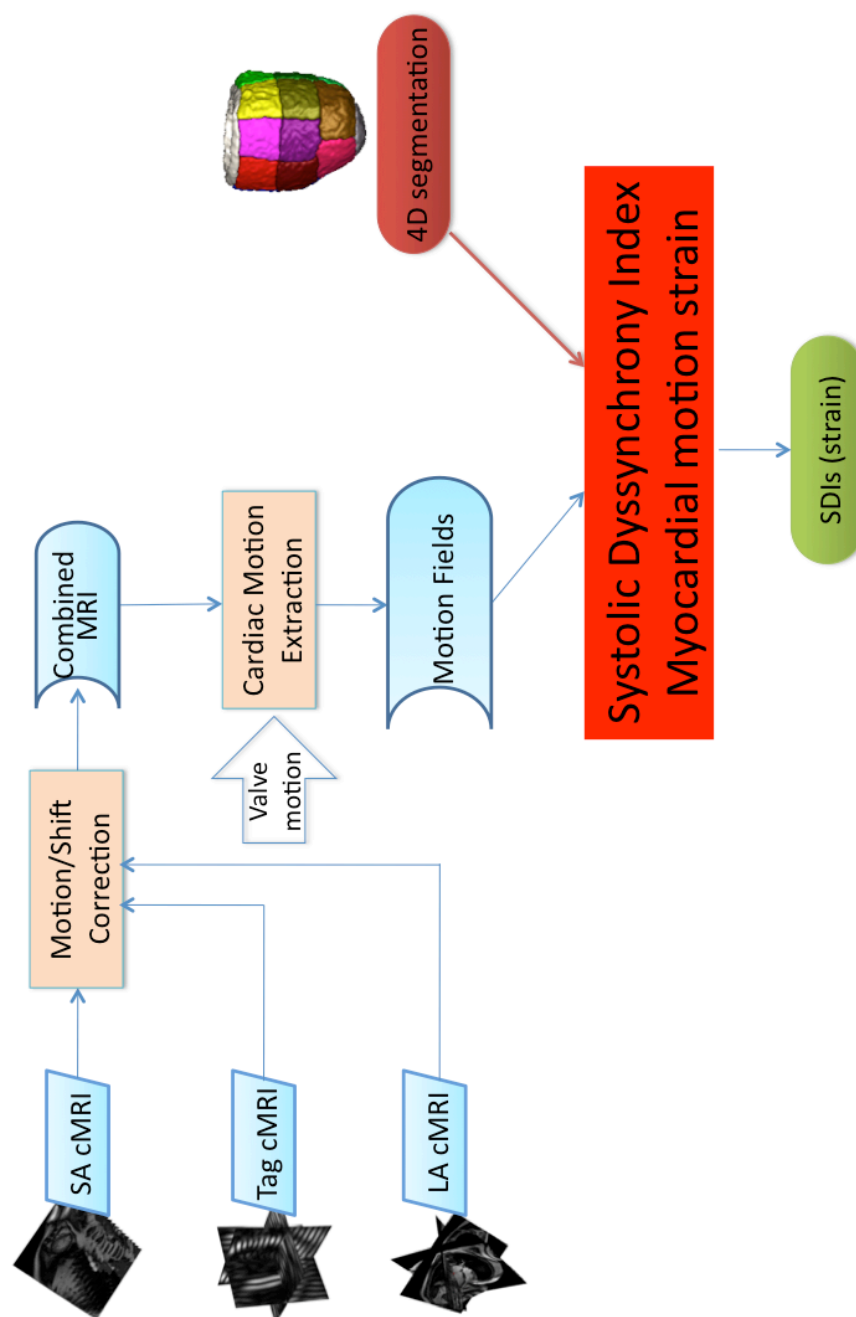
surfaces for wall thickening computation; and (3) extraction of deformation fields within the myocardium for myocardial motion and strain computation. A 3D model of the heart was developed from the end diastolic slices and all the subsequent slices were registered to this to correct for slice misalignment. Myocardial surface detection and deformation fields were computed from cine and tagged CMR. The myocardial wall thickening value, and strain fields were all mapped onto the coordinate of the anatomical CMR, where the 16 segments of the LV myocardium (bull's-eye) were defined from the segmentation results.

For each subject 16 segments of the LV myocardium were defined according to the same definition used by the Tomtec software. This was done by first manually labelling the myocardium of the LV at the end diastolic (ED) phase of the cine CMR. A pre-constructed myocardium model which has 16 segments defined was then fitted onto the manually segmented myocardium using automatic image registration<sup>130</sup>. As corresponding 16-segment labelling of the myocardium at ED phase CMR for each subject was thus achieved.



**Figure 18**

Workflow of how tagged images are used to develop global motion and strain dyssynchrony assessment



### **Myocardial Wall Thickening from Cine CMR**

Cine CMR provides good image quality, high signal and contrast to noise ratio. The endo- and epi-cardial surfaces of the LV for each phase of the cardiac cycle were segmented to achieve the segmentation of ED phase using manual delineation as described earlier.

- 1) Other phases from the cine CMR were then extracted and the *registration and propagation* procedure from the ED phase was applied to achieve automatic segmentation. In this procedure, the ED phase image is selected as the reference image. The reference image is then registered to all the other phases and the corresponding segmentation is propagated<sup>130</sup>. The serial propagation registration was used to model the large deformation field required for the registration between the phases that are far apart from the ED phase. In the serial propagation the neighbouring phase of the ED phase to the reference image is first registered, and the resulting transformation is used to initialize the registration of the next phase. This process continues until all the phases are registered with the reference image.
- 2) Having achieved the segmentation of endo- and epi-cardial surfaces for all cardiac phases, the surface distance between the two surfaces was computed for each segment of the LV myocardium.

### **Myocardial Deformation from Cine and Tagged CMR**

Myocardial strain is computed from the deformation field of the myocardium, which is achieved by registering the ED phase CMR to all the other phases

(Figure 18). Having the deformation fields  $v(x,p)$  for voxel  $x$ , from the ED phase to phase  $p$ , the myocardial motion is computed as follows:

$$m(x) = |v(x,p)|$$

The term strain was defined as a material point with original volume  $V(sa,sl)$  and current volume  $V'(sa',sl')$  where  $sa$  is short-axis area and  $sl$  is long-axis length with the following equations:

$$S(x) = \frac{sa' * la}{sa * la'}$$

So that longitudinal strain is reverted so the strain term could represent the muscle function during the systolic cycle.

### **Systolic Dyssynchrony Index**

To assess global LV dyssynchrony the time taken to reach maximum muscle thickness or peak strain for 16 segments was calculated as a percentage of the cardiac cycle. A SDI was then defined as the standard deviation of these timings with a high SDI denoting more dyssynchrony. Expressing the SDI as a percentage of the cardiac cycle allows comparison between patients with different heart rates.

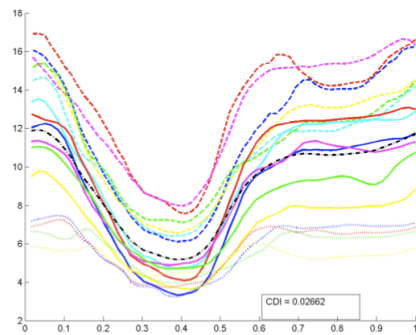
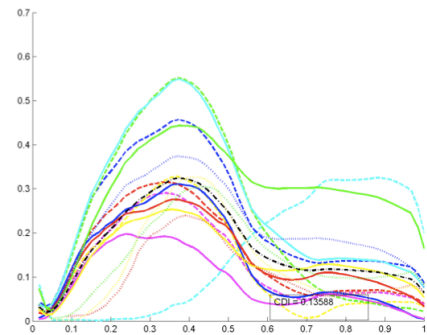
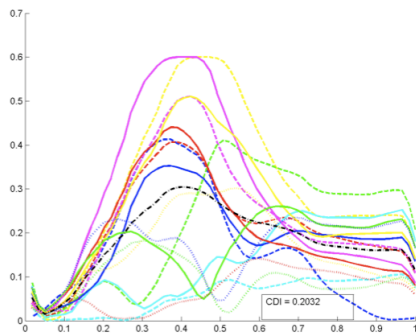
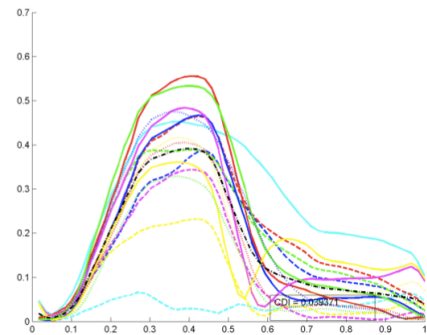
Only segments that had  $\geq 5\%$  thickening defined from the diastolic wall thickness were included in the SDI for muscle thickening.

Graphs with curves for each of the 16 segments for the change in volume, thickening and strain (radial, longitudinal and circumferential) over the cardiac

cycle were formed for all patients to allow a visual representation of how each method compared during LV contraction. (Figure 19)

**Figure 19**

Curves for a volunteer with normal LV function representing the time to peak volume change **(A)** and time to peak strain for all 16 myocardial segments **(B)** Longitudinal strain, **(C)** Radial strain, **(D)** Circumferential strain.

**A****B****C****D**

### **Implant and Acute Haemodynamic Measurements**

All patients had a standard CRT implant (Table 6). During CRT implantation in 27 patients haemodynamic evaluation was performed with a 0.014-inch pressure sensor-tipped percutaneous transluminal coronary angioplasty guide wire (Radi Medical Systems, Uppsala, Sweden) with a 500-Hz frequency response introduced into the LV through a 4-Fr multipurpose catheter from either a femoral or radial access site.<sup>131</sup> Subsequently the multi-purpose catheter was removed or withdrawn into the aorta, leaving the soft tip of the pressure wire in a stable position within the LV cavity. Once venous access had been acquired for pacing lead implants, 2500 Units of heparin were given followed by saline flush. At steady-state conditions LV-dP/dt<sub>max</sub> was calculated electronically from every heartbeat for a period of at least ten seconds. The results were averaged for the complete measurement period. A waiting period of at least twenty seconds was respected after any change in pacing settings or lead position in order to achieve haemodynamic stabilisation<sup>18, 38</sup>. LV-dP/dt<sub>max</sub> was measured during intrinsic rhythm and atrial pacing (AAI 10 beats above intrinsic with consistent capture) and with LV CS pacing (DDLV (fixed AV delay 100ms) or VVI (patients in atrial fibrillation (AF)), 10 beats above intrinsic). In patients with AF baseline was considered as RV pacing 10 beats above intrinsic rhythm.<sup>132</sup> Results were expressed as a percentage of variation from the baseline (AAI pacing, 10 beats above intrinsic). Baseline drift in LV-dP/dt<sub>max</sub> was determined by calculating the mean standard deviation over the course of the procedure.



### **Classification of Acute Response**

Improvement in  $LV-dP/dt_{max} \geq 10\%$  compared with fixed rate atrial / RV pacing (baseline) was used as the cut-off for an acute response. This cut-off value has been used in previous studies <sup>37, 51</sup>.

### **Classification of Reverse Remodelling and Responders**

Patients were deemed to have RR if there was a  $\geq 15\%$  reduction in LV end-systolic volume (ESV) as measured using modified Simpson's biplane method on 2D echo images<sup>48, 49</sup>. Evaluation of symptomatic response was made using NYHA class, six-minute walk distance and QOL score. <sup>50</sup> Patients were labeled clinical responders if the NYHA class fell by  $\geq 1$  or if there was a  $\geq 10\%$  improvement in six minute walk distance or a  $\geq 10\%$  reduction in QOL score.

### **Comparison and Reproducibility of Methods**

Using the framework developed to assess strain and muscle thickening also allowed assessment of volume SDI comparable to the Tomtec method. To establish the agreement between the two methods statistical analysis proposed by Bland and Altman<sup>133</sup> was used.

For volume SDI derived from TomTec 4D LV-Analysis software intra-observer and inter-observer agreements were assessed according to the statistical methods proposed by Bland and Altman. The measure of reproducibility used was two standard deviations (SD) of the intra-observer and inter-agreement

indices. Therefore, the intra-observer coefficient of variation (COV) was equal to two SD of

$$\frac{|x_{1st}-x_{2nd}|}{(x_{1st}+x_{2nd})/2}$$

And the inter-observer COV was equal to 2 SD of

$$\frac{|x_a-x_b|}{(x_a+x_b)/2}$$

The process to develop muscle thickening and strain SDI is an automotive process so intra-observer or inter-observer assessment is not appropriate.

### **Statistical Analysis**

Statistical analysis was performed using JMP software (version 8.0.2, Marlow, Buckinghamshire, UK). A Shapiro-Wilk test was used to ensure variables were normally distributed. Continuous variables were expressed as mean  $\pm$  SD and compared with parametric (ANOVA) and non-parametric (Wilcoxon rank sum) tests. Nominal variables are expressed as absolute count and percentages and compared with a Fisher's exact test. Outcomes were assessed with logistic regression to create receiver-operator characteristic (ROC) curves. P values of  $<0.05$  were considered statistically significant.

## Results

Forty-eight patients were recruited, (42 male,  $63.8 \pm 13.9$  years), NYHA class  $2.8 \pm 0.5$  (Table 5). All patients had LBBB with QRS duration  $155 \pm 24$ ms. Two patients were recruited with QRS duration less than 120ms. These two patients had severe LV impairment and would have been 100% RV paced and therefore it was felt they would benefit from CRT. Twenty-five patients had DCM and 23 ICM. Forty-four (92%) patients were followed up at 6 months. Of the four patients that were not followed up at six months one patient with DCM had died of heart failure, one patient declined any further intervention after the LV lead displaced twice, one patient had their LV lead turned off due to diaphragmatic pacing and one patient declined a device post recruitment.

## Acute Response

In twenty seven patients, LV-dP/dt<sub>max</sub> was measured at the time of implant. (Table 7) The baseline (AAI or RV pacing) LV-dP/dt<sub>max</sub> was  $823 \pm 199$ mmHg/s, this increased to  $940 \pm 216$ mmHg/s with LVCS pacing ( $P < 0.001$ ). The average number of baseline readings was  $4.2 \pm 1.2$ . Baseline drift in LV-dP/dt<sub>max</sub> was  $58 \pm 19$  mmHg/s. The average percentage increase in LV-dP/dt<sub>max</sub> from baseline with LVCS pacing was  $16 \pm 17\%$ . Eighteen (66%) of the patients had a  $\geq 10\%$  increase in LV-dP/dt<sub>max</sub> and were deemed acute responders.

## Measures of Dyssynchrony Predicting Acute Haemodynamic Response

A wider QRS duration strongly predicted AHR ( $P = 0.008$ ) with a moderate correlation between QRS width and % rise in LV-dP/dt<sub>max</sub> ( $r = 0.73$ ). For measures

of global dyssynchrony a high volume derived SDI strongly predicted AHR ( $P=0.008$ ) with a moderate correlation between high SDI and % rise in LV- $dP/dt_{max}$  ( $r=0.7$ ). (Figure 20) (Table 8) For all other measures of dyssynchrony I found no relationship between AHR and derived SDI. (Figure 21)

Receiver-operating characteristics (ROC) analysis (Table 8) showed an SDI derived from volume change of  $\geq 10.3\%$  was sensitive (0.76) and specific (0.88) for predicting AHR. None of the other methods for deriving a SDI were comparable. Using ROC analysis, QRS duration of  $\geq 158\text{ms}$  was found to have a sensitivity of 0.71 and specificity of 0.89 for predicting AHR.

The only echocardiographic measure of dyssynchrony that was found to predict AHR was IVMD ( $P=0.03$ ) and volume SDI derived from 3D echo ( $P=0.02$ ). The ROC analysis showed that an SDI of  $\geq 7.2\%$  had a sensitivity of 0.92 and specificity of 0.63 and IVMD of  $\geq 60\text{ms}$  had a sensitivity of 0.61 and specificity of 0.89 for predicting AHR.

**Table 7** Characteristics of patients in whom AHR was measured at the time of CRT implant

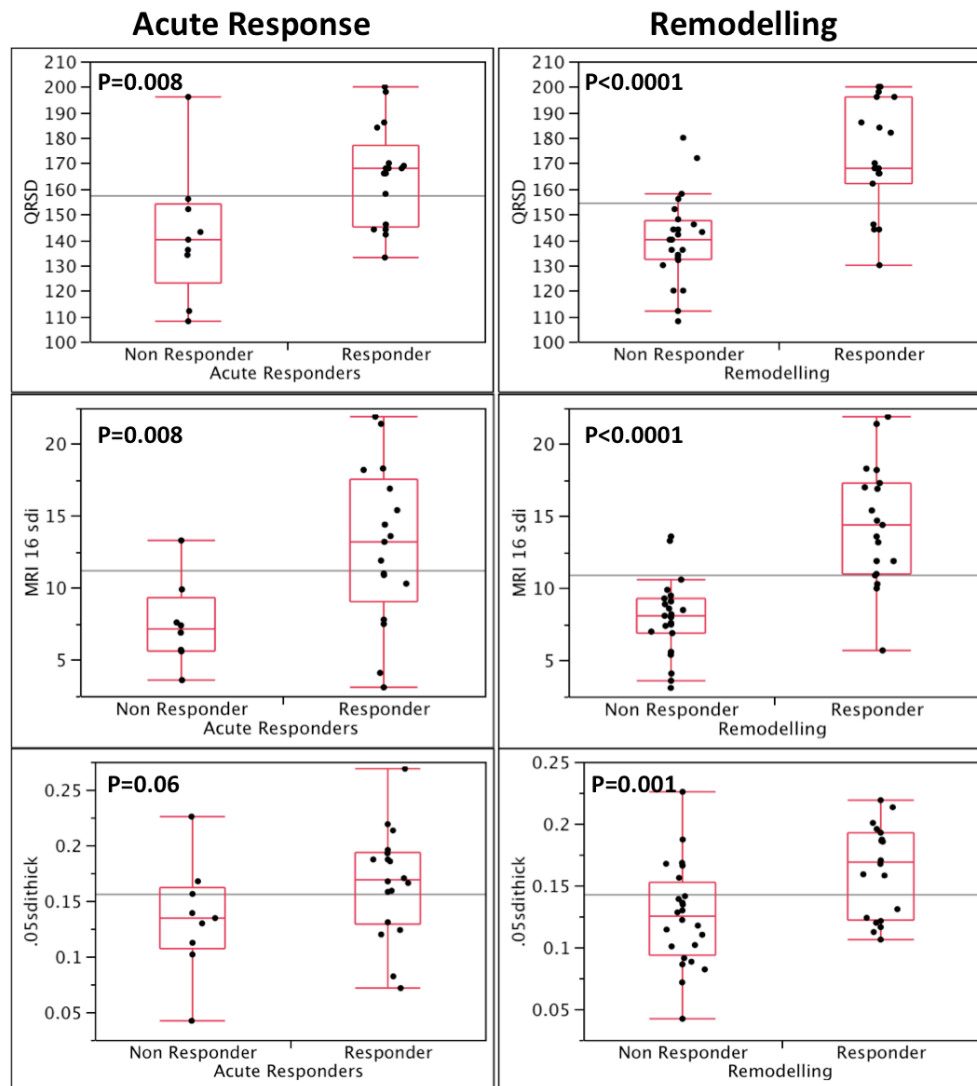
	All Patients	AH patients
	N=48	N=27
Age (years)	63.8±13.9	64.4±11.7
Sex (male/female)	43/5	23/4
Aetiology	25 DCM	18 DCM
	23 ICM	9 ICM
NYHA status	2.9±0.5	2.7±0.5
QOL score pre CRT	50.9±24	48±22
QRS duration (ms)	154±24	158±24
Rhythm	42 SR	22 SR
	6 AF	5AF
6 minute walk distance (m)	255±112	270±108
Ejection fraction (%)	25±9	25±9
End diastolic volume (ml)	230±70	233±64
End systolic volume (ml)	175±67	177±62

**Table 8** Shows the P values for each SDI derived from the various methods to predict AHR. Receiver-operating characteristic are shown with the area under the curve (AUC) and the cut-off values and sensitivities and specificities for each method shown.

	P value to predict	AUC	Cut-Off	Sensitivity	Specificity
AHR					
<b>QRS duration (ms)</b>	0.008*	0.81	≥158ms	0.71	0.89
<b>Volume SDI</b>	0.008*	0.82	≥10.3%	0.76	0.88
<b>Thickening SD</b>	0.06	0.7	≥15.8%	0.72	0.78
<b>Radial strain SDI</b>	0.4	0.5	≥22.2%	0.28	0.89
<b>Longitudinal strain SDI</b>	0.3	0.56	≥12.5%	0.83	0.33
<b>Circumferential strain SDI</b>	0.1	0.62	≥6.0%	0.72	0.56
<b>Combined strain SDI</b>	0.3	0.58	≥4.4%	0.94	0.33

\*Significant relationship

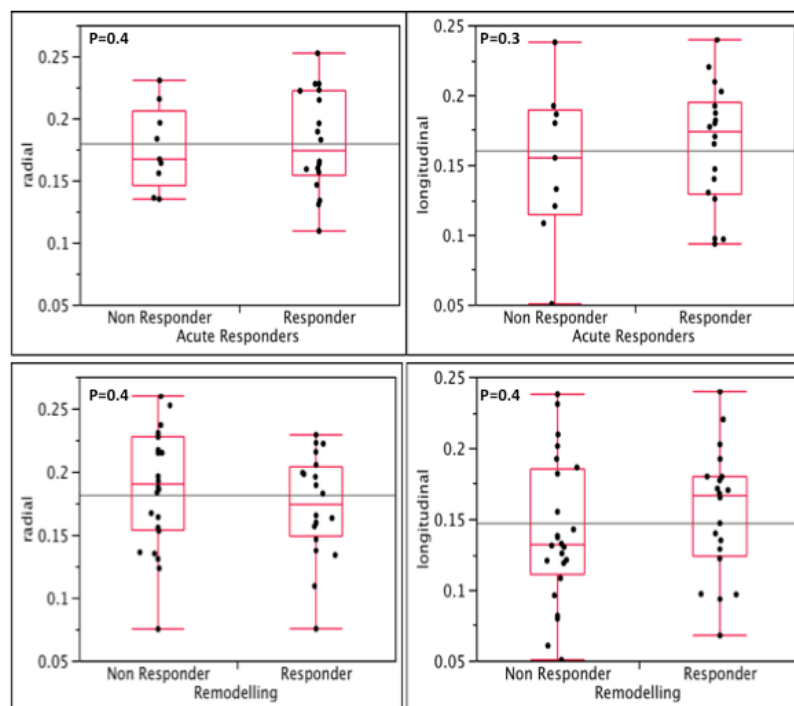
**Figure 20** Shows the ANOVA plots for QRS duration, volume and muscle thickening derived SDI to predict AHR and RR



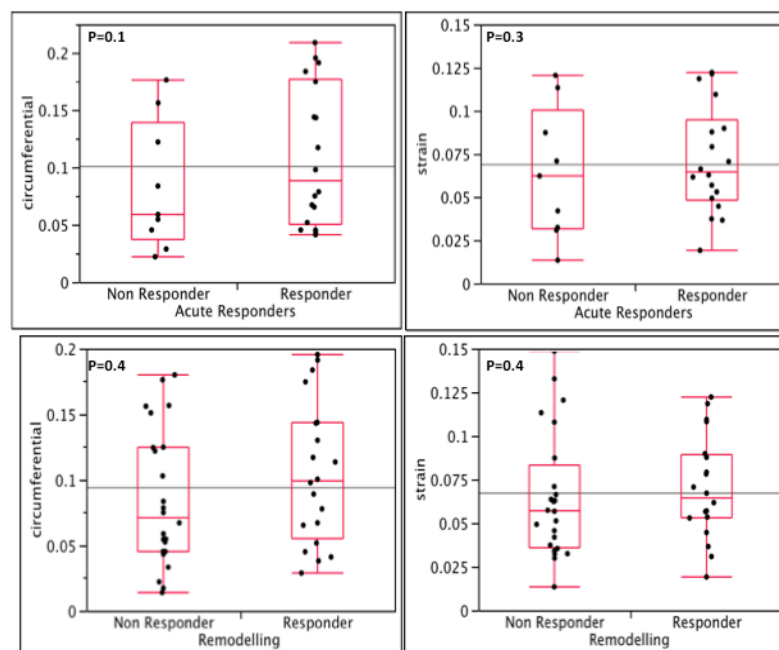
MRI 16 sdi = CMR volume SDI, 0.5sdi thick = SDI derived from CMR muscle thickening

**Figure 21A & B** Shows the ANOVA plots for SDI derived from various types of strain to predict AHR (top rows) and RR (bottom rows).

**A**



**B**





### **Reverse Remodelling**

Pre-implant LVESV and LVEF were  $175 \pm 64$  ml and  $25.0 \pm 8.5\%$  respectively. These improved over the follow-up period to  $155 \pm 68$  ml ( $P < 0.01$ ) and  $31.8 \pm 10.2\%$  respectively.

QRS duration predicted RR ( $P < 0.0001$ ). Using ROC analysis QRS duration of  $\geq 162$  ms was sensitive (0.79) and specific (0.92) for predicting RR. (Table 9) (Figure 20)

Volume derived SDI strongly predicted RR ( $P < 0.0001$ ) (Figure 20). ROC analysis showed that an SDI of  $\geq 10\%$  was highly sensitive (0.94) and specific (0.87) for predicting which patients are likely to RR. SDI derived from muscle thickening predicted RR ( $P = 0.001$  for thickening of  $> 0.5$  mm) (Figure 20). SDI derived from thickening was much less sensitive and specific than QRS duration or volume derived SDI at determining which patients were likely to RR. None of the SDIs derived from strain (radial, longitudinal, circumferential and combined) were predictive for RR (Table 9) (Figure 21).

For standard echocardiographic measures of dyssynchrony (Table 10), LVPE ( $P = 0.003$ ) and IVMD ( $P = 0.0008$ ) predicted RR. TDI derived indices of dyssynchrony did not predict RR. Volume derived SDI from 3D echocardiography showed predicted RR ( $P = 0.02$ ).

**Table 9** P values for each SDI derived from the various methods to predict RR. Receiver-operating characteristic are shown with the area under the curve (AUC) and the cut-off values and sensitivities and specificities for each method shown.

	<b>P value</b>	<b>AUC</b>	<b>Cut-Off</b>	<b>Sensitivity</b>	<b>Specificity</b>
	<b>to</b>				
	<b>predict</b>				
	<b>RR</b>				
<b>QRS duration (ms)</b>	<0.0001*	0.88	≥162ms	0.79	0.92
<b>Volume SDI</b>	<0.0001*	0.92	≥10.0%	0.94	0.87
<b>Thickening SDI</b>	0.001*	0.75	≥15.8%	0.65	0.79
<b>(&gt;0.5mm)</b>					
<b>Radial strain SDI</b>	0.8	0.59	≥22.2%	0.95	0.29
<b>Longitudinal strain</b>	0.8	0.59	≥20.7%	0.83	0.4
<b>SDI</b>					
<b>Circumferential strain</b>	0.9	0.60	≥8.9%	0.6	0.62
<b>SDI</b>					
<b>Combined strain SDI</b>	0.7	0.58	≥5.6%	0.8	0.46

\*Significant relationship

**Table 10** Sensitivity, Specificity and AUC for echo measures of dyssynchrony to predict RR

Assessment method	P value to predict RR	AUC	Cut- off	Sensitivity	Specificity
LVPE (ms)	0.003*	0.74	≥160	0.68	0.75
IVMD (ms)	0.0008*	0.83	≥60	0.67	0.83
TDI Septal/lateral delay (ms)	0.4	0.56	≥90	1.0	0.17
SDI (%)	0.02*	0.71	≥12.1	0.69	0.84
N=26					

### Clinical Response

Thirty six (82%) patients had a reduction of at least one NYHA class at 6 months, and 38 (86%) had a  $\geq 10\%$  improvement in quality of life score. Twenty-six of the patients performed six-minute walks pre and post CRT implantation. Seventeen of the patients (65%) had a  $\geq 10\%$  improvement in six-minute walk distance.

QRS duration was predictive for reduction in NYHA score ( $P=0.0005$ ). LVPE ( $P=0.02$ ), IVMD ( $P=0.005$ ), CMR volume SDI ( $P=0.02$ ) and muscle thickening SDI ( $0.002$ ) predicted reduction in NYHA score. None of the strain indices showed a relationship with improvement in NYHA class. Only muscle thickening SDI was found to predict improvement in QOL score ( $P=0.01$ ). No relationship was found between improvement in six-minute walk duration and any measure of dyssynchrony.

**Aetiology: DCM vs ICM**

Differences between patients with DCM and ICM pre CRT are shown in table 11. There was significantly greater RR in patients with DCM compared to ICM patients (decrease in ESV for DCM  $36\pm 55\text{ml}$  vs  $1.0\pm 51\text{ml}$  for ICM,  $P=0.02$ ). Fourteen (61%) of patients with DCM reverse remodeled, compared to only six (29%) of the patients with ICM.

For patients with DCM, QRS duration and SDI derived from CMR volume change and muscle thickening predicted RR (Figure 22). SDI derived from radial and circumferential strain weakly predicted RR (Figure 23). For echo derived indices of dyssynchrony, LVPE, IVMD and volume derived SDI with 3D echocardiography predicted RR (Table 12).

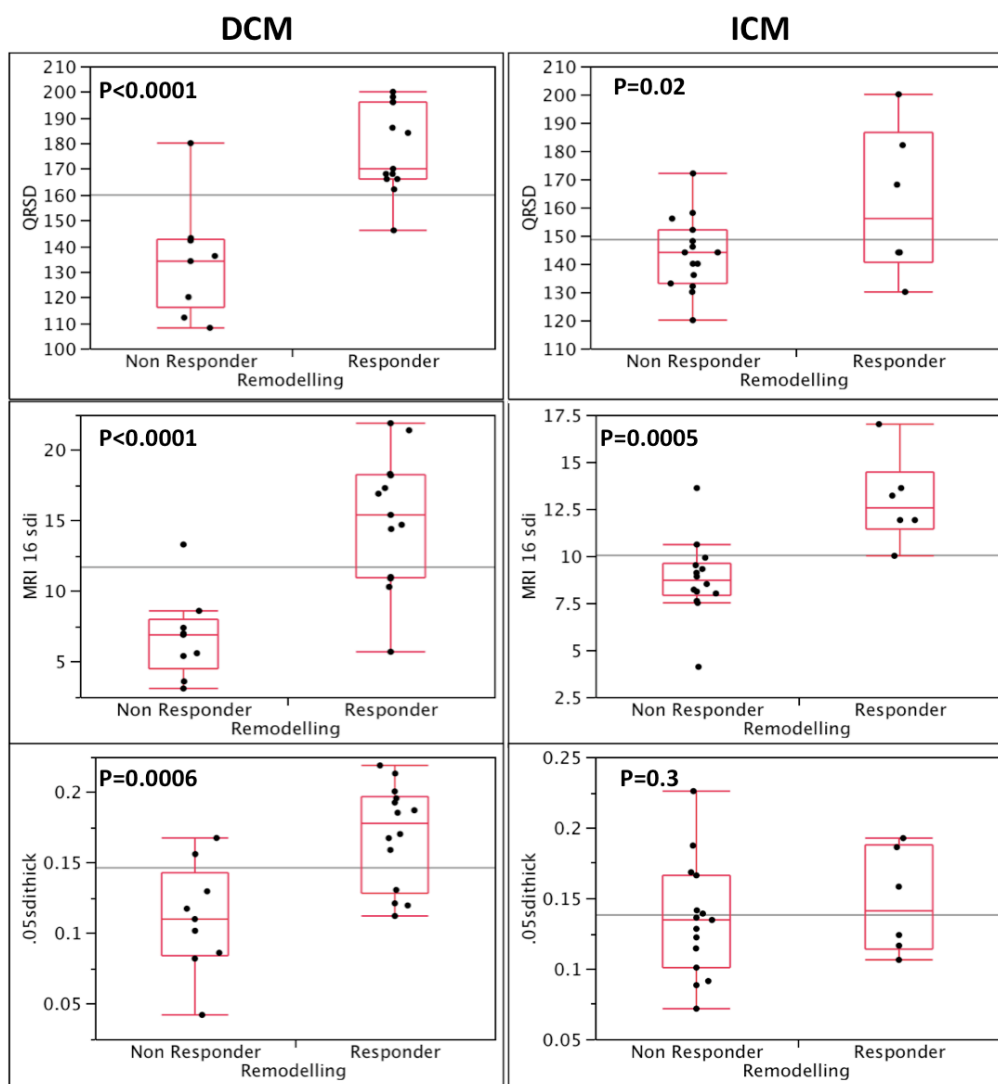
For patients with ICM, SDI derived CMR volume change was highly predictive for RR. QRS duration (Figure 22) and IVMD were also predictive for RR, however had weaker relationship (Table 12).

**Table 11** Difference between DCM and ICM patients pre and post CRT

	DCM			ICM		
	N=23			N=21		
	Pre CRT	Post CRT	P	Pre CRT	Post	P
			value		CRT	value
<b>NYHA Score</b>	2.9±0.5	1.7±0.8	<0.001	2.8±0.4	1.7±0.8	<0.001
<b>QOL score</b>	52±22	26±19	<0.001	51±27	30±25	<0.001
<b>Six minute walk distance (m)</b>	258±111	374±115	<0.001	248±117	303±160	0.07
<b>QRS duration (ms)</b>	160±28			148±19		
<b>Ejection Fraction (%)</b>	25±10	34±11	<0.001	25±8	29±9	0.04
<b>End systolic volume (ml)</b>	175±70	139±71	<0.002	171±62	173±62	0.5

**Figure 22**

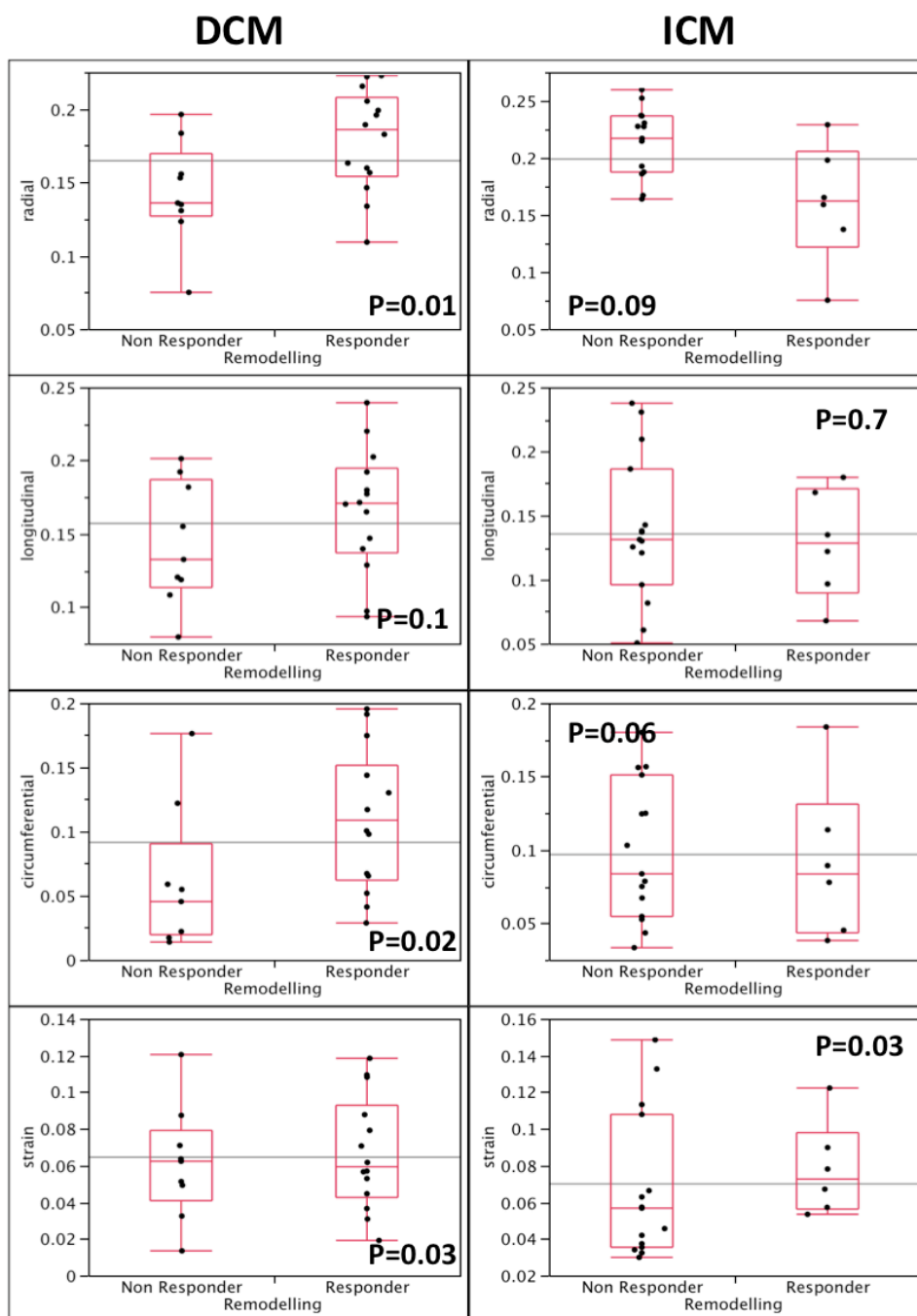
Shows the ANOVA plots for QRS duration, volume and muscle thickening derived SDI in both DCM and ICM patients.



MRI 16 sdi = CMR volume SDI, 0.5sdi thick=SDI derived from CMR muscle thickening

**Figure 23**

Shows the ANOVA plots for SDI derived from various types of strain for DCM and ICM.



MRI 16 sdi = CMR volume SDI, 0.5sdi=SDI derived from CMR muscle thickening

**Table 12** P values for echocardiographic measures of dyssynchrony for predicting RR in DCM and ICM patients

	P value for predicting $\geq 15\%$ decrease ESV for DCM pts	P value for predicting $\geq 15\%$ decrease ESV for ICM pts
<b>QRS duration</b>	<0.0001*	0.02*
<b>LVPE</b>	0.03*	0.2
<b>IVMD</b>	0.002*	0.02*
<b>TDI, septal/lateral delay</b>	0.9	0.3
<b>3D echo 16 seg SDI</b>	0.01*	0.1

\*Significant relationship



### **Aetiology and Clinical Response**

For patients with ICM; QRS duration ( $P=0.03$ ), SDI derived from muscle thickening ( $P=0.007$ ), SDI derived from volume change ( $P=0.02$ ) and IVMD ( $P=0.04$ ) predicted improvement in NYHA score. For improvement in heart failure score there was no relationship found with any marker of dyssynchrony in ICM patients. Only SDI derived from volume change predicted improvement in six-minute walk distance in ICM patients ( $P=0.02$ ).

For patients with DCM only QRS duration ( $P=0.004$ ) predicted improvement in NYHA score. For improvement in heart failure score only SDI derived from volume change ( $P=0.03$ ) and muscle thickening ( $P=0.003$ ) predicted improvement in score. For improvement in six-minute walk distance no measure of dyssynchrony showed a relationship in DCM patients.

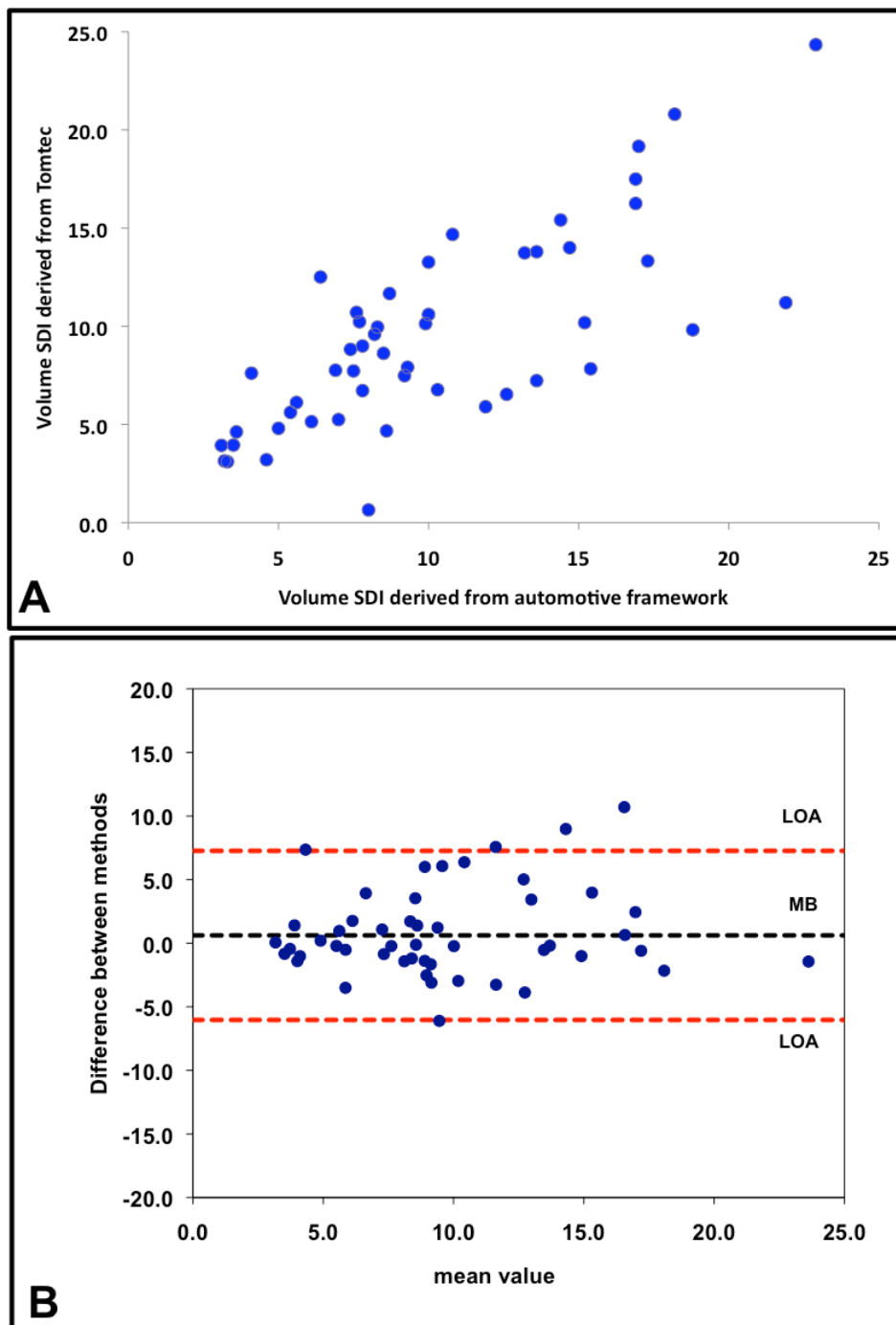
### **Agreement of Methods and Reproducibility**

To assess agreement of methods and reproducibility, ten subjects (five patients and five volunteers with normal LV function) had repeat scans. Between the two methods to assess volume SDI there was a good agreement, with a mean difference of  $0.61\% \pm 3.39\%$  (Figure 24). Both methods for deriving a volume SDI were assessed to see agreement between two CMR scans. There was excellent agreement with mean difference for 4D Tomtec analysis derived SDI  $0.57 \pm 1.26\%$  compared with  $0.66 \pm 2.15\%$  for the automotive method.

In the five patients and five volunteers selected for intra and inter-observer variability for volume SDI derived from Tomtec 4D LV-Analysis software was

excellent. The intra-observer average difference was  $0.04 \pm 0.3\%$  and COV was  $1.8 \pm 1.2\%$  and the inter-observer average difference was  $0.55 \pm 1.4\%$  and COV was  $4.2 \pm 4.6\%$ .

**Figure 24:** **A** Scatter plot of two different methods to assess volume dyssynchrony. **B** Bland and Altman plot for the difference between volume SDI assessed with Tomtec 4D LV-Analysis software and via automotive framework.



## Discussion

Using a framework that enabled comparable measures of global dyssynchrony (SDIs for volume, muscle thickening and peak radial, circumferential, longitudinal and combined strain) the ability of these indices to predict both acute response and RR in patients referred for CRT was assessed.

The following was shown:

1. A SDI of  $\geq 10\%$  derived from volume change is sensitive and specific and superior to other mechanical dyssynchrony measures at predicting acute response and reverse remodelling.
2. A SDI derived from peak strain (radial, longitudinal, circumferential or combined) is poor at predicting which patients will respond acutely to CRT or RR.
3. Muscle thickening SDI does not predict acute response, but is strongly predictive of RR although is less sensitive and specific than volume SDI.
4. Other than QRS duration volume SDI is the only global measure that is predictive of RR both for DCM and ICM patients.

## Systolic Dyssynchrony Index Measurements

In this work radial, longitudinal, circumferential and combined strain measurements did not help predict which patients would respond to CRT. Although surprising, considering the focus of previous studies on measures of myocardial strain, this apparent separation of volume and thickening measures of dyssynchrony from strain indices may be explained by a closer look at the mechanics involved in myocardial contraction. Ejection is due to wall thickening

and apical-basal shortening. In a normal subject, wall thickening contributes 25-48% to stroke volume and is the result of a combination of shearing and elongation along the laminar sheets that make up the myocardium and has a limited correlation with fibre shortening that is more closely related to measures of strain.

The use of longitudinal, radial and circumferential strain dyssynchrony measurements that are not aligned with the orientation of the helical cardiac microstructure is fraught with physiological limitations. The measured strain is then made up of a combination of different muscle fibre orientated segments and sheets and the intrinsic variation in the time taken for different regions of the heart to contract and reach their peak strain in the healthy heart obscures any changes in synchrony that may occur with heart failure. The timing of peak contraction in the heart varies transmurally, circumferentially and in the apex to base directions. This variation is significant with an 83ms dispersion in time to peak strain across the heart wall in canines compared with a QRS duration of approximately 60ms and the time to peak circumferential strain variations of 121ms in human LV, where the QRS duration is approximately 80ms. The distribution of timing of peak deformation is consistent with the distribution of electrical activation only amplified. This increased heterogeneity in the spatial variation in deformation is potentially facilitated by multiple factors including the non-uniformity of fibre and sheet orientation, activation times, regional cavity curvature, contractile function, electrophysiology and passive material properties. Therefore using indices of strain to measure myocardial motion does

not provide a useful measure of dyssynchrony and explains why these measures are not useful in predicting which patients are likely to respond to CRT.

This is clearly seen in volunteers with normal ventricles (Figure 19). The volume SDI is low, indicating synchrony, but SDI for peak strain (longitudinal, radial and circumferential) is high, which indicates dyssynchrony even though the volunteers ventricles are normal. Using cruder measures of myocardial dyssynchrony such as volume SDI gives a clear indication of how well coordinated the ventricular contraction is as it does not take into account the difference forces working with and against each other during systole.

### **Aetiology**

Part of the aim of the study was to use muscle thickening and strain derived SDI to take into account the difference between active and passive myocardial motion. It is known that position and extent of myocardial scar affect the likelihood of response to CRT.<sup>134</sup> Using a volume derived SDI does not take into account the difference between active and passive motion that occurs in scarred akinetic regions. Patients with DCM are much more likely to RR (61%) compared to ICM (29%). I found SDI derived from volume change was highly predictive for RR in both DCM and ICM patients. I would have expected an SDI derived from muscle thickening or strain derivatives to be more helpful in patients with ICM as these parameters give a better understanding of the dyssynchrony seen in active muscle contraction but no such relationship was found. The reasons for this are unclear. The aim of CRT is to synchronise contraction in a failing ventricle to

improve ventricular efficiency. A volume derived index of dyssynchrony may be better at predicting which patients are likely to respond to CRT as it gives a far more accurate assessment of mechanical dyssynchrony and therefore the possible treatable substrate for CRT. Furthermore the inherent problems with strain measurements already discussed may explain this.

### **Comparing Imaging Techniques**

Volume SDI derived from 3D echo showed a significant relationship with both AHR and RR, but not with any clinical measures of response. It is interesting that similar volume derived measure of dyssynchrony both predict AHR and RR. The relationship for 3D echo derived SDI is not as strong as for CMR volume derived SDI. This is probably due to the poor image quality and therefore a less accurate assessment of dyssynchrony. For 3D echo SDI the image quality was only good enough to accurately analyse in 26 (60%) patients. Only IVMD was comparable to volume SDI derived from CMR at predicting RR. However, this was much less sensitive (0.67 compared with 0.94).

### **Understanding Relationships Between SDI and LBBB**

The aim of CRT is to synchronise the contraction of the LV. It is implied that the greater LV dyssynchrony, the greater the substrate for CRT and the more likely a patient will respond. It is inferred that the broader the QRS duration the more electrical dyssynchrony there is and more mechanical dyssynchrony is present. The relationship between QRS duration and mechanical dyssynchrony is not clear. I found that the correlation between QRS duration and volume SDI was

only moderate ( $r=0.6$ ). Having a broad QRS does not always lead to mechanical dyssynchrony and vice versa. All patients had LBBB, with a QRS duration  $\geq 120$ ms yet only 45% RR. Therefore current use of QRS duration of  $\geq 120$ ms is very poor at selecting which patients will respond to CRT.

Current guidelines for patient selection for CRT are a QRS duration greater than 120ms. The broader the QRS the more likely patients are to RR. This is underpinned by QRS duration of 162ms being the best cut-off for sensitivity and specificity in this study. Using a cut-off of 10% for volume derived SDI from CMR, 21 (47%) patients had an SDI  $\geq 10\%$ , of those 18 (86%) RR. Using a volume derived SDI of  $\geq 10\%$  is a far better discriminator at predicting which patients are likely to RR than QRS duration of  $\geq 120$ ms.

### **Measurement Techniques**

Previous echocardiographic-based studies<sup>135</sup> have showed the poor reproducibility of particularly strain based measures of dyssynchrony. I found excellent intra and inter-observer agreement for volume derived SDI. The measures of agreement between two difference scans were also good for volume derived SDI. The framework that was developed as part of this project to allow assessment of muscle thickening and strain involved a complex procedure, which was long and time consuming and not practical in the clinical arena. Assessment of volume SDI was easy to perform providing valid results within five minutes. This provides a simple clinical tool to improve patient selection for CRT.



## Limitations

For this study both RR and clinical indicators were used to determine response to CRT. SDI for volume change and muscle thickening were predictive for RR. Although a weak relationship with improvement in NYHA class and SDI derived from volume change and muscle thickening, and a weak relationship with muscle thickening SDI and improvement in QOL score were found, no other statistically significant relationship with functional measures were identified. It has been shown that RR is an independent predictor of clinical outcome at up to five years<sup>136</sup>, but RR does not predict symptomatic response and that there is a discordance between symptomatic response and survival benefit of CRT. It is therefore important that a volume derived SDI of  $\geq 10\%$  strongly predicts RR. Furthermore this study is underpowered to show the true relationship between functional measures of improvement and SDI.

When the patients were separated into aetiology, only six of the patients with ICM RR, all having a volume SDI  $\geq 10\%$ . A highly significant relationship for volume and RR in ICM and DCM patients was found. For muscle thickening SDI a significant relationship in DCM patients but no relationship in ICM patients was identified. Due to the small numbers of patients that RR particularly in the ICM group it is difficult to interpret these results and a larger study is required to answer this question.

A major limitation of the echo data was the image quality, where particularly the 3D echo image quality was only good enough for accurate analysis in 26 (60%)

patients. This is one of the major limitations of echo assessment of dyssynchrony and a clear benefit of CMR due to superior image quality.

## **Conclusions**

A volume derived systolic dyssynchrony index from cine CMR strongly predicts reverse remodelling in heart failure patients referred for cardiac resynchronisation therapy. Volume derived systolic dyssynchrony index is superior to echo measures of dyssynchrony and muscle thickening at predicting reverse remodelling. Different strain based measures of dyssynchrony do not predict reverse remodelling. Furthermore, volume derived SDI is a highly reproducible measurement that has significant potential clinical implications in the future for improving patient selection for cardiac resynchronisation therapy.

## **Chapter 4**

# **Relationship Between Acute and Chronic Response to CRT**

### **Introduction**

What follows is the methodology and results for the study of acute haemodynamic response and its relationship with chronic response to CRT. To study this, invasive maximum rate of LV pressure rise (LV-dP/dt<sub>max</sub>) was used to guide conventional coronary sinus LV lead placement in an unselected group of heart failure patients at the time of CRT implant. The relationship between LV-dP/dt<sub>max</sub> and reverse remodelling was then investigated.

### **Methods**

Patients with severe heart failure fulfilling standard criteria for CRT (NYHA class III-IV drug refractory heart failure, LVEF  $\leq 35\%$ , LV end-diastolic diameter  $\geq 55\text{mm}$  and prolonged QRS  $> 120\text{ms}$ ) were recruited. Clinical characteristics of the patients are presented in Table 13. Symptomatic response was assessed using a quality-of-life questionnaire, which was repeated six months post CRT.

**Table 13** Patient Characteristics

	All Patients	DCM	ICM	P value
	N=33	N=21	N=12	DCM vs ICM
<b>Age (years)</b>	63.6±12.1	62.3±12.7	65.9±10.9	N/S
<b>Sex (male/female)</b>	29/4	18/3	11/1	N/S
<b>NYHA status</b>	30 class III	20 class III	10 class III	N/S
<b>QOL score pre CRT</b>	52±22	50±23	53±21	N/S
<b>QRS duration (ms)</b>	160±23	162±28	156±13	N/S
<b>Rhythm</b>	27 SR	16 SR	11SR	N/S
	6 AF	5AF	1AF	
<b>Ejection fraction</b>	25±8%	24±9	26±5	N/S
<b>End diastolic volume (ml)</b>	239±69	250±83	229±56	N/S
<b>End systolic volume (ml)</b>	185±67	193±77	170±43	N/S
<b>B Blockers (%)</b>	86	88	75	
<b>ACE/ARB (%)</b>	100	100	100	
<b>Diuretics (%)</b>	64	78	45	
<b>Aldosterone antagonists (%)</b>	39	41	36	

N/S=Non significant

### Echocardiographic Assessment

Prior to CRT implantation patients underwent echocardiogram, acquired on a GE vivid 7 scanner (General Electric-Vingmed, Milwaukee, Wisconsin). Analysis was performed using EchoPac version 6.0.1 (General Electric-Vingmed, Milwaukee, Wisconsin). Ejection fractions and LV dimensions were measured using 2D biplane Simpson's modified method. Echocardiography measures of dyssynchrony were measured as described in chapter 3.

### **Implant and Acute Haemodynamic Measurements**

All patients underwent CRT implantation (Table 14). During CRT implantation haemodynamic evaluation was performed using a 0.014 inch diameter high fidelity Certus PressureWire and PhysioMon software (Radi Medical Systems, Uppsala, Sweden) with a 500 Hz frequency response introduced into the LV.<sup>131</sup> (chapter 3 for more details of method)

LV-dP/dt<sub>max</sub> was calculated electronically from every heartbeat for a period of at least ten seconds to ensure steady-state conditions. The results were averaged for the complete measurement period. A waiting period of at least twenty seconds was respected after any change in pacing settings or lead position in order to achieve haemodynamic stabilization<sup>18</sup>. This method has previously been shown to reliably measure LV-dP/dt<sub>max</sub><sup>38</sup>.

**Table 14** Implant details

<b>Implant</b>	
<b>Device</b>	8 St Jude Promote Q CD3221 16 St Jude Promote RF 3213-36 5 St Jude Pacesetter Atlas II HF v-367 4 St Jude Frontier II 5596
<b>LV lead position</b>	2 Posterior vein 19 Postero-lateral vein 11 Lateral vein 1 Middle cardiac vein 1 Antero-lateral vein
<b>Types of LV lead</b>	27 Quickflex® (St Jude Medical) 6 Quartet Model 1458Q (St Jude Medical)
<b>LV lead threshold</b>	1.4±0.7
<b>RV lead threshold</b>	0.7±0.3

### **Haemodynamic Measurement Protocol and Data Analysis**

An occlusive venogram was performed and the LV lead was then placed in branches of the coronary sinus that were considered potential targets to allow multiple measurements of  $dP/dt_{\max}$ . In these sites the LV- $dP/dt_{\max}$  was measured during intrinsic rhythm and atrial pacing (AAI 5-10 beats above intrinsic atrial rate to ensure consistent capture) and with LV coronary sinus pacing (DDDLV (fixed AV delay 100ms) or VVI (patients in atrial fibrillation (AF) 5-10 beats above intrinsic). In patients with AF, baseline was considered as right ventricular (RV) pacing 5-10 beats above intrinsic ventricular rate.<sup>132</sup>

Results at each pacing site were expressed as a percentage of variation from the baseline (AAI pacing, 5-10 beats above intrinsic rate). The best position for the LV lead location was defined as the site with the largest percentage rise in LV- $dP/dt_{\max}$  from baseline. Baseline drift in  $dP/dt_{\max}$  was determined by calculating the mean standard deviation over the course of the procedure. At the end of the procedure, pressure wire guided AV and VV optimization was performed.

### **Reverse Remodelling and Responders**

Patients were deemed to have RR if there was a  $\geq 15\%$  reduction in LV ESV as measured using Simpson's modified biplane method on 2D echo images.<sup>48, 49</sup> Evaluation of symptomatic response was made using NYHA class and quality-of-life questionnaire.<sup>50</sup> To assess sensitivity and specificity for  $dP/dt_{\max}$  to predict RR patients were deemed acute responders if the percentage improvement in  $dP/dt_{\max}$  was  $\geq 10\%$  compared with fixed rate atrial / RV pacing (baseline). This

cut-off value has been used in previous studies.<sup>37, 51</sup> Patients were labeled clinical responders if the NYHA class fell by  $\geq 1$  or if there was a  $\geq 10\%$  reduction in quality-of-life questionnaire score.

### **Statistical Analysis**

Statistical analysis was performed using JMP software (version 8.0.2, Marlow, Buckinghamshire, UK). A Shapiro-Wilk test was used to ensure variables were normally distributed. Continuous variables were expressed as mean  $\pm$  SD and compared with parametric (One-way ANOVA) and non-parametric (Wilcoxon rank sum) tests. Changes with in variables were compared using paired t tests. Nominal variables are expressed as absolute count and percentages and compared with a Fisher's exact test. Outcomes were assessed with logistic regression to create receiver-operator characteristic (ROC) curves. Optimal cut-offs were selected as the level with the highest (Sensitivity- (1-Specificity)). P values of  $< 0.05$  were considered statistically significant.

### **Results**

Thirty-three patients were recruited (29 males, age  $63.6 \pm 12.1$  years), with mean ejection fraction of  $25 \pm 8\%$ . All patients had LBBB, QRS duration  $160 \pm 23$ ms. Twelve had ICM and 21 DCM (Table 13). Assessment of LV-dP/dt<sub>max</sub> was successfully achieved in all patients. All patients had a BIV pacemaker inserted at the time of the pressure wire study (Table 14). Average procedure time was  $138 \pm 38$  minutes and fluoroscopy time  $20.7 \pm 7.4$  minutes. One patient had a groin haematoma from the pressure wire, and one a wound haematoma, neither



requiring further intervention. One patient had RV lead displacement that required repositioning the following day. One patient had a coronary sinus dissection, however a LV lead was still successfully implanted. One patient with an ICM post implant had excessive diaphragmatic pacing, which led to the LV lead being turned off and this patient being excluded from six-month follow up.

The mean intrinsic LV-dP/dt<sub>max</sub> was 722±148 mmHg/s compared with AAI/RV pacing 10 beats above intrinsic which was 801±194 mmHg/s (p<0.001) (used as baseline). The baseline drift in LV-dP/dt<sub>max</sub> over the course of the implants was 68±17 mmHg/s. There was a highly significant increase in LV-dP/dt<sub>max</sub> from baseline to DDDL V pacing in the optimal (best AHR) position (801±194mmHg/s to 924±203mmHg/s P<0.001, 18±18% rise)(Figure 25) (Table 15). In 30 of the patients at least two separate branches of the coronary sinus were paced. There was a highly significant difference between best and worst LV pacing site (924±203mmHg/s best site, 782±160mmHg/s worst site P<0.001)(Figure 25 & 26). Using a 10% cut-off to define acute response, 23 (70%) of patients were acute responders to DDDL V pacing.

**Table 15** RR and acute haemodynamic response depending on LV lead position

	<b>≥ 15%</b>	<b>Intrinsic</b>	<b>AAI pacing</b>	<b>DDD-LV pacing</b>	
	<b>reduction in</b>				
	<b>ESV</b>				
		<b>Mean</b>	<b>Mean</b>	<b>Mean</b>	<b>%</b>
		<b>dP/dt<sub>max</sub></b>	<b>dP/dt<sub>max</sub></b>	<b>dP/dt<sub>max</sub></b>	<b>Change</b>
<b>†All patients n=33</b>	18 (56%)	722±148*	801±194	924±203*	18±18
<b>LV lead</b>	11 (64%)	730±123*	828±174	978±222*	19±16
<b>†Posterolateral vein</b>					
<b>n=18</b>					
<b>LV lead Lateral vein</b>	5 (45%)	725±164	795±255	894±178*	18±23
<b>n=11</b>					
<b>LV lead Posterior vein</b>	1 (50%)	745	831	978	18
<b>n=2</b>					
<b>LV lead middle</b>	1 (100%)	519	516	599	15
<b>cardiac vein n=1</b>					
<b>LV lead anterolateral</b>	0 (0%)	780	948	982	4
<b>vein n=1</b>					

\*Significant difference from AAI pacing (P<0.05)

†One patient excluded from long-term follow up

**Figure 25** Change in LV-dP/dt<sub>max</sub> for various pacing modes and difference between best and worst LV-dP/dt<sub>max</sub> for DDDLV pacing.

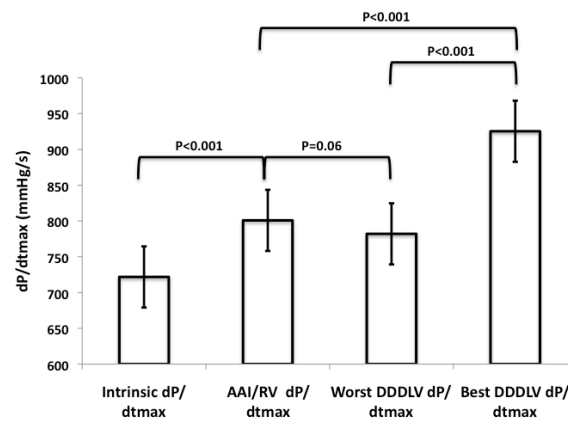
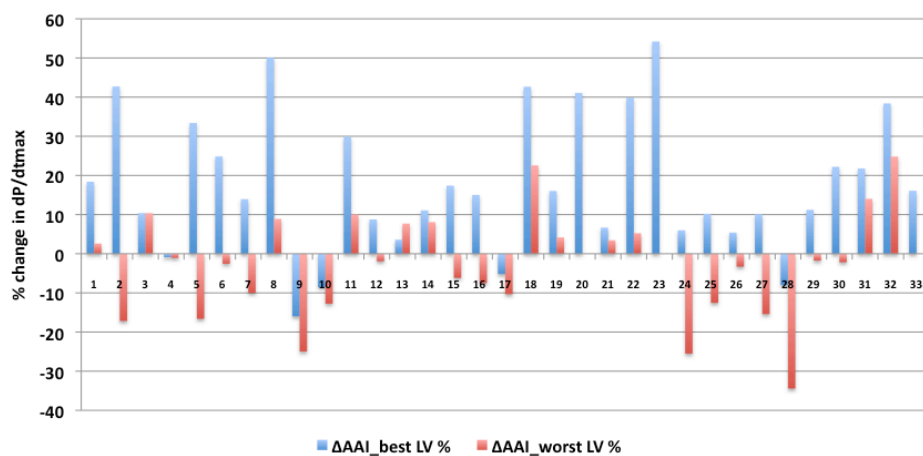


**Figure 26** Best and Worst Sites for Each Individual pacing position

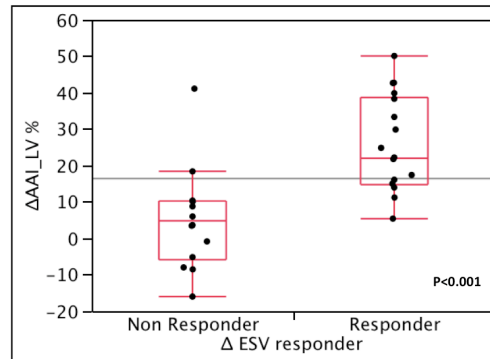


Percentage of change in LV-dP/dt<sub>max</sub> from AAI or RV baseline LV-dP/dt<sub>max</sub> for each individual patient at best (blue bar) and worst (red bar) LV lead position.

### **Response and Reverse Remodelling**

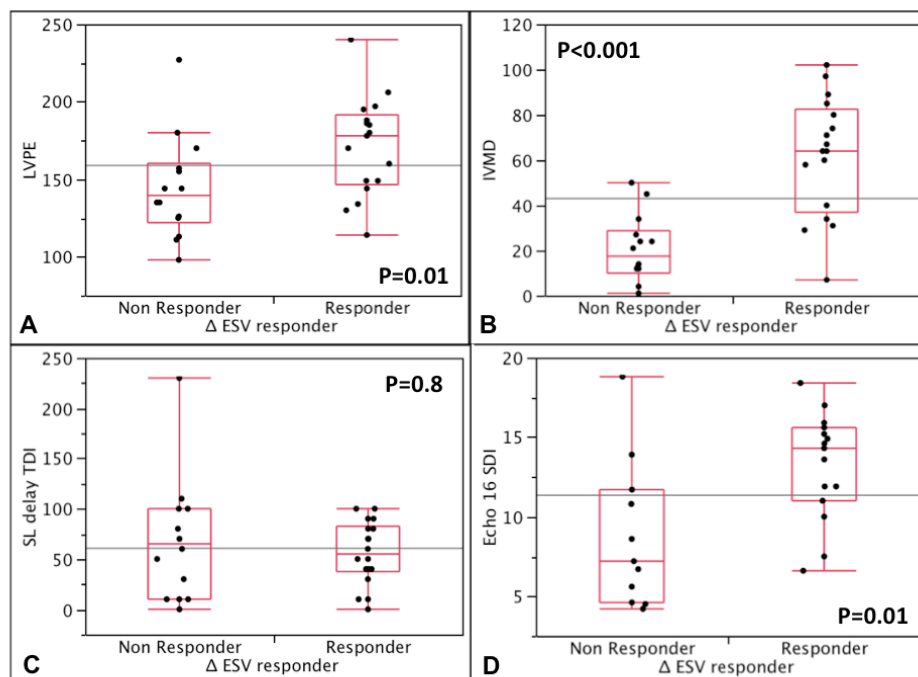
Pre-implant LV ESV and LV EF were  $185 \pm 67$  ml and  $24.8 \pm 8.0\%$  respectively. These improved over the follow-up period to  $157 \pm 69$  ml and  $32.8 \pm 9.7\%$ . This represented a 15% relative reduction in LV ESV and a 41% relative improvement in LV EF (both  $p < 0.001$ ). Eighteen (56%) patients RR. Percentage rise in  $dp/dt_{\max}$  with DDDL V pacing strongly predicted RR ( $P < 0.001$ ) (Figure 27), as did QRS duration ( $P < 0.001$ ). Using echocardiographic measure of dyssynchrony, LVPE, IVMD and SDI measured with 3D echocardiography were found to predict RR ( $P = 0.01$ ,  $P < 0.001$  and  $P = 0.01$  respectively). It should be noted that seven (21%) of the 3D echo data sets were not analyzable due to poor image quality. Septal-lateral delay with TDI showed no association with RR ( $P = 0.8$ ) (Figure 28).

**Figure 27** ANOVA plot showing the percentage change in LV-dP/dt<sub>max</sub> from baseline for DDD-LV pacing plotted against the presence or absence of RR.



AAI\_LV= %rise in LV-dP/dt<sub>max</sub> with DDDL V pacing from baseline AAI pacing.

**Figure 28** Shows the ANOVA plots for echocardiographic parameters of dyssynchrony to predict RR



**A** LV pre ejection period; **B** Interventricular mechanical delay; **C** Septal lateral delay measured with tissue Doppler imaging; **D** Systolic dyssynchrony index measured with 3D echocardiography.

A greater than 10% improvement in LV-dP/dt<sub>max</sub> from baseline with DDDL V pacing was more sensitive at predicting which patients were likely to RR than echocardiographic parameters (Table 16). Seventeen (77%) of the 22 patients that RR had a  $\geq 10\%$  rise in LV-dP/dt<sub>max</sub>, with only one patient that had a 10% rise in LV-dP/dt<sub>max</sub> not RR (sensitivity 0.94,  $P < 0.001$  compared with best echo parameter LVPE sensitivity 0.82,  $P = 0.06$ ). Receiver-operating characteristics (ROC) (Table 17) 11.1% rise in LV-dP/dt<sub>max</sub> from baseline had a sensitivity of 0.94 and specificity of 0.86 ( $P = 0.009$ ) to predict RR. This supports the use a 10% cut-off value to distinguish between responders and non-responders. A QRS duration cut off of 146ms was found to be good predictor of RR. With ROC analysis the only echocardiographic parameter of dyssynchrony that had comparable sensitivity and specificity was IVMD with a cut off of 29ms (sensitivity 0.94, specificity 0.79,  $P = 0.003$ ).

**Table 16** Sensitivity and Specificity for 10% rise in LV-dP/dt<sub>max</sub> for LV pacing as well as standard echocardiographic measures of dyssynchrony predicting RR

Assessment method	Cutoff	Total	n	%	Sensitivity	Specificity	P
	Met?						
<b>% rise LV dP/dt<sub>max</sub> ≥ 10%</b>	Yes	22	17	77	0.94	0.64	<0.001
<b>N=32</b>	No	10	1	10			
<b>LVPE ≥ 140ms</b>	Yes	21	14	67	0.82	0.5	0.06
<b>N=31</b>	No	10	3	30			
<b>IVMD ≥ 40ms</b>	Yes	15	13	86	0.76	0.86	<0.001
<b>N=31</b>	No	16	4	25			
<b>TDI Septal lateral ≥ 80ms</b>	Yes	8	4	50	0.22	0.71	0.7
<b>N=32</b>	No	24	14	56			
<b>SDI ≥ 10.3%</b>	Yes	16	12	75	0.8	0.64	0.02
<b>N=26</b>	No	10	3	30			

**Table 17** Sensitivity, Specificity and Area under the curve for RR

Assessment method	AUC	Cut-off	Sensitivity	Specificity
QRSD (ms) N=32	0.84	146	1	0.64
% rise LV dP/dt <sub>max</sub> N=32	0.89	11.1	0.94	0.86
LVPE (ms) N=31	0.75	160	0.65	0.79
IVMD (ms) N=31	0.91	29	0.94	0.79
TDI Septal lateral (ms) N=32	0.5	90	0.88	0.29
SDI (%) N=26	0.8	11.9	0.73	0.82

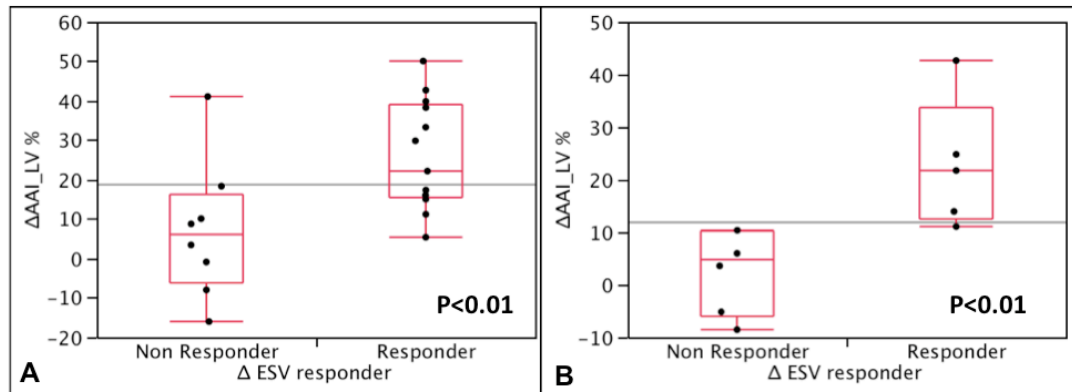
Table uses receiver-operating characteristics curve analysis to investigate whether changing the cut-off values used in table 16 could give a better prediction of improvement in ESV



### **Aetiology and Reverse Remodelling**

Differences between patients with DCM and ICM pre CRT are shown in table 18. Reverse remodeling occurred in 13 (61%) patients with DCM and five (45%) with ICM (Table 18). There was a trend towards patients with DCM having a greater percentage reduction in ESV ( $19\pm 21\%$  vs  $8\pm 28\%$ ) compared to ICM patients although this was non-significant. AHR predicted RR for both DCM and ICM patients ( $P=0.01$  and  $P=0.006$  respectively) (Figure 29). Similar QRS duration predicted RR, for both DCM and ICM patients ( $P=0.01$  and  $P=0.04$  respectively). For patients with DCM, SDI, ( $P=0.004$ ) and IVMD predicted RR ( $P=0.006$ ). For patients with ICM the only echocardiographic parameter that was useful for predicting RR was IVMD ( $P=0.006$ ).

**Figure 29** Shows the percentage rise in LV-dP/dt<sub>max</sub> from baseline with DDDL<sub>V</sub> pacing in patients with DCM (**A**) and ICM (**B**).



AAI\_LV = %rise in LV-dP/dt<sub>max</sub> with DDDL<sub>V</sub> pacing from baseline AAI pacing.

**Table 18** Differences in AHR and RR between DCM and ICM

<b>Pts</b>	<b>% decrease in ESV</b>	<b>≥ 15% decrease in ESV</b>	<b>AAI pacing</b>	<b>DDLV pacing</b>	
			<b>Mean</b>	<b>Mean</b>	<b>%</b>
			<b>dP/dt<sub>max</sub></b>	<b>dP/dt<sub>max</sub></b>	<b>change</b>
<b>All</b>	16±24	18 (56%)	798±197	910±188*	16±17
<b>N=32</b>					
<b>DCM</b>	19±21	13 (61%)	766±205	887±185*	19±18
<b>N=21</b>					
<b>ICM</b>	8±28	5 (45%)	857±173	953±193*	12±14
<b>N=11</b>					

\*Significant difference between AAI pacing (P<0.05)

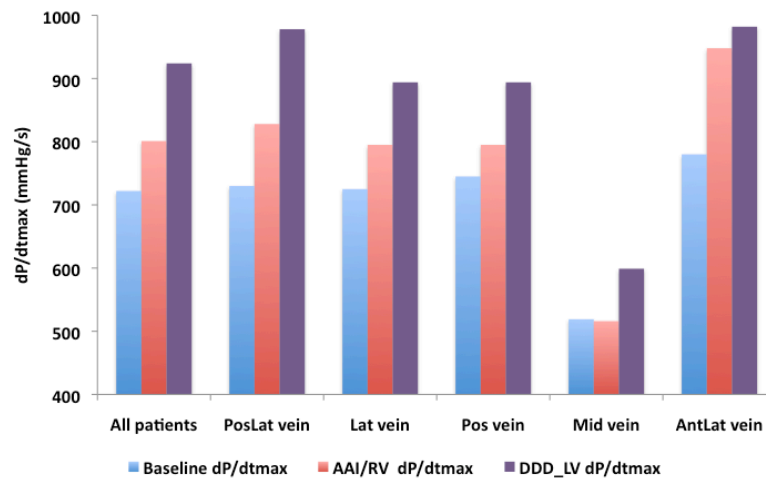
### Lead Position

With respect to LV lead position in 18 (54%) patients the largest rise in LV-dP/dt<sub>max</sub> was in a posterolateral vein (one patient had LV lead turned off due to diaphragmatic pacing and was therefore excluded from long-term follow up). Of these 11 (64%) reverse remodelled. In 11 (33%) patients the largest rise in LV-dP/dt<sub>max</sub> was in a lateral vein, and five (45%) of these RR. In two patients the largest rise in LV-dP/dt<sub>max</sub> was in a posterior vein with of these patients RR. In one patient the largest rise in LV-dP/dt<sub>max</sub> was in the middle cardiac vein, and the patient RR. In one the best position was the anterolateral vein, but the subject did not RR (Table 15, Figure 30 and 31).

### Clinical Response

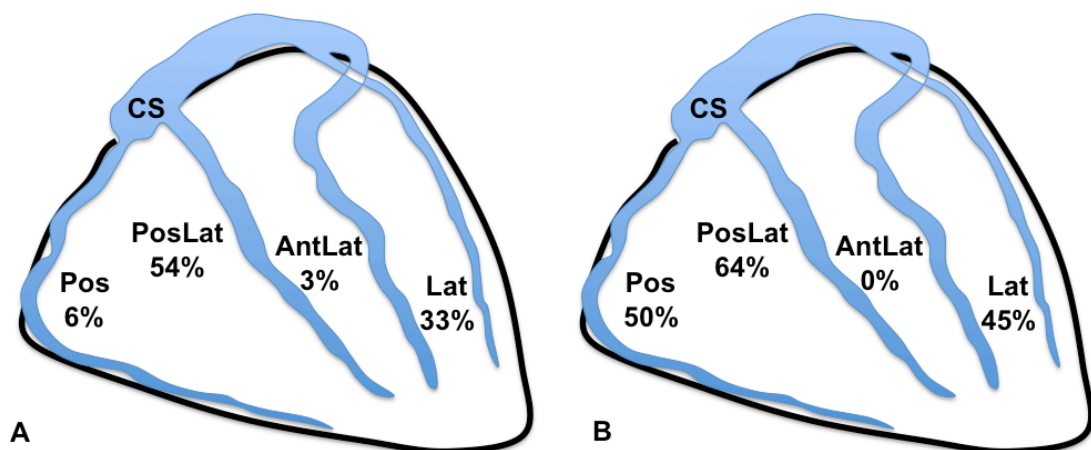
Twenty-nine (91%) patients improved by at least one NYHA class and 30 (94%) patients had a  $\geq 10\%$  reduction in quality-of-life score. There was a statistically significant relationship between percentage rise in LV-dP/dt<sub>max</sub> and improvement in NYHA score and 10% reduction in quality-of-life score ( $P=0.02$  for both). No relationship between QRS duration or echocardiographic measures of dyssynchrony and measures of clinical improvement were found.

**Figure 30** Comparison of LV-dP/dt<sub>max</sub> for intrinsic, AAI, DDDL V pacing for the different final LV lead positions.



PosLat=Posterolateral vein, Lat=Lateral vein, Pos=Posterior vein, Mid=Middle cardiac vein, AntLat=Anterolateral vein.

**Figure 31 A** shows the percentage of LV leads positioned in the branches of the coronary sinus. **B** shows the percentage of patients that remodelled.



The middle cardiac vein is not represented on this diagram

## Discussion

Using invasive acute haemodynamic response at the time of CRT implant this study shows:

- 1) There is a strong relationship between the magnitudes of rise in LV-dP/dt<sub>max</sub> from baseline for DDDL<sub>V</sub> pacing and RR.
- 2) For DDDL<sub>V</sub> pacing giving a  $\geq 10\%$  increase in LV-dP/dt<sub>max</sub> from baseline is a highly sensitive and specific predictor of RR which was under-pinned by the receiver operator characteristics giving a cut off of 11.1%.
- 3) The percentage rise in LV-dP/dt<sub>max</sub> for LV pacing is better at predicting RR than QRS duration greater or equal to 120ms and is at least as good as the best echocardiographic parameters of dyssynchrony (IVMD).
- 4) LV-dP/dt<sub>max</sub> varies significantly depending on site of LV lead positioning and maybe useful for guidance.

## Aetiology and Reverse Remodelling

More of the patients with DCM than with ICM reverse remodelled (61% vs 45%). There was a trend towards increased RR in DCM patients although this was not statistically significant. However the acute response appeared to be similarly predictive of RR in both groups. The fact that fewer ICM patients RR can be explained by the presence of myocardial scar, which may give rise to a more varied response to CRT. Nevertheless, the rise in LV-dP/dt<sub>max</sub> may reflect contractile reserve and therefore provides an indicator of how a patient is likely to respond<sup>137</sup> independent of aetiology. There was a good relationship between QRS duration and RR for both DCM and ICM patients. For echocardiographic

parameters of dyssynchrony only IVMD delay was found to be predictive of response in ICM patients. This underpins that  $\text{LV-dP/dt}_{\text{max}}$  may be particularly usefully in determining which ICM patients are likely to respond, as conventional methods are less helpful.

### **LV Pacing Site**

Although in the majority of patients the greatest percentage rise in  $\text{LV-dP/dt}_{\text{max}}$  was in a posterolateral or lateral lead position (88%), there were four patients (12%) where the optimum position based on the rise in  $\text{LV-dP/dt}_{\text{max}}$  was in either a posterior, middle or anterolateral vein. Of these four patients, 50% RR. Only one of these four patients had an ICM. This patient had extensive transmural inferior lateral scar, a lead was placed in the anterolateral vein and they showed a less than 10% increase in  $\text{LV-dP/dt}_{\text{max}}$  and did not RR. It is unlikely this patient would have RR due to position and extent of scar. Recent published data have demonstrated that pacing the site of latest mechanical activation was associated with a better long-term prognosis and RR at six months<sup>14</sup>. A further study<sup>34</sup> using an individually based approach showed that there was marked individual variation between patients and  $\text{LV-dP/dt}_{\text{max}}$  measured at different LV pacing sites and concluded that an individual based approach to pacing is possibly superior to empirical placement of the lead in a posterolateral or lateral vein. In this study epicardial pacing via the coronary sinus was used, which limits the potential targets (three patients had only one suitable vein). However I found, using a targeted approach with  $\text{LV-dP/dt}_{\text{max}}$ , that empirical implantation of the LV lead in a posterolateral or lateral vein does not always

produce the best AHR. It is interesting that in some positions LV lead placement was no better than AAI or RV pacing (Figure 25 & 26). This emphasises the importance of optimising the final site for the LV lead.

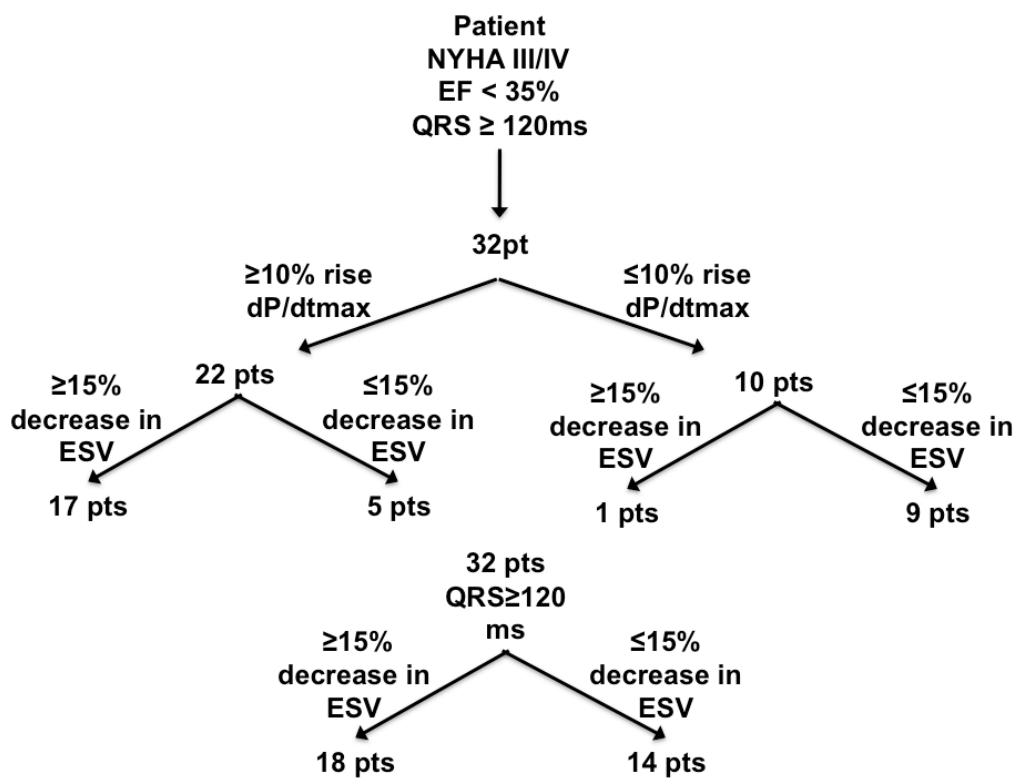
### **Role of LV-dP/dt<sub>max</sub>**

Patients were recruited on the basis of QRS duration  $\geq 120$ ms. On this basis, only 18 (56%) patients RR. For LV-dP/dt<sub>max</sub> 17 (94%) of the 18 patients that RR had a  $\geq 10\%$  rise in LV-dP/dt<sub>max</sub> and only one patient with a  $\geq 10\%$  rise in LV-dP/dt<sub>max</sub> did not RR (figure 32). The receiver operator analysis showed a QRS cut off of 146ms was a far more sensitive predictor of RR than 120ms. Of 10 patients with a QRS between 120-149ms only one RR, this patient did have a  $\geq 10\%$  rise in LV-dP/dt<sub>max</sub>. Although the numbers are small it is possible that LV-dP/dt<sub>max</sub> could be particularly useful in determining responders in this group as it would appear that if the QRS is  $< 150$ ms and there is a  $< 10\%$  rise in dP/dt<sub>max</sub> RR it is very unlikely to occur.

IVMD was nearly equivalent in its predictive value for RR as LV dP/dt<sub>max</sub>. When groups were separated into DCM and ICM, only IVMD was found to be predictive of RR for both aetiologies. No relationship for septal lateral delay and RR was seen. 3D Echo-derived SDI was predictive of RR overall and in DCM patients, but did not give superior discrimination compared to QRS duration alone and was not helpful in ICM patients. Furthermore seven (22%) data sets were not analyzable due to poor image quality.



**Figure 32** Breakdown of patients that RR that had  $\geq 10\%$  rise in LV-dP/dt<sub>max</sub>.



Assessment of LV-dP/dt<sub>max</sub> is highly invasive (requires arterial access) whereas conventional 2D echocardiographic assessment of dyssynchrony is not. However dp/dt<sub>max</sub> measurement is a more practical method to assess response during the procedure, whereas echocardiography would be more difficult. The real benefit of using both echocardiography and dP/dt<sub>max</sub> is complimentary - echocardiography should be used to predict pre-procedure who would respond, while dP/dt<sub>max</sub> should be used intra-procedure to identify best site for response.

### **Clinical Implications**

With respect to symptomatic response, 29 (91%) patients improved by at least one NYHA class and 30 (94%) patients had a  $\geq 10\%$  reduction in quality of life questionnaire score. There was a statistically significant relationship between percentage rise in LV-dP/dt<sub>max</sub> and improvement in quality of life questionnaire and NYHA score. For QRS duration and echocardiographic parameters no relationship was found. It has been shown that up to 28% of patients experience clinical response without significant LV RR.<sup>46</sup> It could be inferred that using LV-dP/dt<sub>max</sub> to guide LV lead placement leads to a high clinical responder rate. However, there are few clinical non-responders and a larger study is required to understand the relationship between rise in LV-dP/dt<sub>max</sub> and clinical response.

### **Study Limitations**

Due to the small number of ICM patients it is difficult to fully understand the relationship between rise in LV-dP/dt<sub>max</sub> and RR. I have been able to show that LV-dP/dt<sub>max</sub> is helpful at predicting RR in all patients undergoing CRT and

although I have shown that rise in  $\text{LV-dP/dt}_{\text{max}}$  seems to be helpful in predicting response in DCM and ICM patients greater numbers are required to fully understand this relationship. The high clinical responder rate means that this study is underpowered to determine if  $\text{LV-dP/dt}_{\text{max}}$  can predict which patients are likely to improve symptomatically.

To keep the pacing protocol simple DDDL<sub>V</sub> pacing was used to determine the LV lead position rather than BIV pacing. It could be argued that determining the LV lead position with DDD<sub>BIV</sub> pacing would be superior as this would be more comparable to a normal resynchronisation pacing strategy, but using DDDL<sub>V</sub> pacing was the only option to ensure steady rate for accurate haemodynamic measurements throughout the study. Also, previous studies have demonstrated the non-inferiority of DDDL<sub>V</sub> pacing compared to DDD<sub>BIV</sub> pacing<sup>35, 37, 138</sup>. We are aware that further studies are required with the LV lead position optimised with BIV pacing to see if there are differences in final lead placement and if this changes the long term outcome although a protocol optimising every lead position with BIV pacing would run the risk of having unfeasible procedure times.

The absence of a control group is a major limitation. Our results do, however, highlight the potential of  $\text{LV-dP/dt}_{\text{max}}$  to guide LV lead placement and improve response rates. This study emphasises the need for a randomised control study of a guided versus conventional approach to CRT.

## Conclusions

I have shown that rise in LV-dP/dt<sub>max</sub> from baseline AAI or RV pacing to guide LV lead position is helpful in predicting which patients are likely to reverse remodel following CRT. Using a 10% rise in LV-dP/dt<sub>max</sub> is superior to QRS duration and at least as good as the best echocardiographic parameters at selecting which patients are likely to reverse remodel both for DCM and ICM patients. This work supports the use of LV-dP/dt<sub>max</sub> to aid in lead placement and this may improve the responder rates in CRT with respect to determining which patients will reverse remodel.

It is logical that rise in LV-dP/dt<sub>max</sub> during LV pacing at the time of CRT implant should help predict which patients are likely to reverse remodel. The energy which is wasted as a result of LV dyssynchrony, may be “harnessed” by LV pacing in order to improve cardiac function. Measuring the LV-dP/dt<sub>max</sub> rise at implant potentially is a marker of how much the cardiac function can be improved during CRT and therefore the likelihood of long term reverse remodeling. Clearly this is a small study and a prospective randomised controlled study will be needed to confirm a favourable effect of LV-dP/dt<sub>max</sub> guided therapy on prognosis and functional status after CRT in the future.

## Chapter 5

### Relationship Between Myocardial Electrical Activation and Motion in Helping to Understand Response to CRT

#### Introduction

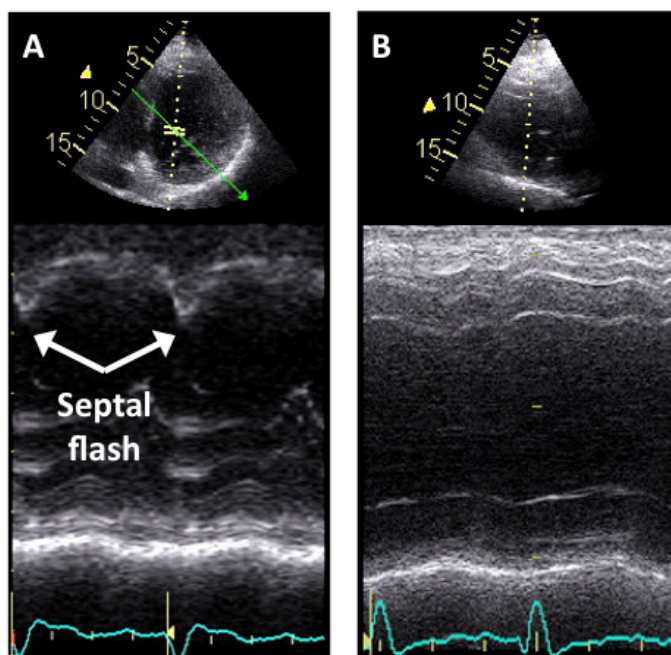
What follows is a brief discussion about LV dyssynchrony and the methodology, results and discussion for work investigating the relationship between myocardial motion and electrical activation of the LV.

A recent study <sup>59</sup> hypothesised that response to CRT is governed by multiple independent mechanisms. One of these was true LV intra-ventricular dyssynchrony, characterised by an early septal contraction and inward motion, stretching the lateral wall, immediately followed by a septal lengthening while the lateral wall starts to contract. This fast inward and outward motion of the septum is within the isovolumic contraction time (between the onset of the QRS complex and aortic-valve opening (AVO)) and is referred to as a *septal flash* (SF). Elimination of the SF results in significant RR and good response to CRT. <sup>59</sup> Groups have reported this abnormal septal motion as a pathophysiological mechanism underlying heart failure in patients with LBBB. <sup>139-142</sup> In these studies, septal abnormalities are associated with abnormal stretching of (non-ischemic) tissues, where LBBB induced anterior and inferior wall stretching

extending towards the lateral wall. <sup>139</sup> Similar findings were reported in the presence of ventricular pacing. <sup>143</sup>

The presence of a SF is visualised on echocardiography in all views showing the septum (short axis (SAX), parasternal long axis (PLAX) and apical four chamber (4CH) views) and can be appreciated using either (slowed down) grey scale or (anatomical) M-mode (Figure 33).

**Figure 33** **1A** Grey scale M-mode image of a patient with a large SF. Septum is seen to have early and fast thickening and thinning. **1B** Patient with no SF.



Non-contact mapping (NCM) has been used in several human studies to characterize the LV endocardial activation pattern <sup>144</sup> in patients with heart failure and intra-ventricular conduction delay. These studies showed the presence of functional lines of block in patients with LBBB, often with the pattern of activation taking a “U-shape” around the area of slow conduction. <sup>53, 145</sup> This “U-shaped” activation wave front was the result of the presence of a line of block that was located anteriorly (about 50% of cases), laterally or inferiorly. <sup>53</sup> Previous work in our institution demonstrated that NCM can identify regions of slow conduction and that LV pacing outside these areas leads to significant hemodynamic improvement. <sup>56</sup>

Mechanical deformation changes the electrical properties of myocardial tissues, <sup>146</sup> with stretching of myocytes decreasing their conductivity. <sup>147</sup> Computer models have shown that electro-mechanical interaction may play a role in LBBB. <sup>148</sup> These concepts have yet to be translated into the clinical arena. Given that in a subset of CRT candidates the SF is present during the LV activation period and that there is evidence for electro-mechanical interaction at the myocyte level, it is hypothesised that evidence of direct electro-mechanical interaction might be present in CRT candidates showing a SF. Conversely this would not be the case in the absence of a SF. Furthermore it would be anticipated that the effects of electro-mechanical interaction would change with LV pacing.

In this study I characterised the electrical activation and mechanical action of the LV during the activation period by directly comparing NCM and echocardiography imaging in patients prior to CRT.

## **Methods**

### **Study Population**

Patients with severe heart failure fulfilling standard criteria for CRT (NYHA class III-IV drug refractory heart failure, LVEF  $\leq 35\%$ , LV end-diastolic diameter  $\geq 55\text{mm}$ ) and with LBBB on ECG (QRS duration of  $> 120\text{ms}$  with QS or RS complex in lead V1 and a monophasic R wave in leads V1 and V6).

### **Echocardiographic Acquisition**

Prior to NCM, standard echocardiograms with tissue Doppler imaging (TDI), were acquired on a GE vivid 7 scanner (General Electric-Vingmed, Milwaukee, Wisconsin). Analysis was performed using EchoPac version 6.0.1 (General Electric-Vingmed).

Ejection fraction and LV dimensions were measured using 2D modified biplane Simpson's method. Transmitral flow velocities were obtained from the apical-4CH view with pulsed-wave Doppler positioned at the tip of the leaflets. End diastole (onset of isovolumic contraction) and end systole (aortic valve closure) were determined using transmitral and aortic Doppler profiles.



### **Assessment of Dyssynchrony and Septal Flash**

Echocardiography assessment of dyssynchrony has been described in chapter 3.

To determine the presence and extent of the SF, two independent clinical experts, who were blinded to the electrophysiology studies, reviewed all echocardiographic images. The existence of a SF was defined as the presence of early inward and outward motion within the isovolumic contraction period seen both visually from the grey scale SAX and 4CH views as well as on M-mode in the PSLAX, SAX and 4CH. Bull's eye plots of the LV were generated, indicating the presence and spatial extent (segments involved) of the SF. Patients were categorised according to the appearance and extent of the SF: a large SF if there was marked fast early septal inward/outward motion with a prominent displacement involving  $\geq 50\%$  of the septal segments in an American heart association (AHA) model; a small SF if there was early inward/outward motion, but with a very limited displacement; or no SF present.

### **CMR Imaging**

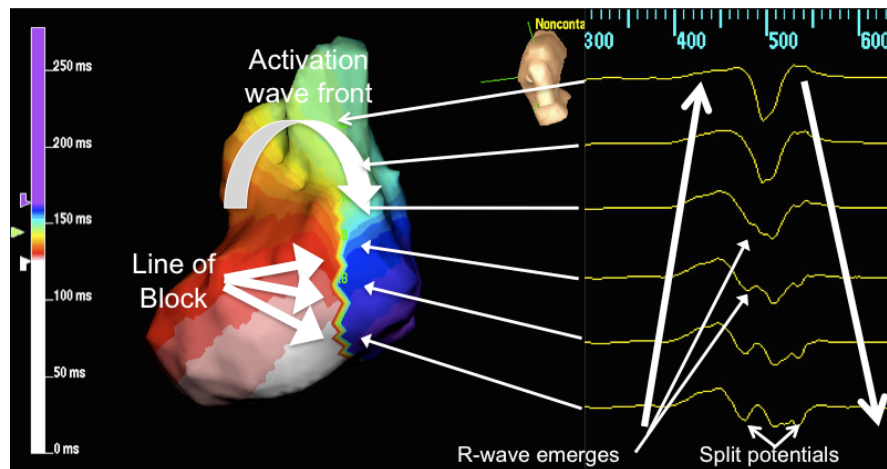
CMR delayed gadolinium enhancement imaging was performed to assess myocardial scar. CMR was performed on a Philips Achieva 1.5T scanner (Philips, Healthcare, Best, The Netherlands). DE-MR was performed 15-20mins following the administration of 0.1-0.2mmol/kg gadopentetate dimeglumine (Magnevist®, Bayer Healthcare, Dublin, Ireland) using conventional inversion recovery techniques.<sup>149</sup>

### **Non-contact Mapping Procedure**

Patients underwent NCM  $11 \pm 8.6$  days prior to CRT implant in our interventional X-ray/MRI catheter laboratory (Philips Medical Systems, Best, Netherlands). Bilateral femoral venous access was used to place 5F Supreme JSN 401443 quadripolar electrode catheters (St. Jude Medical, Minnetonka, MN, USA) to the high right atrium and right ventricular apex to perform atrial and RV ventricular sensing and pacing, a 5F Supreme CRD-2 401860 quadripolar electrode catheter (St. Jude Medical, Minnetonka, MN, USA) was positioned at the His bundle. The coronary sinus was intubated using a pre-shaped 8F Fast-Cath SL3 406842 guiding sheath (St. Jude Medical, Minnetonka, MN, USA) and a multipolar Pathfinder 16 electrode catheter 01-16-1003 (Cardima Inc., Fremont, CA, USA) was passed to a postero-lateral or lateral branch of the coronary sinus to perform epicardial LV pacing to replicate standard CRT. A NCM Ensite Array EC1000 (St. Jude Medical, St Paul, MN, USA) was passed via the femoral artery retrogradely across the aortic valve to the LV cavity. Via the other femoral artery, a decapolar steerable 6F Livewire 401915 electrode catheter (St. Jude Medical, Minnetonka, MN, USA) was passed to the LV cavity along with a high fidelity pressure wire (Radi Medical Systems, Uppsala, Sweden) with a 5-Fr multipurpose catheter. The chamber geometry was reconstructed using a locator signal from the decapolar catheter.<sup>150</sup>

The following pacing protocol was performed; (100 beats per minute with consistent capture, AV delay 100ms, VV simultaneous): AAI (atrium sensed and paced), DDDR<sub>V</sub> (atrium and ventricle sensed and paced from RV), DDDL<sub>V</sub> (atrium and ventricle sensed and paced from coronary sinus) and DDBIV

(conventional CRT). AAI pacing at 100 beats per minute was used as baseline for assessment of LV-dP/dt<sub>max</sub> measurements and was performed prior to each change in pacing mode.<sup>34</sup> Ensite data, pacing parameters and percentage rise in LV-dP/dt<sub>max</sub> for each pacing mode were recorded once steady state pacing had been achieved for at least one minute. Capture without fusion was confirmed using VVI pacing and examining the paced QRS morphology. Endocardial maps were obtained in sinus rhythm and in each pacing configuration. Electrograms were acquired at 1200Hz, giving a temporal resolution of 0.83ms. High pass filter was set at 8Hz. Virtual unipolar electrograms recorded from the endocardial surface were analysed to measure the duration of LV activation. Peak negative dV/dt is a universally accepted indicator of the onset of activation in a region of myocardium. Thus the onset of activation was taken as the time to the first peak negative 8 Hz high-passed unipolar virtual electrogram anywhere in the chamber. The end of LV activation was defined as the time of the latest peak negative 8 Hz unipolar electrogram on the virtual endocardial surface.<sup>151</sup> QRS duration was obtained from the surface 12 lead ECG. Lines of block were interpreted from both the patterns of activation observed in isopotential maps and the associated morphological features of electrograms (Figure 34).

**Figure 34** Patient with a large SF

Unipolar isochronal map with NCM electrograms showing fragmented signals (development of split potentials) indicating a reduction of conduction and inability to cross throughout the inferior region. The NCM mapping electrograms show the criteria used by Auricchio et al to define block, with the emergence of R-wave, smallest and earliest at the superior part of the block (where area of block begins) with largest negative peak. Bold white arrows on the electrogram indicate how the electrical activation spreads superiorly in a U-shape pattern leading to the development of split potentials.

Bull's eye activation maps were generated from the NCM data sets by computing the long axis from the manual identification of the ventricular apex and the centre of the mitral valve in at least two views. I estimated the short axis by identifying the ventricular septum, and lateral wall and drawing a perpendicular line through the long axis. From this information, temporal bull's eye plots were constructed representing the percentage of activated tissue (black in the figures) through time. In parallel, bull's eye plots were generated of the presence and

location of mechanical septal motion visually identified with echocardiography as well as the position and extent of scar determined by DE-MR imaging. These visualisation tools allowed a multimodal analysis and integration to directly compare different factors involved in the studied pathophysiology, mainly mechanical septal motion, presence and location of scar and presence and location of lines of conduction blocks. Lines of conduction block are areas of tissue where propagation of the activation wave front is halted for several tens of milliseconds. This is visualised as a stagnation of the black-white transition during several frames in the series of bull's eyes plots (Figure 35). Acute haemodynamic responders were considered as an increase in  $LV-dP/dt_{max}$  of  $\geq 10\%$  from baseline AAI pacing.<sup>37</sup> Patients were followed up six months after CRT with a repeat echocardiogram.

### **Statistical Analysis**

Statistical analysis was performed using SPSS software package (IBM, Chicago, IL, USA). Continuous variables were expressed as mean values  $\pm$  SD. Where appropriate continuous variable were assessed with a Student's t test and 1-way ANOVA. P values of  $< 0.05$  were considered statistically significant.

### **Results**

Thirteen patients were recruited (aged  $63 \pm 10$  years, ten males and three females). At baseline all were in NYHA class 3, with LBBB (QRS duration of  $158 \pm 24$ ms). Eight patients had DCM and five ICM. Ejection fraction  $22.8 \pm 5.8\%$ ,

inter ventricular delay  $47.8 \pm 23.6$ ms, septal-lateral delay from TDI  $79.2 \pm 40.3$ ms and SD of 12 segments TDI  $50.2 \pm 13.5$ ms (Table 19).

**Table 19** Comparison of patients with varying size of SF

	All patients	Large SF	Small SF	Absent SF
<b>Number</b>	13	5	4	4
<b>Age</b>	63±10	66±7	57±13	67±12
<b>Sex</b>	10 M:3 F	4 M:1F	4 M	2 M:2F
<b>Etiology of HF</b>	8 DCM	4 DCM	1 DCM	3 DCM
	5 ICM	1 ICM	3 ICM	1 ICM
<b>QRS duration (ms)</b>	158±24	172±25*	156±18	143±21
<b>Ejection fraction (%)</b>	23±6	22±7	23±4	24±8
<b>EDV (ml)</b>	255±67	270±66	248±89	245±62
<b>ESV (ml)</b>	198±59	211±65	196±83	185±30
<b>IVMD (ms)</b>	48±24	69±14*	41±17	22±29
<b>Septal/lateral delay TDI (ms)</b>	79±40	56±53	83±22	105±21
<b>TDI 12 segment SD (ms)</b>	50±14	51±16	47±14	52±13
<b>TIVT (ms)</b>	186±128	304±72*	222±57	125±72
<b>IVCT (ms)</b>	68±63	133±29	59±55	38±49
<b>IVRT (ms)</b>	118±88	171±68*	163±81	89±41

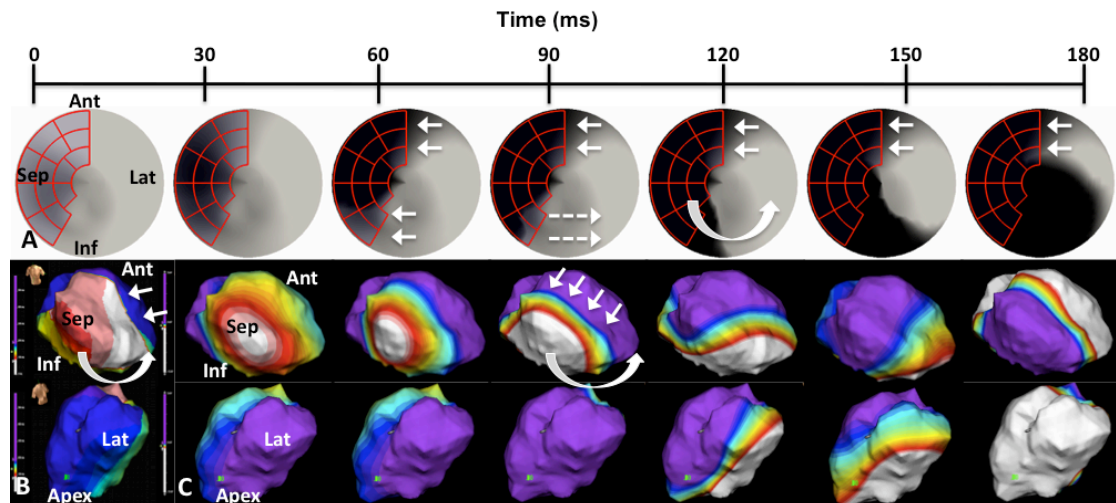
\*Significant difference between patients with a large SF and small/absent SF

(P<0.05)

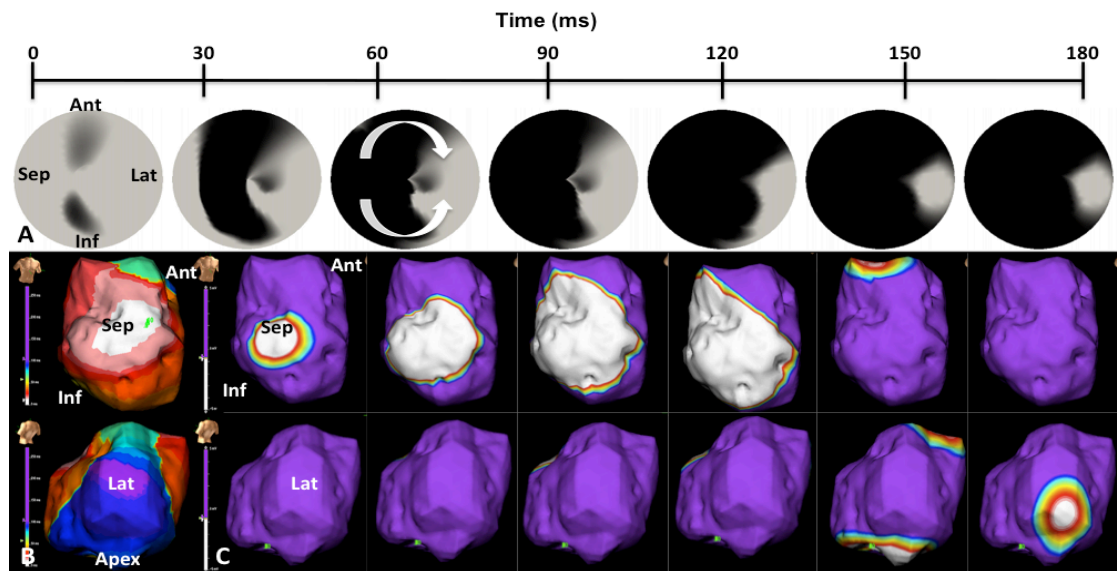
### **Baseline Analysis**

Five patients had a large SF, four small SF and four no SF (Table 19). Figures 35 and 36 shows the comparison of the NCM and echo bull's eye plots from a typical patient with or without a SF. While the activation spreads homogenously over the endocardial surface when no SF is present, there are definite areas of conduction block surrounding the region of the large SF (Fig 35). A very specific pattern of conduction slowing is present in the large SF cases. After the initial activation of a small septal region, there is a delay of further activation during 2-3 frames on the ensite activation map corresponding to 20-40 ms. Next, the activation continues either anteriorly or inferiorly (Fig 35) and the opposite area (inferior or anterior (Fig 35) respectively) remains blocked until it is activated retrogradely. The persistence of one part of the initial conduction block results in an overall U-shaped activation with a persistent line of block in either the anterior or inferior region. In patients with a small or no SF there was no conduction block (Figure 36) except in one of the patients with a small SF and an ICM where there was an area of block associated with anterior-lateral scar. Figures 37 to 39 show activation maps for all patients.



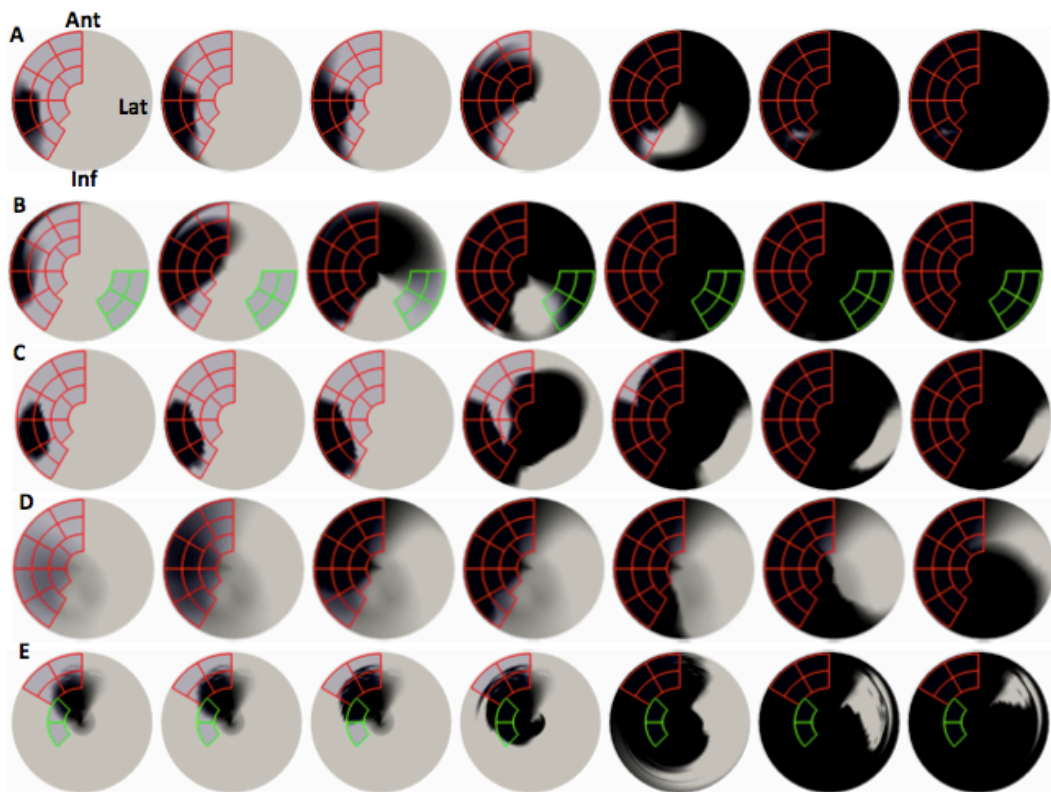
**Figure 35** Patient with a large SF

**A** Fused activation and echo bull's eye plots. Black area indicates activation pattern, red segments area with SF. There is initial depolarisation of the ventricular septum, followed by slowed conduction (20 to 40ms) both anteriorly and inferiorly. Areas of block indicated with white arrows. There is breakout of activation inferiorly although slowed depicted by the dashed arrows. Block remains anteriorly. Activation continues inferiorly until the anterior wall is retrogradely activated. **B** Unipolar isochronal map. **Top row anterior: Bottom row posterior.** There is a line of anterior block with activation spreading inferiorly. **C** LV NCM unipolar activation map. The activation breaks out in the ventricular septum, instead of spreading uniformly there is an anterior line of block shown by white arrows. The activation spreads inferiorly, leading to a U-shaped activation pattern. Ant=Anterior, Sep=Septum, Inf=Inferior, Lat=Lateral.

**Figure 36** Patient with no SF

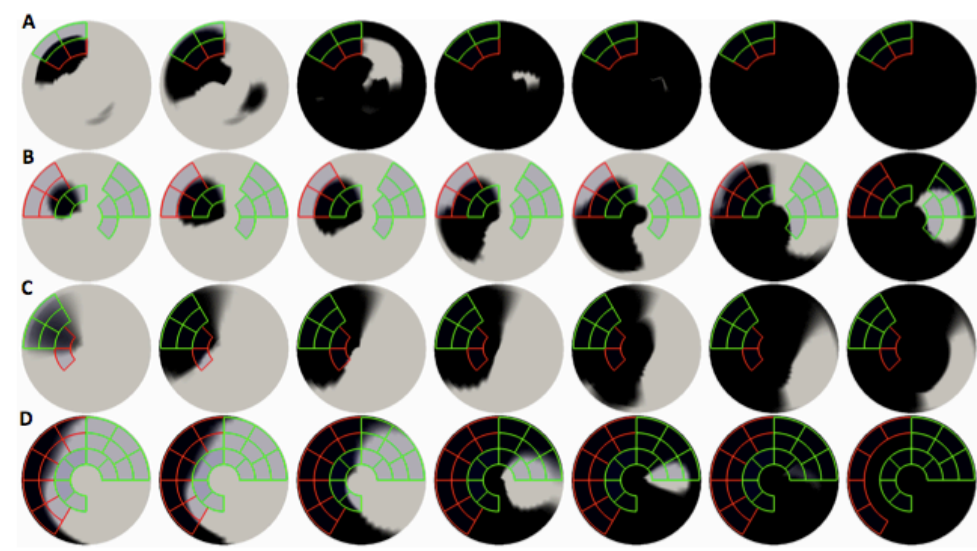
**A** Fused activation and echo bull's eye plots. There is uniform activation both anterior and inferiorly with no block. **B** Unipolar isochronal map. **Top row anterior: Bottom row posterior.** Uniform activation with no block. **C** LV NCM unipolar activation map. The activation breaks out in the ventricular septum, and spreads uniformly with no areas of block.

**Figure 37** Activation maps for all patients with a large SF



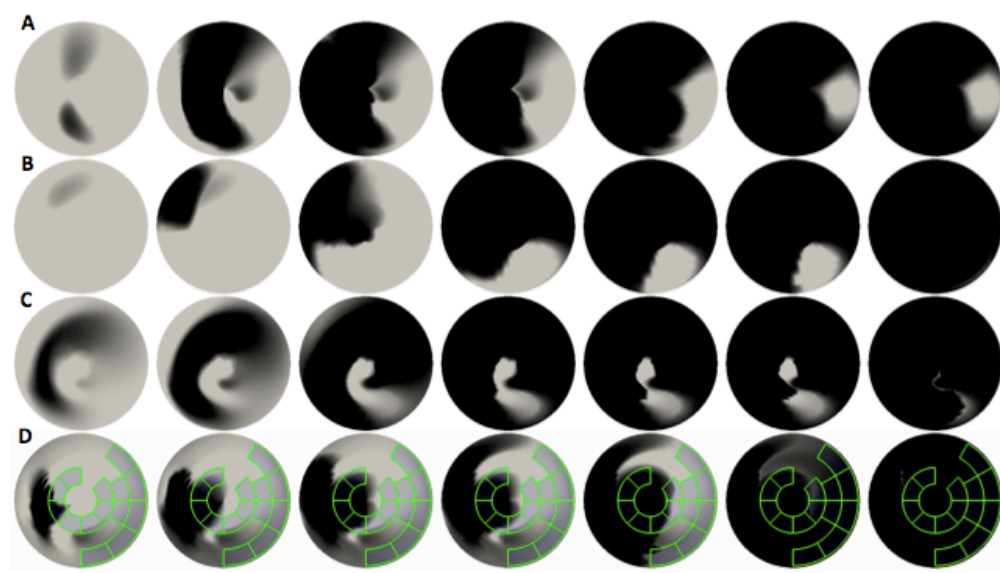
In all patients, early breakthrough is seen in the septum there is then slowing and even halting of activation at the borders of the SF (3 patients inferior block, **A**, **B** & **C**, 2 patients anterior block, **D** & **E**). This is followed by a period of no further activation (lasting about half of the total activation time). Next, a further breakthrough of the activation is observed, either from the anterior or inferior side of the SF propagating homogeneously over the rest of the LV. Row **B** shows a patient with an ICM with the area of scar shown by the green gridded area. The other rows are all patients with DCM. Ant=Anterior, Inf=Inferior, Lat=Lateral.

**Figure 38** Activation maps for all the patients with a small SF



There is no area of block seen except in **B** where there is an area of block associated with scar seen by the green grid. Rows **B**, **C** and **D** are patients with ICM with the scar depicted with the gridded area. Row **A** is a patient with a DCM.

**Figure 39** Activation maps for all the patients with no SF

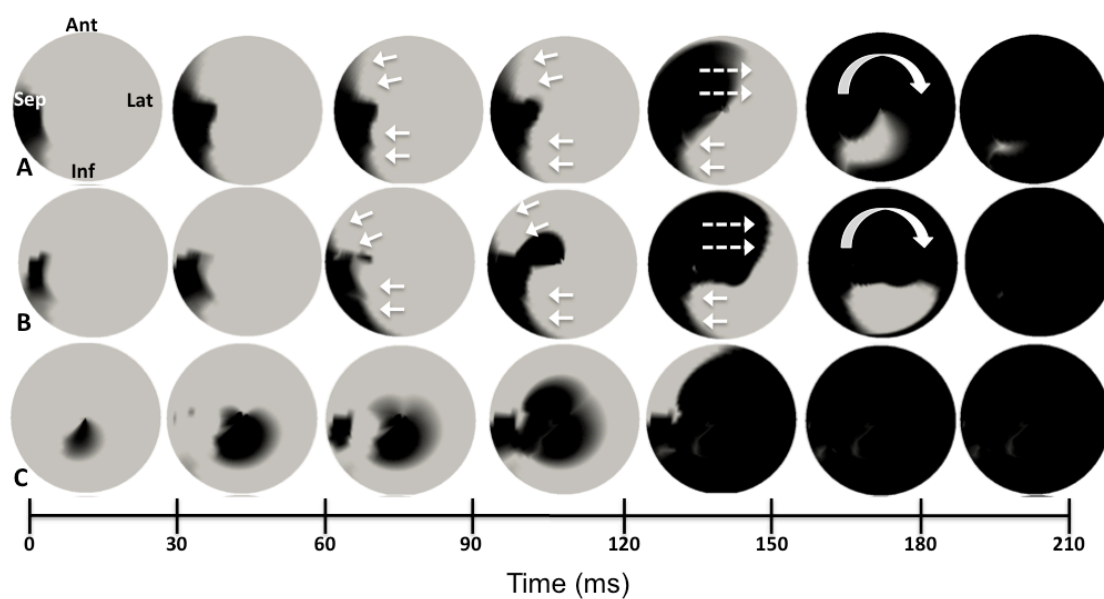


Row **D**, patient with an ICM with extensive myocardial scar as depicted by the green gridded area. Other rows show patients with DCM.

### Influence of BIV and RV Pacing

Patients with a large SF the conduction block was seen to disappear with BIV pacing, but remained with RV pacing (Figure 40).

**Figure 40** Activation maps of patient with a large SF



Row **A**, baseline with area of block and late anterior breakthrough. Row **B**, RV pacing showing the area of anterior block remains. Row **C**, BIV pacing. Functional conduction block has disappeared.

### **Acute Haemodynamic Response**

Overall there was a significant increase in acute response to both DDDL V and DDDDBIV pacing (baseline AAI pacing LV-dp/dt<sub>max</sub> 782±214mmHg/s, DDDL V pacing 916±219mmHg/s (p<0.05) and DDDDBIV pacing 998±254mmHg/s (p<0.05)). Comparing percentage rise in LV dP/dt<sub>max</sub> from baseline for both DDDL V and DDDDBIV pacing patients with a large SF had a larger response than patients with a small or no SF (Table 20). Using a cut off of 10% rise in LV dP/dt<sub>max</sub> from baseline all patients with a large SF were acute haemodynamic responders for DDDL V and DDDDBIV pacing. One patient with a small SF did not respond to DDDL V pacing and two did not respond to DDDDBIV pacing. No patients without a SF responded to LV pacing and one did not respond to BIV pacing.

**Table 20** Acute haemodynamic response with different pacing modes

	<b>AAI</b>	<b>DDDLV</b>	<b>%</b>	<b>DDDBIV</b>	<b>%</b>
	<b>Baseline</b>	<b>pacing</b>	<b>Increase</b>	<b>pacing</b>	<b>Increase</b>
	dP/dt <sub>max</sub>	dP/dt <sub>max</sub>		dP/dt <sub>max</sub>	
<b>All</b>	782±214	915±219*	20±18	998±254*	31±24
<b>patients</b>					
<b>Large SF</b>	828±240	1038±229*	28±14	1141±256*	42±28
<b>Small SF</b>	713±216	876±182*	25±14	835±141	21±22
<b>No SF</b>	880±112	856±179	-4±9	1063±152	22±24
<b>Combined</b>	797±179	866±161	11±19	949±181*	22±21
<b>small &amp; no</b>					
<b>SF</b>					

\*Significant difference from AAI pacing (p<0.05)

**Clinical Response and Reverse Remodelling (Table 24)**

At six months one patient with no SF had died. All except one patient (small SF) improved by at least one NYHA class (responder rate 92%, ( $P<0.05$ )). The SF was no longer present after CRT. With respect to RR (decrease in ESV  $\geq 15\%$ ) the overall responder rate was 64% (average decrease in ESV  $19.8\pm 21.4\%$ , ( $P<0.05$ )). All patients with a large SF RR (decrease in ESV  $37.1\pm 21.2\%$ ), two patients RR with a small SF (decrease in ESV  $11.5\pm 7.4\%$ ) and none with no SF (decrease in ESV  $1.9\pm 13.7\%$ ). (Table 21) Comparing large SF to small or no SF there was a greater improvement in EF, larger reduction in ESV and NYHA score.



**Table 21** NYHA class and echocardiographic parameters pre and post CRT

	All patients		Large SF		Small SF		Absent SF	
	N=13		N=5		N=4		N=3†	
	Pre CRT	Post CRT	Pre CRT	Post CRT	Pre CRT	Post CRT	Pre CRT	Post CRT
<b>NYHA class</b>	3±0	1.6±0.8*	3±0	1.0±0.7	3±0	2.3±0.5	3±0	1.7±0.6
<b>EF (%)</b>	23±6	32±11*	22±7	37±13	23±4	31±5	24±8	23±7
<b>EDV (ml)</b>	256±67	228±71*	270±66	211±83	248±89	245±83	245±62	231±16
<b>ESV (ml)</b>	198±59	158±56*	211±65	137±61	196±83	171±69	185±30	175±7
<b>TIVT(ms)</b>	186±128	147±107	304±72	173±61	222±57	144±98	127±72	139±120
<b>IVCT(ms)</b>	68±63	48±47	171±68	33±19	59±55	53±37	38±49	64±62
<b>IVRT(ms)</b>	118±88	99±74	133±29	140±65	163±81	91±63	89±41	74±69

\*Significant difference from pre CRT measurements

†One patient died

## Discussion

Comparing mechanical events with intra-cardiac electrical activation, I have demonstrated that in the presence of a large SF, there is a spatially related functional conduction block resulting in a U-shaped activation. With LV or BIV pacing there is restoration of a more normal pattern of electrical activation without areas of slow conduction, which was associated with disappearance of the SF. Patients without a prominent SF did not show an abnormal electrical activation pattern. These results suggest for the first time, in a clinical setting, that there is a direct electro-mechanical interaction at the macroscopic level during the activation period of the LV in a subset of patients with LBBB.

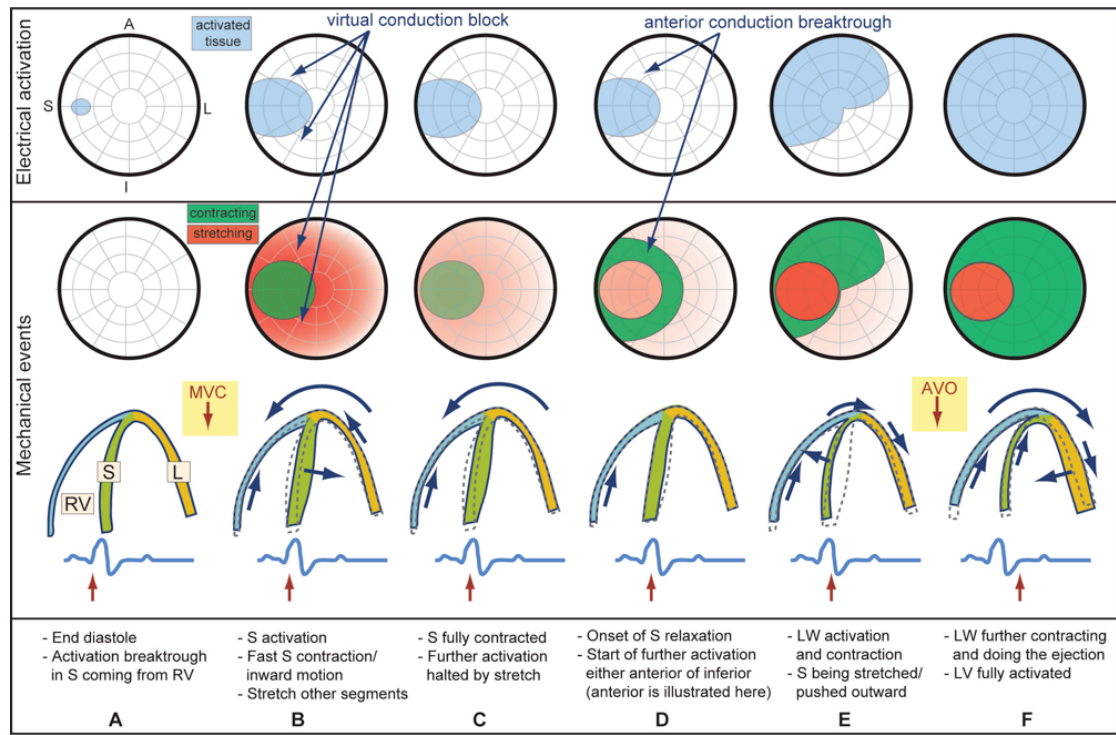
Figure 41 summarises this hypothesis with regard to the electrical activation, mechanical events, and their interaction, in patients with LBBB and a SF. Shortly after the onset of the activation (breaking trough at the mid/basal septum, coming from the right side) (Fig 41 A), the fast and large contraction of the septum during the initial phase of the SF (Fig 41 B) leads to mechanical stretching of the surrounding tissues, thus changing its conductivity and slowing down or halting further activation. When activation slowly surpasses the stretched region (around half of the total activation time, while only a limited area of the LV is activated at this point), either anterior or inferior of the SF region (Fig 41 C/D), it rapidly conducts further over the LV endocardium, activating the rest of the ventricle and initiating mechanical activity in the free

walls, which start to contract and exhibit force on the contracted septum, which in its turn is stretched, resulting in the outward/lengthening portion of the SF. (Fig 41 E/F).

As a result, total activation time is long (QRS width in large SF patients is the longest), the isovolumic contraction period is long, since during the SF period, septal contraction is used for stretching surrounding tissue and the first mechanical activity of the free walls for stretching the septum. During this period, all mechanical energy is used for stretching tissue instead of building up pressure (very low LV  $dP/dt_{max}$  in SF patients while the tissue does show substantial mechanical activity) and aortic valve opening is very late.

While RV pacing does not change the activation pattern within the LV (breakthrough of activation and the pattern of propagation, including the presence of the SF, remain the same), both LV and BIV pacing induce an additional activation wave front initiation within the LV and preventing the septum from stretching the surrounding region and changing its conductivity. As a result, the whole ventricle is activated faster, there is no longer detrimental mechanical interaction between the opposing free wall and the IVT is markedly reduced.

**Figure 41** Electrical activation and associated mechanical events in patients with LBBB and a *Septal Flash*



A=anterior wall, AVO=Aortic valve opening, I=Inferior wall, L=lateral wall, MVC=mitral valve closure, RV=Right ventricle, S=Septum.

The area of the induced functional conduction block corresponds very closely to the borders of the area observed to be involved in the SF. The consequent progression of activation, which seems in about half of the patients anteriorly and in the other half inferiorly, results in the previously described U shaped activation pattern.

### **LBBB: Measures of Dyssynchrony and the Septal Flash**

All patients had LBBB, however the presence of large SF was only seen in five. LBBB is a complex electrical disease resulting from conduction delay located at several anatomical levels of the activation sequence.<sup>53</sup> The group with a large SF seemed to have a predisposition to a longer QRS duration (large SF,  $172.4 \pm 25.0$ ms, small SF,  $155.5 \pm 18.0$ ms, no SF,  $142.8 \pm 21.0$ ms), however it is known that surface ECG recordings are unable to characterize the location and extent of specific ventricular delays.<sup>54</sup>

Looking at inter-ventricular dyssynchrony, patients with a large SF have a larger delay (large SF,  $69 \pm 13.9$ ms, small SF,  $40.5 \pm 17.2$ ms, no SF,  $21.8 \pm 29.1$ ms). This fits the hypothesis that the presence of the SF results in a much longer TIVT and IVCT in the LV, which is confirmed by our findings, while the RV is activated almost normally. Previously reported parameters to describe intra-ventricular dyssynchrony, the septal/lateral delay show the opposite. Patients with a large SF appear less dyssynchronous. This is possibly due to the measurement method. Firstly, the peak velocity in patients with a SF is often outside the ejection period (AVO/AVC) and therefore excluded from the measurements. Secondly, since the

SF induces stretching/unstretching of the different segments of the LV, this is not necessarily reflected in the velocity of the basal segments. When a 12-segment standard deviation is used there does not appear to be any difference between the groups, again emphasizing that measurement based on velocities might not be the appropriate way to assess the intra ventricular dyssynchrony. A recent multicenter trial, showed that velocity based parameters was no better than the QRS duration in predicting response to CRT.<sup>103</sup>

### **Clinical Implications for CRT**

In previous studies<sup>59</sup> the correction of the SF by CRT has been shown to be associated with significant RR. This study has shown in patients with a large SF that CRT improves the mechanical inefficiency resulting from the stretching/unstretching of tissue as well as inducing more homogeneous and faster activation. By showing that a LV lead corrects the conduction abnormality leading to a more normal electro-mechanical interaction this may explain the high response rates.

### **Study Limitations**

Although this study shows a spatio-temporal relation between the presence and extent of the SF and the changes in conduction pattern of the myocardium, I can only hypothesise with respect to their causal relationship. Given that there is much evidence from basic science on the existence of electro-mechanical interaction, that is consistent with this hypothesis, and the observation from the changes induced by LV and BIV pacing, it is a possible explanation of the findings.

Given the invasive and complex nature of these clinical measurements, the study has a small number of patients with only five having a large SF. There are definite trends that patients with a large SF have a greater acute response to LV and BIV pacing and the presence of a large SF leads to greater reverse remodelling at six months. However, due to these small numbers it is not possible to determine whether these differences are significant.

The design of the bull's eye plots was crude. For further assessment a better method of quantifying the SF is required, including a truly quantitative analysis of the extent and location of the deformation association with the SF. To understand fully the relationship between the SF and LV activation pattern we would need a larger study.

## **Conclusions**

In left bundle branch block with a septal flash there is a strong interaction between electrical activation and mechanical deformation. Early deformation of the septum, stretching adjacent tissue may induce functional changes in conductivity. This information may be valuable in understanding and predicting response to cardiac resynchronisation therapy.

## Chapter 6

### **A Method for Imaging Coronary Veins and Myocardial Scar during a Single CMR Acquisition**

#### **Introduction**

What follows is a brief summary of previous studies and techniques to visualize coronary veins as well as the methods, results and discussion for a novel CMR protocol to examine both coronary veins and scar in a single examination.

The most common method by which the LV lead is implanted in CRT is transvenously through the CS using a posterior lateral, or lateral coronary vein. Failure to implant a LV lead is up to 12% in large clinical trials.<sup>23</sup> There is marked individual variation in coronary venous anatomy, which can make it difficult to find a suitable position for the LV lead.<sup>106</sup> One reason for leads having unacceptable pacing parameters is implantation in areas of myocardial scar.<sup>151</sup> Therefore, knowledge of the coronary venous anatomy as well as location of myocardial scar provides extremely useful information for procedure planning.

152, 153

At present the coronary venous anatomy is usually imaged at the time of implant with invasive coronary venography. An occlusive balloon catheter is inserted into the CS followed by iodine-based contrast injection under X-ray fluoroscopy. The limitation of this method is that venous anatomy is determined only at the time



of the implant and it does not provide any information on scar or viable myocardium. Non-invasive methods for assessment of coronary venous anatomy are developing both with computer tomography (CT) <sup>154</sup> and CMR imaging. <sup>107-109,</sup>  
155

Multislice CT has been used to visualize coronary veins in three dimensions <sup>154,</sup>  
<sup>156</sup>, but involves ionizing radiation and nephrotoxic contrast agents. CMR has a number of advantages over CT as it provides information about LV scar <sup>157, 158</sup>, dyssynchrony <sup>124</sup> and function <sup>159</sup>. CMR has previously been used to assess coronary veins using an intravascular contrast agents <sup>107, 108</sup> or without a contrast agent by employing an MTC-prepulse <sup>109</sup>. Although the use of an intravascular contrast agent has been shown to give excellent CV anatomy, <sup>108</sup> very limited information with respect to myocardial scar can be obtained. A recent retrospective study <sup>110</sup> evaluated CMR angiograms of 31 patients for the ability to visualize coronary venous anatomy using conventional extravascular contrast agent. The average ejection fraction in the patient group was over 50%. The clinical relevance of this study is therefore limited as heart failure patients requiring CRT have ejection fractions of less than 35% and often have fast irregular heart rhythms and irregular breathing patterns leading to technical challenges with respect to MR image acquisition.

Recently, the slow infusion of the extravascular contrast agent dimeglumine-gadobenate ((Gd-BOPTA), Bracco Imaging SpA, Milan, Italy) has been proposed for whole-heart coronary artery MRA <sup>160</sup> exploiting the high relaxivity ( $r_1=9.7(\text{mmol/L})^{-1} \text{ s}^{-1}$  at 1.5 Tesla) and the weak interaction of the contrast agent

(CA) with serum albumin. In particular, whole heart CMR was combined with an inversion recovery (IR) preparation to improve contrast between the coronary arteries and myocardium. Studies have shown that Gd-BOPTA can be used for the assessment of myocardial scar and viability <sup>161, 162</sup>, which were found to be comparable to other gadolinium based contrast agents <sup>163</sup>. This agent has not previously been used for the combined assessment of coronary vein and myocardial scar.

In this study I investigated a CMR-examination in patients with heart failure using a slow infusion protocol of a high relaxivity CA Gd-BOPTA to evaluate the coronary venous anatomy, myocardial scar and left ventricular function. In patients with myocardial scar the relationship between myocardial scar and the coronary veins was assessed. The potential of CMR to aid implant planning was also assessed by comparing the imaging data from the occlusive venogram taken at the time of CRT implantation with the CMR venous anatomy.

## **Methods**

### **Study Population**

Fourteen heart failure patients (ejection fraction from transthoracic echocardiography  $27 \pm 7.0\%$ ) having a CMR as part of assessment for CRT implants, along with two patients with normal LV function were recruited. Seven patients had ICM and seven DCM (Table 22). Subjects with contraindications to MRI or history of anaphylaxis to contrast agent or GFR of  $< 30\text{ml/min/1.73m}^2$  were excluded.

**Table 22** Demographics of heart failure patients

<b>Heart Failure Patients</b>	
<b>Sex</b>	12 men
	2 women
<b>Age</b>	59.3±14.5yrs
<b>Aetiology</b>	7 Non-ischaemic cardiomyopathy
	7 Ischaemic cardiomyopathy
<b>Weight (Kg)</b>	86.0±12.5kg
<b>Average NYHA class</b>	2.9±0.4
<b>Heart rate during MRI scan</b>	66.8±9.3bpm
<b>Rhythm</b>	10 in sinus rhythm
	3 in sinus rhythm with ventricular ectopics
	1 in atrial fibrillation
<b>Ejection fraction (trans thoracic ultrasound)</b>	27±7%

## Data Acquisition

The patients were scanned using 1.5T MR-scanner (Achieva, Philips Healthcare, Best, Netherlands) with a 32-element cardiac coil (12 patients) and a 5-element cardiac coil (4 large patients due to claustrophobia). Cardiac gating was performed with vector electrocardiography (VECG). After localization and a coil sensitivity reference scan an interactive real-time scan was performed to determine the geometry of the SA, 4CH, 3CH and 2CH. A multiple slice (M2D) cine steady state free precession (cine-SSFP) scan was performed in SA orientation to assess the ventricular function (FA=60°, TR/TE=2.9/1.5ms, resolution 2.2x2.2x10mm, 30 heart phases). The 4CH, 3CH and 2CH views were used to assess LV function for regional wall motion abnormalities. Furthermore, visual assessment of the 3CH (FA=60°, TR/TE=3.0/1.5ms, resolution 2.5x2.5x10mm, 60 heart phases) view was used to determine timing of the end systole. For the contrast enhanced coronary vein scan, Gd-BOPTA (dose of 0.1 mmol/kg) was slowly infused at a rate of 0.3ml/sec with subsequent saline flushing as proposed by Bi et al <sup>160</sup> for coronary arteries. In order to determine the optimal start point of the whole heart coronary vein MR-scan, a dynamic ECG-triggered 2D-scan with inversion recovery (IR) preparation (TI=300ms) was used. For coronary vein visualization, an ECG-triggered respiratory navigated 3D IR-SSFP MR-scan was applied to acquire the whole-heart during a short interval (60-80ms) in end systole using a centric profile order and the following parameters: FA=50°, TI=300ms, TR/TE=4.25/1.44ms, SENSE=3-4 (with SENSE =2 AP direction and SENSE=1.5-2 in RL-direction), resolution 1.5 x 1.5 x 2mm (average number of slices 180±15). The overall scan time for the protocol was 3.5 min (assuming a 100% respiratory gating efficacy). After the coronary vein scan a delayed

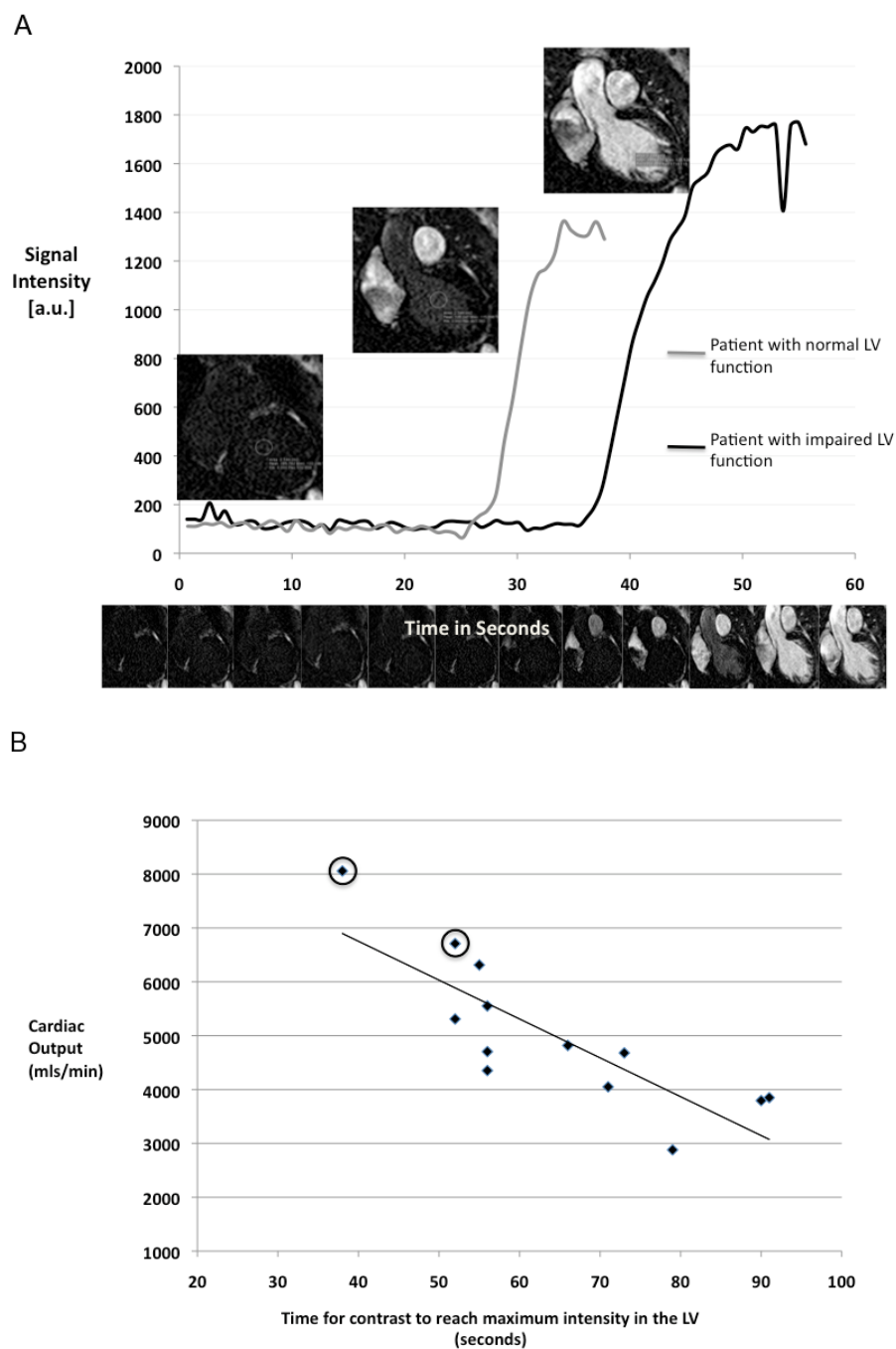
contrast-enhanced multi-slice IR gradient echo sequence (FA=25°, TR/TE=5.8/2.0ms) was performed at end systole to depict areas of scar. A preceding Look-Locker sequence was used to determine the optimal inversion time TI (320±22ms) to null the signal of the myocardium.

### **Data Analysis**

LV volumes were derived from the M2D-cine SSFP data by manually drawing endocardial borders (Philips, Viewforum). Papillary muscles were excluded and EDV and ESV were calculated for the LV, from which the ejection fraction and cardiac output (CO) were derived. The arrival of contrast agent bolus in LV was determined from dynamic ECG-triggered IR-scan. A linear regression analysis was performed between the times taken for contrast to reach maximum signal intensity for the different cardiac output (Figure 42).

**Figure 42**

**A** Time difference for contrast to reach maximal signal intensity within the LV in a patient with normal and impaired LV function. **B** Correlation between cardiac output and time for contrast to reach maximum signal intensity in the left ventricle. The two-circled points indicate the patients with normal LV function.



Volume rendering of the whole-heart coronary vein scan (3D IR-SSFP) was performed (Philips, Viewforum) to identify the CS and its tributaries. The ostium of the CS was defined as the site where the CS makes an angle with the right atrium. The origin of the Great cardiac vein (GCV) was considered immediately after the bifurcation of the Posterior vein of the left ventricle (PVLV) when visible or after the Posterior inter-ventricular vein subjects. Cardiac veins were classified according to Ortale et al and adopted terminology of Jongbloed et al.<sup>154,</sup>

164

In all the patients with late enhancement two clinical experts reviewed the position and transmural of the scar. To determine the relationship between scar and veins I co-registered the 3D whole heart images with the scar imaging using Osirix software.<sup>165</sup> For this, I superimposed a cast of the LV volume from the 3D whole heart image with the veins on the scar image. To further visualize the coronary venous anatomy and position in relation to myocardial scar I manually segmented the 3D whole heart images with ITK-SNAP software<sup>166</sup> to form high fidelity models. The scar was manually segmented using Osirix software and then registered to the 3D segmentation of the left ventricle using geometry information stored in the DICOM header. Once registered, scar segmentation images were projected onto the LV segmentation to provide 3D visualization of the scar geometry. Using all this information the number of veins that were related to areas of scar was determined.

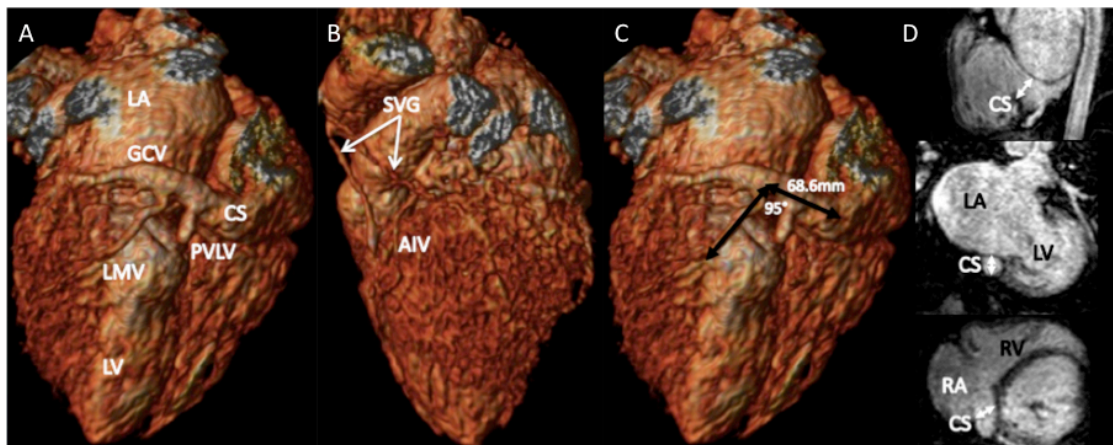
In patients that went on to have a CRT implant at our institute (n=11) I compared the occlusive venogram with the CMR imaging to determine the correlation

between the two imaging techniques and to determine if the vein used for final LV lead position was seen on the CMR imaging.

### Quantitative Analysis

Multiplanar reformatting was used to determine the size of the ostium of the CS in anteroposterior and superoinferior direction and to measure the starting diameter of each tributary. The distance between the ventricular tributaries was measured from the volume rendered reconstructions (Figure 43).

**Figure 43**



**A** and **B** Whole heart 3D reconstruction with the coronary sinus (CS) and tributaries. Also seen are two saphenous vein graphs (SVG). **C** An example of the distance between the origin of the CS and the Left marginal vein (LMV) and also the angle the LMV makes with the Great cardiac vein (GCV). **D** shows the measurement of the diameter of the CS in various plans. LV, Left ventricle; LA, Left atrium; AIV, Anterior inter-ventricular vein.

The signal to noise ratio was measured by drawing a region of interest (ROI) in the CS to measure mean signal intensity and two areas in the background define



background noise. Since a SENSE acquisition was used the image noise is spatially varying and usually highly suppressed outside the body. Therefore, two ROI inside the lung were used to define background noise.

Image quality of 3D coronary vein images was graded using an image quality score of 0 to 4. 0=CS/GCV not visible, 1=CS/GCV visible with markedly blurred borders or edges, 2=CS/GCV visible with moderately blurred borders or edges, 3=CS/GCV visible with mildly blurred borders or edges, 4=CS/GCV visible with sharply defined borders or edges.<sup>167</sup> For inter observer variability two experienced independent observers analyzed the data sets.

## Results

The ejection fraction calculated from M2D-cine SSFP for heart failure patients was  $27\pm 10\%$ , End diastolic volume was  $308\pm 140\text{ml}$  and cardiac output was  $4.6\pm 0.9\text{ l/min}$ . Twelve of the patients went on to have a CRT implant, in one of those the implant was performed at another institute and in another patient it was not possible to implant a LV lead due to inability to find a stable lead position. Of the two that did not go on to have implants, one patient, although referred with an ejection fraction of 35% from their transthoracic echocardiogram, was found at MRI assessment to have an ejection fraction of 55%, and one was too unwell to have an implant.

The time taken for the contrast agent to reach the LV was  $71.1\pm 27.2$  seconds (Figure 42A). In one patient with severe LV impairment the bolus track sequence

was completed before the contrast reached the left ventricle (maximum duration of bolus track sequence 120 seconds). The time taken for contrast to reach maximum signal intensity and cardiac output were correlated with  $r=0.82$  (Figure 42B).

The scan-time for the ECG-triggered respiratory navigated 3D IR-SSFP MR-scan varied within all 16 patients due to different respiratory gating efficiencies. In 13 patients the scan time was  $12.8 \pm 3.2$  min (gating efficiency  $29 \pm 7\%$ ) whereas there was a very low gating efficiency (12-15%) in 3 patients resulting in long scan times of up to 30 min.

### **Anatomical Observations**

The CS and GCV were visualized (Table 23) in all subjects with example reformatted images and segmentations given in figures 44 and 45. A PIV and LMV was seen in 12 patients (75%), PVLV in 8 patients (50%) and an AIV in 11 patients (69%). The mean ostial diameter of the CS and coronary vein branches as well as the mean distance from the ostium of the CS to the various tributaries is shown in table 24.

**Table 23** Anatomical observations and the correlation with vein anatomy during occlusive venography

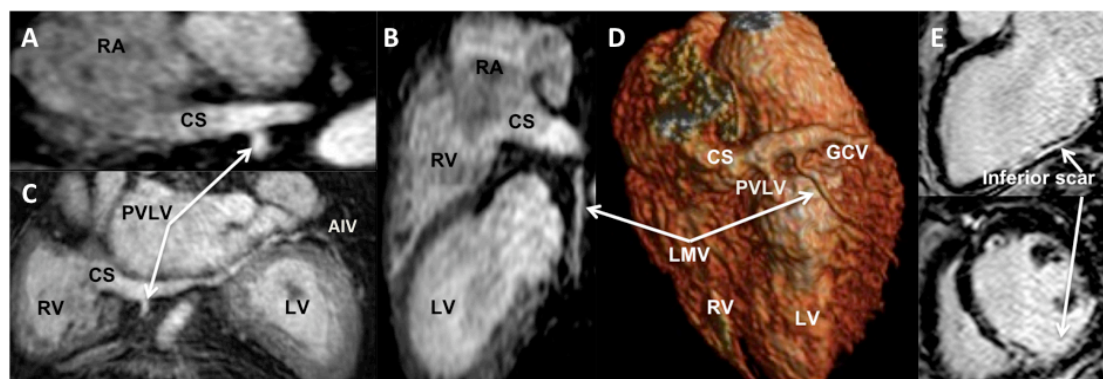
<b>Vessel seen</b>	<b>Number of vessel seen by CMR for all patients (n=16)</b>		<b>Number of vessel seen by venography for CRT patients (n=11)</b>	<b>Number of vessels seen by CMR for CRT patients (n=11)</b>	<b>% of vessels seen by CMR compared to venogram</b>
<b>Coronary sinus</b>	16	100%	11	11	100%
<b>Great cardiac vein</b>	16	100%	11	11	100%
<b>Posterior Inter- ventricular vein</b>	12	75%	8	8	100%
<b>Posterior vein of the LV</b>	8	50%	7	7	100%
<b>Left marginal vein</b>	12	75%	8	8	100%
<b>Anterior inter- ventricular vein</b>	11	69%	9	7	78%
<b>Additional lateral veins</b>	4	25%	2	2	100%
<b>Additional posterior veins</b>	1	6%	0	0	N/A

**Table 24** Ostial diameters of the identified vein and the distance from the ostium of the coronary sinus to the identified vein and measurable vessel length.

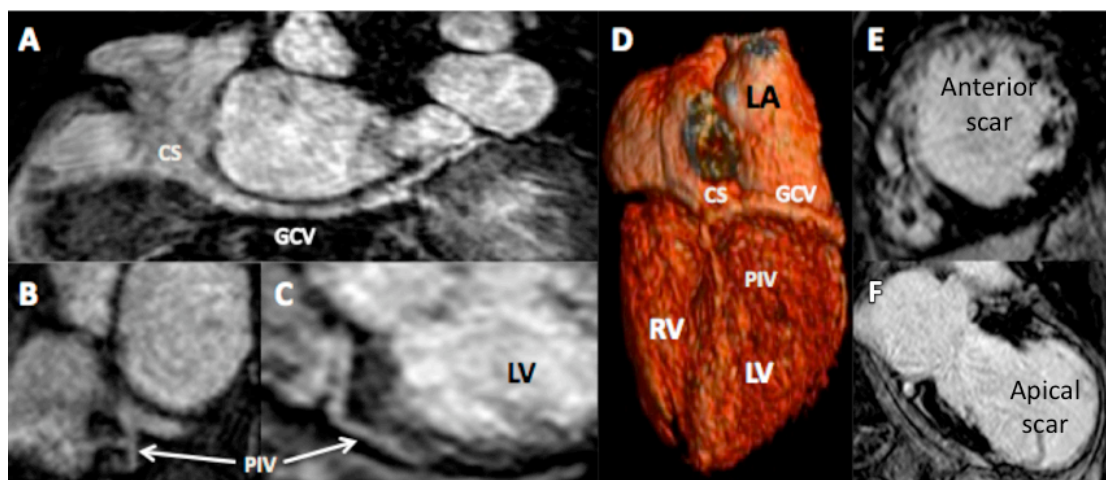
<b>CS</b>	<b>Ostial diameter of</b>	<b>Ostial diameter of</b>	<b>Average Angle</b>	<b>Average</b>	<b>Average</b>
<b>Tributary</b>	<b>identified vein</b>	<b>identified vein</b>	<b>Between the</b>	<b>distance from</b>	<b>Length of</b>
	<b>Superior/inferior</b>	<b>Anterior/posterior</b>	<b>Tributary and</b>	<b>the ostium of</b>	<b>the</b>
	<b>(mm)</b>	<b>(mm)</b>	<b>the CS or GCV</b>	<b>the CS (mm)</b>	<b>identified</b>
					<b>vein (mm)</b>
<b>CS</b>	12.5±4.1	13.9±5.7	N/A	143.8±50.0†	N/A
<b>PIV</b>	5.0±0.8	4.7±1.2	74.7°±27.6°	12.0±4.3	35.8±13.6
<b>PVLV</b>	5.4±1.5	5.4±1.0	108.3°±30.7°	32.6±16.4	42.0±34.3
<b>LMV</b>	4.8±1.0*	4.7±1.2*	99.1°±32.0°	68.8 ±19.4	33.3±23.5
<b>AIV</b>	3.2±1.0*	3.1±0.8*	119.6°±28.7°	146.5±27.6	23.9±16.1

\*Unable to accurately measure in 2 patients

†Total length of vessel measurable (length from Coronary sinus to end of Anterior intra-ventricular vein)

**Figure 44**

**A** and **B** MPR images of the CS and GCV with the PVLV. **C** MPR image showing the extent of the coronary vein from the CS to the AIV. **D** 3D reconstruction of the coronary venous system with the various branches. **E** Late enhancement images showing inferior scar.

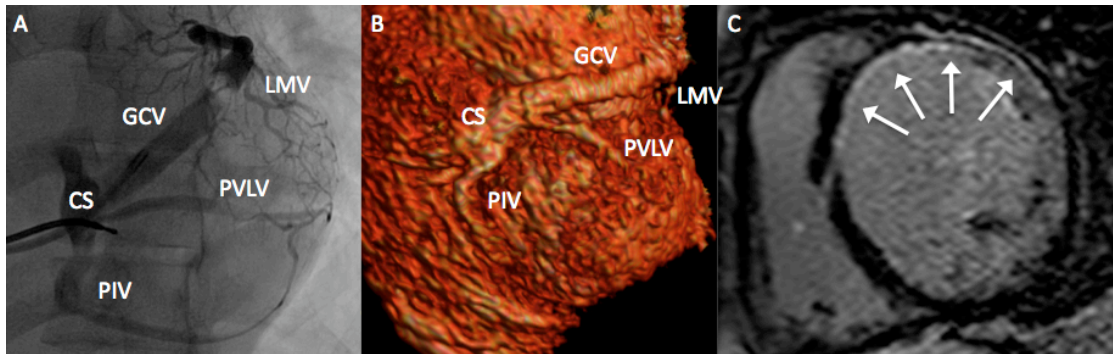
**Figure 45**

**A**, **B** and **C** MPR images of the CS and the GCV. **D** 3D reconstruction of the coronary venous system. **E** and **F** Late enhancement images with extensive anterior apical scar.

### Scar Imaging

Seven patients with ICM had late enhancement (Figure 44 and 45) and one of the non-ischemic patients had late enhancement attributed to an embolic event. Of the patients with scar one had anterior scar, two anterior/lateral scar, one anterior/septal scar, one lateral scar and three inferior scar. For six of the patients with scar we were able to attribute at least one coronary vein to an area of scar (Figure 46 and 47) (Table 25).

**Figure 46** Shows a patient with a dilated cardiomyopathy and anterior scar

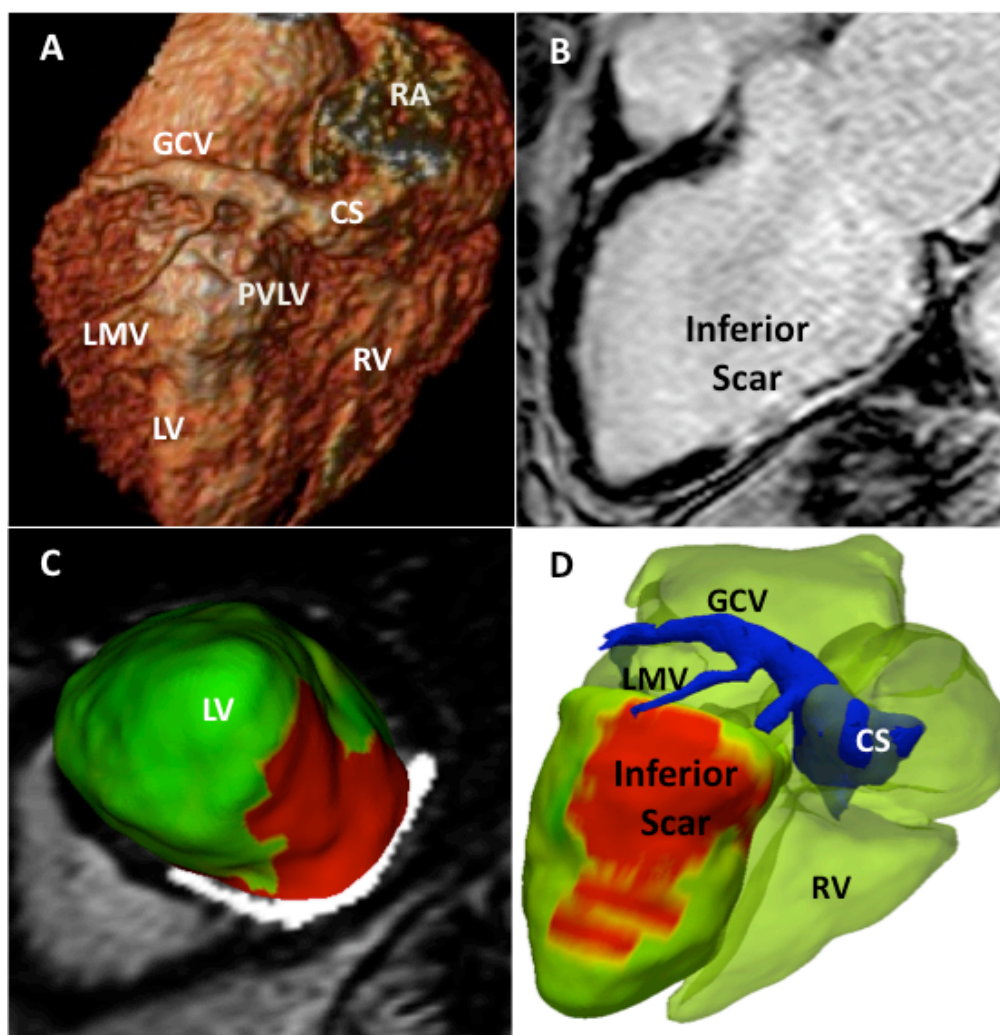


**A** Occlusive venogram performed at time of CRT implant. **B** Volume rendered 3D reconstruction of the heart and coronary veins showing the correlation with the occlusive venogram. **C** Mid ventricular short axis late gadolinium enhanced image showing sub endocardial anterior scar of 50 to 75% transmural.

**Table 25** Position, transmuralty of scar and number of veins associated with scar

Case Number	Aetiology	Scar area	% scar thickness	Number of veins associated with scar
1	ICM	Inferior, basal/mid	75-100%	2*
2	ICM	Inferior basal/mid	50-100%	1
4	ICM	Anterior/septal/lateral	Basal/mid 25-50% Apex 100%	1
5	ICM	Anterior/lateral Mid/apical	100%	0
7	ICM	Anterior/septum Mid/apical Apex	100% 100%	0
9	ICM	Anterior/septum Lateral Apex	75-100% 75-100% 100%	1
10	DCM	Anterior	75-100%	1
15	ICM	Inferior	25-50%	1

\*Images for this patient seen in figure 47

**Figure 47**

**A** 3D reconstruction of the heart with the coronary venous system. **B** 2 chamber multislice delayed contrast-enhanced MR-scan showing inferior late enhancement **C** Segmented LV registered to the scar imaging in the short axis view. The scar has been manually segmented and is imposed on the segmented LV shown as red in the image. **D** Segmented whole heart with the coronary veins and scar all superimposed.



### **Comparison of CMR Venous Anatomy and Venography at Implantation**

In all 11 patients that had implants at our institute there was 100% correlation between the CS, GCV, PIV, PVLV, LMV and additional lateral veins seen on CMR compared with the occlusive venography (Figure 46). In two of the patients the AIV was not seen with CMR imaging, but was visible at venography. In all of the patients the vein used for final LV lead placement was visualized (Table 23).

### **Image Quality**

The average score for the CS was 3.0 and GCV 2.6 with a good agreement between two observers. With respect to the vessels seen the observers agreed for in all cases for the CS, GCV and PIV. Observer 1 identified an AIV vein that observer 2 did not and also two additional lateral veins. The average signal to noise ratio for all patients was 19.5.

### **Discussion**

This is the first study to demonstrate that CMR can be used to accurately assess function, coronary venous anatomy and myocardial scar in a group of patients with heart failure and dilated ventricles awaiting CRT in a single MR examination. I have shown that this CMR protocol can be used to delineate the coronary venous anatomy and correlates well to the occlusive venography. Due to the resolution of the 3D whole heart image (1.5 x 1.5 x 2mm) the venogram gives more detailed information about small vessels and the distal parts of coronary vein branches, however the CMR imaging provides an accurate non invasive assessment of the CS and main tributaries. When comparing the CMR venous anatomy to the venogram in only two patients I was unable to see main

vessels, which were visible on the venogram. In both patients the vessel was the AIV, which, is not normally a target for LV lead placement in CRT. Furthermore using MPR and volume rendered images allowed measurement of the CS ostium diameter and the distance potential target vessels are from the CS ostium as well as the angle of take off from the GCV. This information can be valuable in CRT-procedure planning. When an occlusive venogram is performed the balloon is blown up some distance from the CS ostium and then contrast is injection. Veins between the CS ostium and the balloon are often poorly filled by contrast and it is possible to miss potential target vessels. The ability to show potential targets vessels are present and their size and distance from the CS prior to the procedure means that these vessels are less likely to be missed by a sub-optimal venogram.

In all patients that underwent CRT the target vessels for LV placement were visualized by CMR as were all the veins for final lead position. Furthermore by overlaying segmented coronary vein anatomy and scar I was able to determine which veins were in areas of scar and transmural of the scar. Using this technique has the potential to guide implanters prior to the procedure on the coronary venous anatomy and the potential of which veins may be related to scar.

Previous studies have used volunteers or patients principally with normal LV size and function.<sup>107, 108, 110, 155</sup> This study demonstrates that it is feasible to provide clinically relevant information in patients with heart failure. This cohort of patient is technically more challenging to scan, as there are often problems with arrhythmias. One patient was in atrial fibrillation and a further three had

multiple ventricular ectopics. Interestingly the patient with atrial fibrillation although having a long scan time had good image quality graded as 3 by both observers for the CS and the GCV. Patients also have difficulty lying flat for long periods due to the nature of heart failure symptoms. This often leads to irregular breathing patterns and therefore difficulty with the navigator efficiency prolonging scan times. All of the patients with heart failure had intra-ventricular conduction delay with significant ventricular dyssynchrony. The 3D whole heart scan was triggered during end systole because although the diastolic quiescent period is longer the area of the CS is larger during the systolic quiescent period making imaging easier.<sup>109</sup> A narrow acquisition window of 60 to 90ms. Although this increased the scan duration it is was important to ensure image quality. The scan times were long due to both irregular heart rates and breathing patterns as well as short acquisition windows. The scan would benefit from new innovations that improve the respiratory gating efficiency.

Due to poor cardiac output of heart failure patients there is marked variation in the time for contrast agent to disseminate within the blood pool and reach the coronary veins compared to subjects with normal LV function. Using a dynamic ECG-triggered IR-scan to measure bolus arrival in the LV I was able to optimize the timing of the 3D IR-SSFP scan (Figure 42A). In one of the patients with a DCM the bolus track sequence had finished prior to contrast entering the LV cavity. This emphasizes the importance of the correctly timing the start of the 3D whole heart scan with centric profile order when using a slow infusion protocol.

Scar imaging was done at the same timing as the 3D IR recovery whole heart acquisition (end systole). This allowed direct comparison between the scar imaging, segmented left ventricle and coronary veins. However, in both scans two different respiratory motion compensation strategies were applied, i.e. a respiratory navigator and breath hold. Two points in the papillary muscles were used as anatomical landmarks to briefly investigate the misalignment between the coronary vein and the late enhancement scan. There was a relatively small displacements of  $3\pm3.5\text{mm}$  in 14 patients and larger displacements of up to 20mm in two patients. In future, the registration between both scans can be improved by using the same respiratory navigator.

### **Study Limitations**

I looked at a small number of heart failure patients (n=14) and now need to get greater numbers in particular with ICM to allow further assessment of the relationship of the coronary veins to the myocardial scar.

I did not compare our technique to other non-invasive imaging modalities nor extra vascular contrast agents. However, the results with respect to vessels seen and measurements of length and diameter are comparable to previous studies, which involved volunteers or patients with normal LV function.

I used a slow infusion to increase the circulating time for the contrast agent and improve imaging of the venous anatomy. Due to the time taken to acquire the 3D whole heart scan it may be more appropriate for a bolus to be given and further

work needs to be done to optimize the methods for contrast infusion. Furthermore, a constant inversion time for the coronary vein scan was used, since a determination of TI using a Look-Locker scan before would delay the start 3D IR-SSFP MR-scan with centric profile order. The use of a constant TI and the different heart rate of the patients resulted in different image contrast among the patients.

As 11 of the patients went onto have devices I was able to show that the CMR imaging compared favourably to the venogram anatomy. Ideally I would have liked to compare the measurements made at CMR with the venogram anatomy. However for a quantitative assessment of the size and length of the different territories numerous X ray views would be necessary which would increase the procedure time and radiation dose to the patient.

## **Conclusions**

This study demonstrates that CMR can delineate the coronary venous anatomy and its relationship to myocardial scar in this patient population. This has been helpful for procedure planning and during device implantation using the segmented volumes together with overlaying software <sup>168</sup>. Although these techniques are in their infancy there is the potential to guide lead placement to avoid areas of scar and to reduce procedure time and exposure to contrast agents as well as radiation.

## Chapter 7

### Image Guidance to Aid CRT Implantation

#### Introduction

What follows is a brief summary of image registration tools and study of their uses to aid in CRT implantations.

Developments in improved imaging of the coronary venous system with both CT<sup>154, 169, 170</sup> and CMR<sup>107-109, 171</sup> have allowed clinically useful knowledge of the coronary venous anatomy to be gained prior to lead implantation. Segmentation tools<sup>166</sup> and advanced image registration software developed<sup>172</sup> enable coronary vein anatomy from three dimensional whole heart acquisitions either from CT or CMR to be used intra-procedurally by using an overlay on the X-ray fluoroscopy. The overlaid segmentations are registered in 3D space with X-ray views in various image planes with the movement of the C arm to guide the implantation of the LV lead.

I studied the feasibility of using advanced imaging techniques registered and fused in real time with fluoroscopy to guide LV lead implantation in patients undergoing CRT. These techniques were used to guide LV lead implantation in a group of patients of whom the majority had undergone at least one unsuccessful attempt at LV lead implantation.

## Methods

Twelve patients with severe heart failure that fulfilled standard criteria for CRT were recruited. Patient demographics are shown in table 26. Eight patients (66%) had previous failed CRT implants due to an inability to successfully site a LV lead and four were primary implants. Eleven patients were male and all were in NYHA III class heart failure, five had ICM and six DCM and one had a viral cardiomyopathy. In those with previous failed implants six had a single previous attempt and two had two previous attempts to implant a LV lead at other institutions by experienced implanters. In five patients (63%) failure to implant initially a LV lead was due to inability to cannulate the CS; one patient had a CS dissection leading to the initial procedure being abandoned, in one the previous implanter had failed to find a position with acceptable pacing parameters and one patient had a left- sided SVC with a massively dilated CS in which it was not possible to identify a target coronary vein to implant an LV lead.

**Table 26** Patient demographics

	<b>Patients</b>
<b>Age (years)</b>	59.0±16.8
<b>Sex</b>	11 male
	1 female
<b>Ejection fraction</b>	28±4%
<b>NYHA status</b>	3±0
<b>Aetiology of heart failure</b>	5 ICM
	6 DCM
	1 Viral myocarditis
<b>Reason for initial failed procedure</b>	5 unable to cannulate CS
<b>(8 patients)</b>	1 CS dissection leading to 1 <sup>st</sup> attempt being abandoned
	1 Unable to find lead position with acceptable pacing parameters
	1 left sided SVC with inability to visualize Coronary vein or implant LV lead
<b>Imaging methods</b>	6 cardiac CT
	6 cardiac MRI



## **Advanced Imaging Protocol**

Six of the patients (50%) underwent CMR to guide their implant. The other six patients already had right-sided pacing leads *in situ* from previous failed CRT attempts and therefore were excluded from having a CMR. In this group cardiac CT imaging was performed. Standard exclusion criteria for contrast CMR and CT were used including contrast allergy, uncontrolled arrhythmia, and renal dysfunction with a creatine serum level of  $>1.5\text{mg/ml}$ .

### ***MRI Examination***

For six patients both respiratory and cardiac-gated CMR images were acquired prior to the initial implant on a Philips Achieva 1.5T MR system (Phillips Medical Systems, Best, Netherlands) with the method described in chapter 6.

### ***CT Examination***

For the six patients who underwent cardiac CT examination images of the coronary veins were acquired using cardiac-gated CT images with a Philips Brilliance 40. A retrospectively- gated coronary CT protocol was adopted using approximately 60 ml of iodinated contrast agent. Craniocaudal coverage was set to include the whole heart with typical reconstructed voxel resolution being  $0.4 \times 0.4 \times 0.4\text{mm}^3$  and the number of slices being approximately 400. The reconstructed phase at 75% of the R-R interval was used for segmentation.

## **Implantation**

### ***Image Segmentation***

For the CT images, the 75% cardiac cycle data were used for generation of a 3D anatomical model. The segmentation of the data was carried out using the fully automatic Philips EP Planner software that produced 3D models of all the cardiac chambers and great vessels, including the first part of the CS, within 30 seconds. This was augmented by manual segmentation of the main branches of the CS to yield a highly detailed anatomical model. For the CMR images, the systolic, end-expiration 3D image data were segmented semi-automatically using the ITK-SNAP software. Four of the patients that had CMR had ICM. The late gadolinium enhanced images were segmented manually for scar information. Using the geometry information stored in the DICOM header scar segmentations were registered to the high fidelity 3D models. In the patients that had CT imaging the right-sided pacing leads were segmented to aid image registration. Furthermore, for both CT and CMR data, the tracheal bifurcation was manually segmented to aid in the image registration process.

### ***Image Registration and Fusion***

CRT Implants were undertaken in a cardiac catheter laboratory using a Philips® Allura Xper FD10 cardiovascular X-ray system, with EP Cockpit layout (Philips Medical Systems, Best, Netherlands). A single experienced CRT implanter undertook all procedures after review of the imaging data. During the implant procedure, the overlay of the anatomical model on to the live X-ray fluoroscopy was achieved using a prototype software <sup>172</sup> using a Philips development

environment (PII, Philips Healthcare, Best, The Netherlands) (table 27 for implant details).

The registration procedure was different depending on the type of anatomical data being used, i.e. CT or CMR. For both types of data, the patient's heart was first isocentred in the X-ray field of view by using the PA and lateral X-ray projections. For patients with CT data, the right-sided implant electrodes acted as fiducials. These electrodes were imaged using PA, LAO 30°, and RAO 30° X-ray projections. The segmented anatomical model was then manually aligned with segmented electrodes that were visible in the X-ray images (figure 48). For patients with CMR data, a standard quadripolar electrode catheter, St Jude Medical Supreme (St Jude, Minnetonka, MN, USA) was looped in the right atrium and imaged using PA, LAO 30°, and RAO 30° projections and then removed. The overlay software was then used by the clinical expert to align the segmented anatomical model to the right atrial catheter. For both types of imaging data, the registration was further aided by aligning the segmented tracheal bifurcation to the X-ray shadow of this structure in the PA view. Subsequent to this registration procedure, which took typically less than 5 minutes, there was complete freedom of motion of the X-ray table and C-arm since the registration was automatically maintained by the internal tracking of these devices by the overlay software. This meant that when the fluoroscopic projection was changed the overlay automatically moved in the same projection.

**Table 27** Implant information

	<b>Patients</b>
<b>Access site</b>	9 left subclavian vein 1 right subclavian vein 1 cephalic vein 1 axillary vein
<b>Guide catheter used to cannulate</b>	10 6Fr AL2 (St Jude Medical, Sylmar, California, USA)
<b>CS</b>	2 6Fr AL1 (St Jude Medical, Sylmar, California, USA)
<b>Guide wire used</b>	11 Whisper View™ EDS CS-J 4639 (Guidant Corp. St.Paul, MN, USA) 1 HI TORQUE IRON MANTM 6725 (Guidant Corp. St.Paul, MN, USA)
<b>Lead used</b>	6 Quickflex XL™ 1158T 86cm (St Jude Medical, Sylmar, California, USA) 4 Quartet™ 1458Q 86cm (St Jude Medical, Sylmar, California, USA) 1 Attain Ability™ 4196 88cm (Medtronic Inc. Minneapolis, MN, USA) 1 unable to find lead position with acceptable pacing parameters
<b>Final lead position</b>	6 lateral vein 5 posterior lateral vein 1 no lead implanted
<b>Pacemaker/ICD model</b>	3 ATLAS II HF V-367(St. Jude Medical, Sylmar, CA, USA) 3 PROMOTETM RF 3213-36(St. Jude Medical, Sylmar, CA, USA) 4 PROMOTETM Q CD3221-36 (St. Jude Medical, Sylmar, CA, USA) 1 Biventricular pacemaker INSYNC® III 8042 (Medtronic Inc. Minneapolis, MN, USA)
<b>R wave (mV)</b>	12.8±6.7
<b>Threshold (V)</b>	1.5±1.3
<b>Screening time (min)</b>	28.4±22.0

TM=trademark

**Figure 48** The workflow of how the CMR images are used to form a 3D road map and then registered during the implant

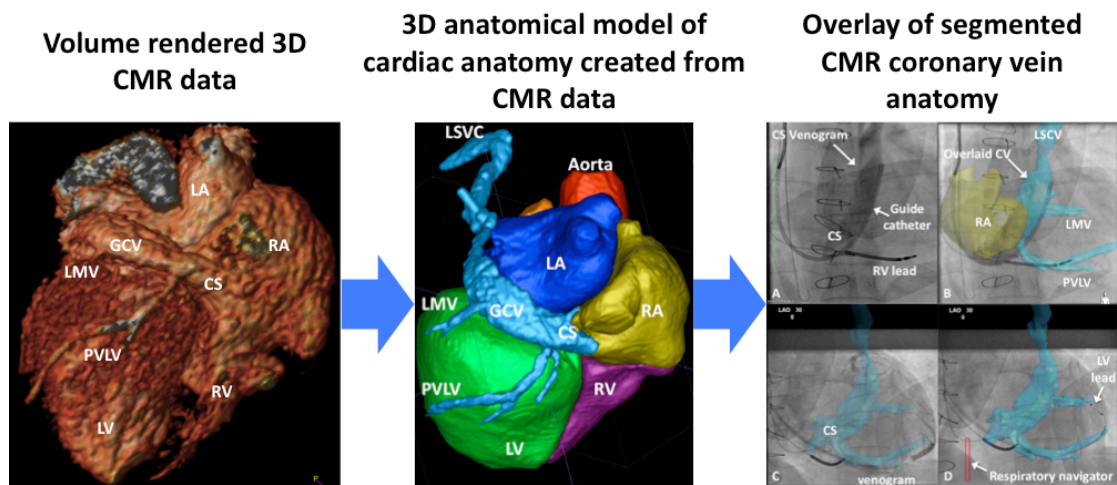
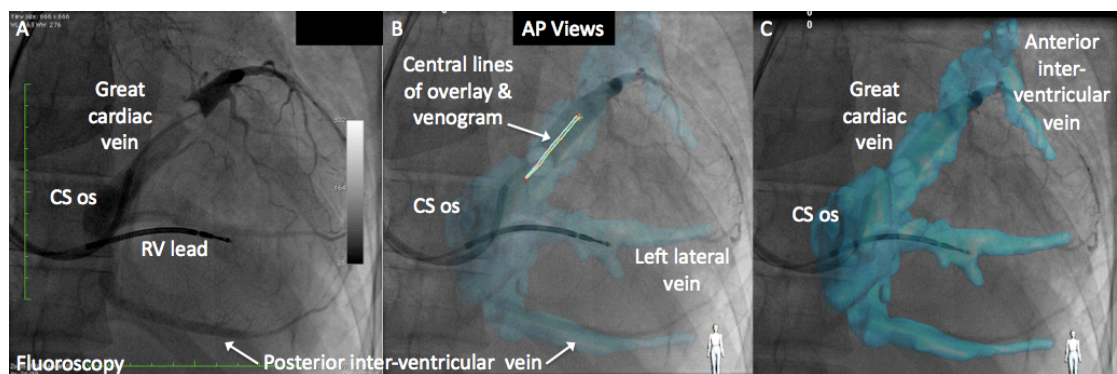


**Figure 49**

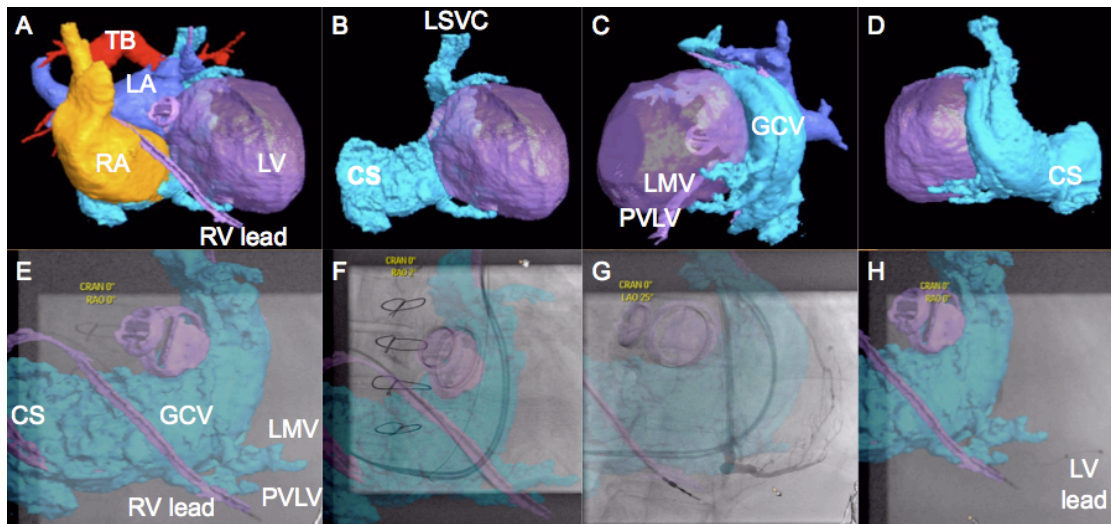


**A** Shows an occlusive venogram. **B** shows the overlay of 3D coronary sinus (CS) segmentation from CMR imaging with a centre line for both the venogram and the overlaid coronary veins. This is used to determine the registration error. **C** Shows how the overlaid coronary veins appear to the operator during an implant. This image was taken during the occlusive venogram to show the close correspondence with anatomy.

After venous access was achieved CS cannulation was performed in all cases using a St Jude OC/135 Guide catheter with a St Jude 6Fr AL2 or St Jude 6Fr AL1 (Sylmar, California, USA) telescoped within it and a Radifocus® Guide Wire M Standard Type RF\*GA35153M (Terumo Europe NV, Leuven, Belgium). The implanter used the overlaid images of the coronary sinus in the LAO projection to guide introduction of the guide catheter into the CS ostium. Once the CS was accessed an occlusion venogram was performed with a 6Fr occlusion balloon catheter (Arrow International Inc, Reading, PA, USA) in PA and LAO views to allow comparison of this with the overlaid images of the coronary sinus and its branches (figure 48 and 49). This was performed in all cases except the patient with a left sided SVC when occlusion venography was not feasible due to the massively dilated coronary sinus (figure 50). Using the overlaid venous anatomy as a roadmap the LV lead was implanted in either a lateral or posterior lateral vein to achieve acceptable pacing parameters.

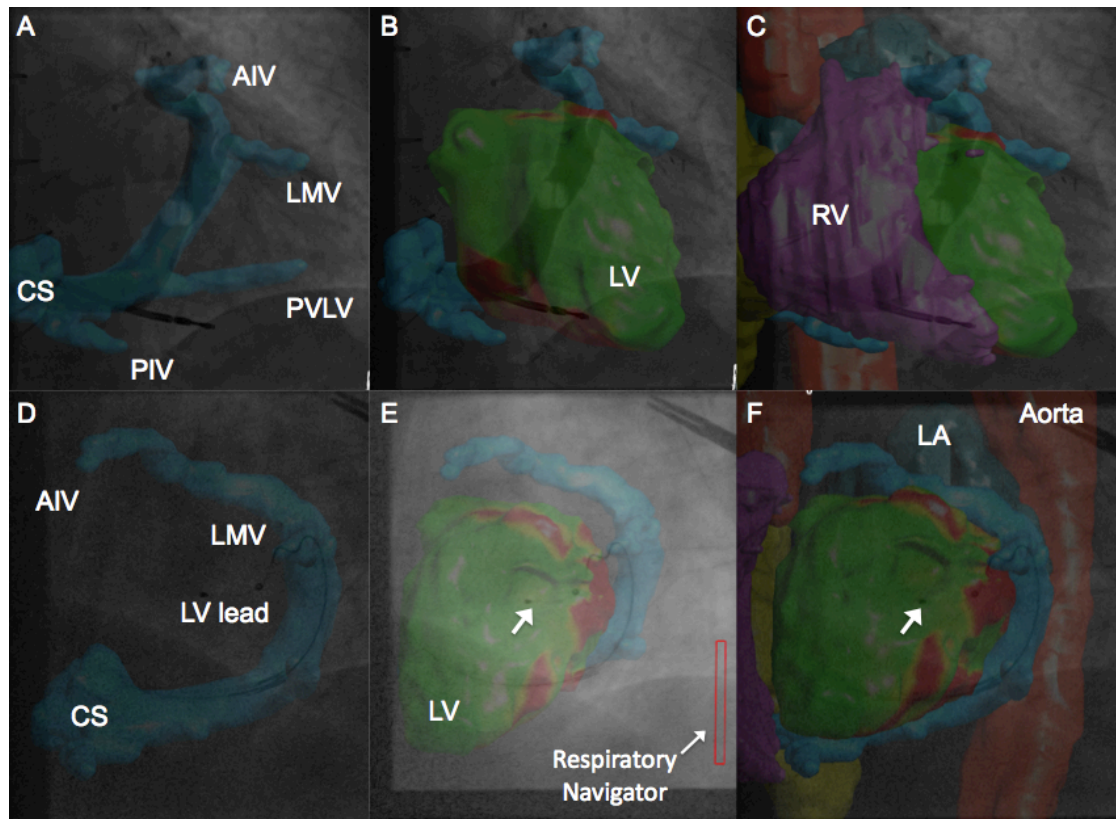
In the four patients that had the overlay of the 3D model with myocardial scar pacing was performed within areas of scar to determine any difference in pacing parameters between scarred and abnormal myocardium (figure 51). In six of the patients that had previous failed LV lead implants pre-existing RA and ventricular leads were already present. In the other cases the right-sided leads were then inserted. The generator was implanted sub-pectorally in eight patients and subcutaneously in four.

**Figure 50** Images from a patient with a left sided SVC draining directly into the coronary sinus



It can also be clearly seen from the images that this patient has had mitral and aortic valve replacements. Images **A** to **D** show the 3D model of the cardiac chambers and a massively dilated CS and tributaries. Images **E** to **H** show the segmented model registered to the fluoroscopy during the left ventricular (LV) lead implant. In **E** and **F** the RV lead can be seen passing down the left sided SVC and through the CS to the RV. The RV lead is segmented to aid registration. Images **G** and **H** show the PVLV with selective venography guided by the overlay being used to implant the LV lead. Image **G** venogram of the PVLV that corresponds closely with the overlaid model. **H** the LV lead is seen implanted in the PVLV. TB=Tracheal bifurcation.

**Figure 51** Shows CMR 3D whole heart images registered as an overlay to the real time fluoroscopy



This patient had myocardial scar that has been registered to the LV and is depicted as red on the overlay. **A** to **C** AP projections taken during the occlusive venogram and shows how accurate the registration is and how well the 3D model correlates to the venogram venous anatomy. **D** to **F** LAO projections showing the overlay used for implantation of the LV lead. The LMV is being used and it can be seen that this is clearly outside an area of scar. In figure **E** and **F** the arrow shows the position of the LV lead.



### ***Registration Error and Statistics***

To evaluate the accuracy of registration between the 3D anatomical models and the live X-ray fluoroscopy, I calculated the distance errors between the central point of the main branch of CS in the 3D anatomical models and the occlusive venogram in 2D X-ray images (figure 49). A centre line of main branch of CS was determined from the venogram as well as a centre line for the overlay in a fluoroscopic overlay. The error was defined as the root mean square distance error between 10 points on the centre line of CS overlay geometry and 10 nearest points on the centre line of CS venogram. Statistical analysis was performed using SPSS software package (Chicago, IL, USA). Mean values  $\pm$  SD was calculated for screening times, echocardiographic measures and pacing parameters. A Student's t test was used to determine significant remodelling determined via echo parameters. P values less than 0.05 were considered statistically significant.

### **Results**

The summary of demographics and clinical characteristics are presented in Table 26. For all patients high fidelity segmentations of all cardiac chambers, great vessels and coronary venous anatomy as well as achieving accurate registration between the 3D anatomical models and the live X-ray fluoroscopy was achieved. This was confirmed by balloon occlusion angiography of the coronary veins from two or more X-ray views. The mean distance between the centre lines of the CS on the overlay and the venogram was  $1.3 \pm 0.68$  mm. In the patient that had a left

sided SVC I was unable to do an occlusive venogram and therefore it was not possible to measure the registration error.

In all patients the CS was cannulated successfully. Eleven of the twelve patients (seven of the eight previous failed implants, 88%) a LV lead was successfully implanted in a posterior lateral or lateral coronary vein with good pacing parameters and no diaphragm stimulation. In one patient (with previous failure due to inability to cannulate the CS ostium), successful cannulation of the CS was achieved without difficulty and the operator was able to navigate freely within the coronary veins. However, due to extensive myocardial scarring he was unable to find a lead position with acceptable pacing parameters and the procedure was abandoned. LV lead parameters for the group are shown in table 27. Average screening time for all patients was  $28.4 \pm 22.0$  minutes. In the four patients having primary implants the screening time was  $17.8 \pm 7.9$  minutes (operators average screening time without overlay  $16.4 \pm 10.4$  minutes), and total procedure time  $136 \pm 58$  minutes. The average R wave at implant was  $12.8 \pm 6.7$  mV and LV lead threshold was  $1.5 \pm 1.3$  V measured at pulse duration of 0.5 msec. At three-month follow-up all implanted leads were functioning satisfactorily with all patients receiving CRT. LV pacing thresholds were slightly lower than at implant,  $1.3 \pm 0.7$  V.

**Table 28** Shows the recorded pacing thresholds and R wave for pacing in and out of areas of myocardial scar as depicted on the overlay

	Scar								Non scar					
	Pos 1		Pos 2		Pos 3		Mean		Pos 1		Pos 2		Mean	
	T	R	T	R	T	R	T (V)	R	T	R	T	R	T (V)	R
	(V)	(mV)	(V)	(mV)	(V)	(mV)		(mV)	(V)	(mV)	(V)	(mV)		(mV)
<b>Case 1</b>	0.8	7.7	0.6	8.1	0.5	17.9	<b>0.63</b>	<b>11.2</b>	0.8	8.7	0.8	13.3	<b>0.8</b>	<b>11</b>
<b>Case 2</b>	6	10.9	1.9	14.6	n/a	n/a	<b>6.6</b>	<b>12.8</b>	0.9	12.7	0.8	13.4	<b>0.85</b>	<b>13.5</b>
<b>Case 3</b>	5.6	8.6	4	10	2	3.3	<b>3.9</b>	<b>7.3</b>	0.5	26	0.5	22	<b>0.5</b>	<b>24</b>
<b>Case 4</b>	7.5	2	7.5	2	0.5	9.5	<b>5.1</b>	<b>4.6</b>	0.8	4.2	0.6	4.2	<b>0.7</b>	<b>4.2</b>

T=Threshold (V) and R= R wave (mV)

All patients (except failed implant) symptomatically improved by at least one NYHA class ( $2 \pm 0.4$  from  $3 \pm 0$ ). Mean left ventricular ejection fraction improved from  $28 \pm 4\%$  to  $37.9 \pm 7\%$  ( $P=0.003$ ) and ESV decreased from  $150 \pm 57\text{mls}$  to  $129 \pm 68\text{mls}$  ( $P=0.15$ ).

In the four patients with overlaid myocardial scar, the average R wave within scar was  $9.0 \pm 3.7\text{mV}$  compared to pacing outside scar where the average R wave was  $13.2 \pm 8.2\text{mV}$ . The threshold within scar was  $4.0 \pm 2.5\text{V}$ , compared to outside scar where the threshold was  $0.7 \pm 0.15\text{V}$ . The breakdown of the pacing thresholds and R waves for all patients with overlaid scar is shown in table 28.

## Discussion

In this series I have demonstrated the feasibility of using an advanced image overlay system using CT or CMR images to guide CRT implantation. This technique allows real time visualisation of the CS and branches overlaid onto fluoroscopy to guide the implanter. Furthermore I have demonstrated its potential to facilitate CRT implantation in a group of patients who have previously had failed LV lead implants.

Such an approach to overlay anatomical data of the CS was recently described by Auricchio et al. In this study the authors demonstrated the feasibility of manually integrating an overlay system between 3D CT anatomical reconstruction and 2D fluoroscopy of the CS and branches. Furthermore this study demonstrated that the registration accuracy was extremely high. These authors did not use the overlay system to guide the CRT implant. Previous work by the same authors had shown the feasibility to use multislice CT to delineate coronary venous anatomy in patients which LV lead replacement is required.<sup>173</sup> Previous work with overlay technology has demonstrated that fusion of CT and fluoroscopy may support electrophysiologists in more accurate delivery of therapy during atrial fibrillation ablation.<sup>174</sup> However, to my knowledge these techniques have not been used to guide CRT implants.

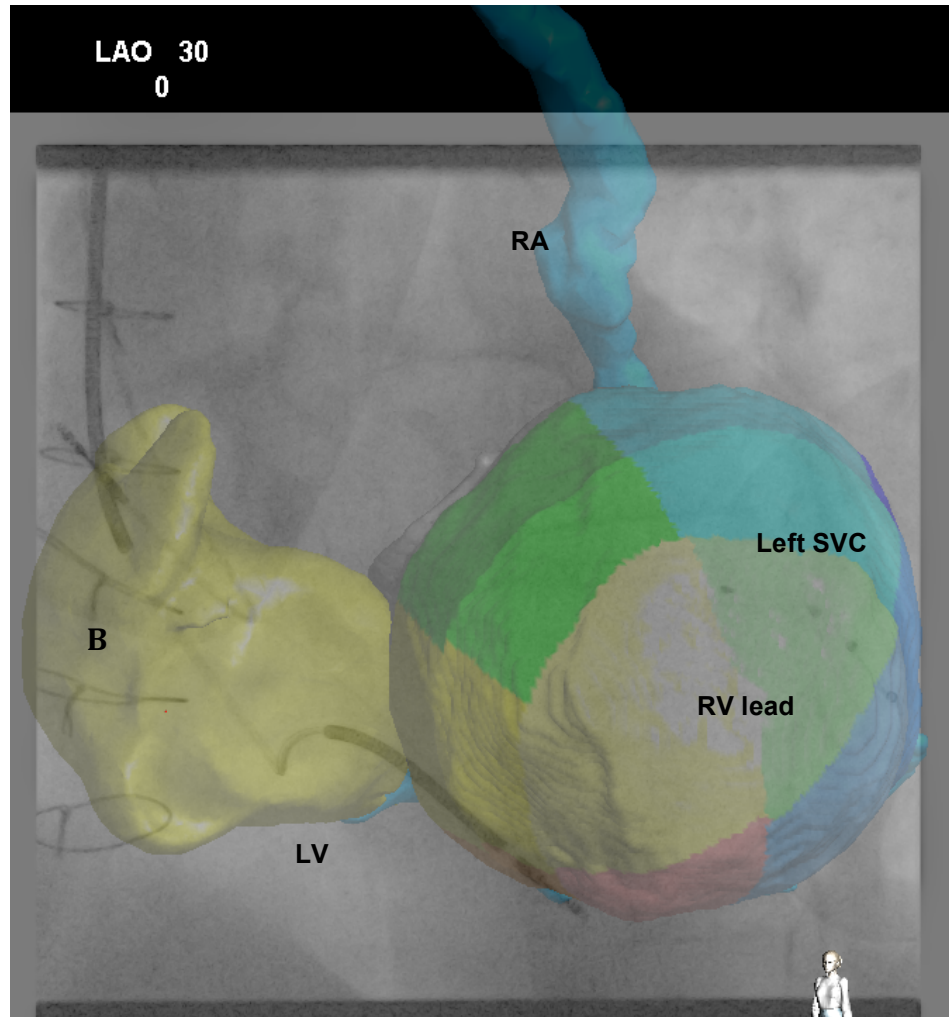
In this series not only was it possible to guide CRT implantation but it also facilitated successful LV lead implants in a group of patients who had previously failed procedures predominantly due to technical difficulty in cannulating the CS ostium. It was of particular help in a patient with a persistent left sided SVC in

which balloon CS angiography was impossible due to massive CS dilatation. In this case the overlay technique offered a potentially unique method of displaying the branches of the CS to guide LV lead implantation.

This technique has wider clinical implications as it is not just restricted to patients that have had failed implants but may be of benefit in all patients undergoing CRT. Cannulation of the CS ostium is often difficult and a key step in the CRT implants.<sup>175</sup> From this patient group five initially had failed implants due to inability to cannulate the CS and one had a dissection of the CS. In all our patients the CS was cannulated within two minutes of central access. It should be noted, that in these cases the procedures were all undertaken by an experienced operator and it is may be that the implants were successful due to this rather than to the overlay. However, using the overlay has particular benefits for less experienced operators as registration of the CS ostium and branches would aid in cannulation of the CS in patients that often have distorted anatomy. LV dilatation and enlargement of both right and left atria lead to distortion of the normal anatomical landmarks for the CS.<sup>176</sup> Using an overlay has the potential to facilitate CS intubation by using the registered image as a guide to the site of the CS ostium. Such techniques therefore may offer the potential to reduce procedure time, contrast dose, X ray exposure and complication rates particularly with inexperienced operators. Furthermore registration of scar may help to avoid pacing in areas of non-viable myocardium. As well as overlaying scar and CVs there is potential to overlay dyssynchrony maps which may also help implanters in placing the LV lead in a position of latest activation and theoretically could lead to improved response rates (figure 52).

**Figure 52**

Shows a 16 segment regional volume map superimposed on the LV volume. This allows the implanter to target areas of latest volume change



The average screening times for all implants is high predominantly due to three patients. In the patient with persistent CS left sided SVC, the procedure was technically very challenging (screening time 30 minutes). Another two patient had two previous failed attempts at CRT with inability to cannulate the CS ostium. In these cases we were able to cannulate the CS. However the procedure were prolonged with multiple pacing sites within the coronary veins used before one of the procedures was abandoned. This highlights that these cases are extremely complicated and the use of the overlay helps to facilitate potential successful implantation.

In the four patients having primary implants the screening times are equivalent to standard techniques ( $17.8 \pm 7.9$  minutes with overlay compared to  $16.4 \pm 10.4$  minutes without overlay). It is important to note that these numbers are not strictly comparable as three of these patients had myocardial scar and the operator paced in various sites to determine different pacing parameters which led to longer than expected screening times. Furthermore one of the patients had very extensive scar meaning it was very difficult to find a lead position with acceptable pacing parameters. It is likely that if the best LV lead position rather was used rather than pacing in different areas to determine the relationship between scar and non-scar that using these image registration techniques would reduce screening and procedure times.

In this series two imaging modalities, CT and CMR were used. With advances in CMR imaging of the coronary veins previously described in chapter six imaging sequence provide comparable information to CT. In patients with no

contraindications to CMR this modality for assessing coronary venous anatomy have a number of benefits over CT. Although images of the coronary veins can be acquired quickly by CT, iodine- based nephrotoxic contrast agents are required in a cohort of patients that often have poor renal function and that will require further nephrotoxic contrast agents for their implant. A further advantage of using CMR imaging over CT is it allows scar to be segmented and registered to the overlay. In the four patients with overlaid scar I was able to show a difference in pacing parameters between overlaid normal and scarred myocardium. It is known that implantation of the LV lead within scar leads to reduced response rates. Overlaying scar has the potential to aid the implanter and may improve response rates to CRT.

### **Study Limitations**

The major limitation is the small number of patients enrolled. Although the CS was cannulated successfully in all patients and implanted a LV lead in 11 (92%) out the 12 patients it is difficult to determine whether the patients would have been implanted successfully without the overlay. It must also be highlighted that in some CRT implants they are not successful not because of inability to cannulate the CS but due to anatomical conditions such as the presence of a valve. Although the pre procedural imaging is able to forewarn the operator of likely difficulties, technical skills and use of different catheters such as a diagnostic EP catheter may lead to successful implant and in these cases an overlay may not help. The small case series is a proof of concept but clearly a larger prospective study to determine if these techniques improve implant



success, shorten procedure time, reduce fluoroscopy dose and response rates is required.

With respect to image registration, further work needs to be done on improving segmentation of myocardial scar. The scar was manually segmented and then superimposed on an endocardial shell of the LV. There are two issues that need to be resolved. As an endocardial shell was used and the veins run along the epicardial surface it sometimes appears that the veins are separate from the myocardial surface. Furthermore myocardial scar was shown as being present (figure 51) the transmuralty of the scar was not depicted. This is an important issue as areas of partial thickness scar may still be viable and provide a good area for pacing. This is supported by one of the patients that we overlaid scar (table 28, case 1). In this patient the pacing parameters within and outside scar were similar. This patient had 50 to 75% endocardial anterior scar and therefore potential viable myocardium. This could explain why there was no difference between pacing parameters between depicted areas of scar and non-scar. Future work developing methods of segmenting CMR images and registering the transmuralty of scar are important to improve the potential of these techniques and further aid our understanding of the effects of scar transmuralty on pacing parameters. In the future to better understand the relationship between transmuralty of scar and pacing parameters I intend to look at the electrograms when we are pacing in and out of overlaid scar. Using the recorded low voltage and/or late potentials I would hope to better understand the relationship between transmuralty of myocardial scar with the timing of pacing artifact and QRS.

## **Conclusions**

This case series shows that advanced imaging and registration techniques can aid CRT procedures. There is much scope to use these techniques in the future not only to aid implants in patients with previous failed LV lead insertion but also to plan and help implanters prior to the initial procedure.

## **Chapter 8**

### **Discussion and Personal Opinion**

The various aspects of each sub study in this thesis have been discussed within each chapter. What follows are my personal opinions of the benefits of the work within this thesis and areas where further work is required.

There are a huge number of heart failure patients worldwide with prevalence increasing as survival from coronary disease improves. Although management of heart failure continues to improve the mortality remains too high.

The development of CRT has led to a further avenue to treat a sub group of heart failure patients with abnormal ventricular conduction. However, there remain a large proportion of patients that undergoing CRT that do not RR or derive clinical benefit. These so called non-responders have driven extensive research in to trying to understand why and how to improve these figures. Much of this work has focused on the use of echocardiographic derived indices of dyssynchrony.

Echocardiography remains a corner stone in the functional assessment of heart failure patients, however its use in stratifying which patients are likely to respond to CRT remains unclear. There are a number of limitations to

echocardiographic assessment of heart failure patients. 1) Poor image quality, 2) Multiple measures of dyssynchrony with no clear consensus on which method should be used, 3) Lack of information on myocardial scar, 4) Lack of information on anatomy such as coronary veins, 5) Difficult to use during procedures. Many of these limitations are not found with CMR.

It is important to understand how CMR can benefit our understanding of heart failure patients referred for CRT. At present we select patients based on QRS duration. It is assumed that electrical dyssynchrony translated into mechanical dyssynchrony and that correction of mechanical dyssynchrony leads to improved myocardial efficiency and response to CRT. Furthermore often is assumed that measures of dyssynchrony derived from strain will determine how and which patients will respond to CRT.

None of these factors take into account structural information such as position and extent of myocardial scar and coronary venous anatomy. It is important to realise that a patient may appear to be highly likely to respond on the basis of QRS duration and measures of dyssynchrony, however, if an implanter is unable to position an LV lead in a good position than that patient will not respond.

The benefit of CMR is that it can provide much of the information that echocardiographic imaging is unable to. Furthermore comparable indices of strain, muscle thickening and volume dyssynchrony can all be measured with potentially better accuracy.

Within this thesis I have attempted to synthesise a novel framework for measuring global myocardial dyssynchrony using strain, muscle thickening and volume change. Using comparable indices to measure dyssynchrony has enabled a better understanding of what is being measured and how it can be used in patient selection for CRT. It is clear that global measures of strain do not aid in patient selection as the forces required to produce synchronous myocardial contraction mean that strain patterns will always appear dyssynchronous even in the normal heart. Using volume-derived motion gives a far better indication of how coordinated ventricular contraction is. This thesis shows that a volume derived SDI is highly predictive of both acute response and remodelling post CRT. This has significant clinical implications.

There has been a lot of work using haemodynamic data to determine which patients are likely to respond to CRT. With recent work showing the AHR to CRT is patient specific it was important to understand both the relationship between myocardial motion and acute response to CRT and also chronic response. The work in this thesis has shown a clear relationship between both acute response and RR. Also patients with a high volume SDI have a large AHR. This has important clinical implications as it validates the use of pressured wires for intra procedural assessment of patients and also the potential to use volume dyssynchrony as a way to stratify likelihood of response or even as a surrogate for the pressure wire assessment.

The position and extent of myocardial scar is known to affect the response to CRT. The relationship of coronary veins to scar therefore has significance. As part

of this thesis I developed a CMR method to assess both in a single examination. This had not previously been done in heart failure patients. Not only does this information provide pre-procedural information to help the implanter, but also with the development of image segmentation and registration techniques I have been able to show how this information can be used in real time to aid implantation. The clinical implications are significant. These novel methods are only in their infancy, however, there is significant potential in the future to improve implant success rates.

I have investigated the relationship between the electrical activation of the ventricle with Ensite mapping and how this relates to the mechanical ventricular motion. Although the method used was crude I showed that areas of slow conduction and block are related to the abnormal septal motion known as the septal flash. This part of the thesis is very important as it provides an explanation as to why sub groups of patients have a good response to CRT.

## **Limitations of this Work**

All this work has been performed in a single centre with a small number of patients (n=50). To truly validate this work larger numbers of patients are required and this is definitely the next step to take this work further. Many of the techniques used within this thesis are experimental. I have shown that it is possible to use CMR images and image registration techniques in real time during a CRT implant. These techniques are novel and, although it would appear from our small patient group that they have potential to aid implant success rates, much more work is required in this area. Furthermore, although it is shown that it is possible to overlay scar and volume dyssynchrony no improvements in patient response rates were demonstrated.

## **The Future**

This thesis explores the development of many potential uses for CMR to aid CRT. There remains much scope to improve the image acquisition, segmentation and registration tools. During this work the CMR examination I used developed. One aspect of this is seen with the introduction of 3D tagging into the exam card. Using 3D tagging reduced acquisition time and improved tagged image quality making post processing easier and more reproducible. The development of better respiratory navigators and 3D imaging has definite potential to improve CMR imaging in heart failure patients. This may progress the ability of this imaging modality to improve patient selection. Furthermore with new CMR fiber tracking techniques there is potential to gain better understanding of the

pathological process that leads to LV failure. Better understanding of ventricular motion could potentially explain why only certain patients respond to CRT and could improve both the patient selection and response rates.

With the development of CMR compatible pacemakers one of the major limitations with respect to following up patients post device implantation will become less of an issue. This will allow improved follow up particularly how CRT affects the measures of myocardial motion.

With no definitive definition of response to CRT more work needs to be done on clarification of this. Although in this thesis I have used AHR and RR it is important to realize that clinical and cognitive improvements are equally important. The development of guidelines that allow assessment of these parameters is important for the future of further work in CRT.



## **Chapter 9**

### **General Conclusions**

This chapter summarizes the overall conclusions and suggests directions for future investigations. This thesis has demonstrated many potential benefits of using CMR to assess heart failure patients prior to CRT. A full assessment of heart failure patients is crucial to determine functional status and the aetiology of heart disease.

The benefits of patients awaiting CRT having a CMR prior to the implant exceed just functional and aetiological assessment. The accurate assessment of global dyssynchrony with volume SDI is a simple yet useful tool enabling stratification of which patients will benefit from CRT. I have demonstrated there exists a good relationship between acute haemodynamic response, reverse remodelling and volume SDI. The use of a pressure wire during an implant is invasive (arterial access) and not without risk of complications. The use of the pressure wire to determine LV lead position is important, but this is not feasible for all implants. However, by using a non-invasive assessment this has the potential to remove the potential of these complications and provide similar information to aid targeted LV lead implants.

By developing an all inclusive CMR examination protocol, which allows accurate assessment of coronary veins, and myocardial scar, I have shown it is feasible to demonstrate the relationship between potential target veins and likely viable and non-viable myocardium. Furthermore, it is demonstrated that it is feasible in real time to use this information during implantation of the CRT device.

The use of CMR is not without its limitations. Although CMR compatible pacemakers are being developed, the inability to do repeat scan post CRT is a major limitation. Ideally we require an imaging modality that enables assessment of function and mechanical changes pre and post implant. Using echocardiography to follow patients up has obvious limitations that need to be addressed.

Although CMR techniques that assess dyssynchrony, coronary veins, and registration-guided implantations have been developed, the studies herein are single centre and involve small numbers of patients. This work highlights the need for larger multicentre trials to assess further the ability of these techniques to improve response rates.

## References

1. Cowie MR, Mosterd A, Wood DA, Deckers JW, Poole-Wilson PA, Sutton GC, Grobbee DE. The epidemiology of heart failure. *Eur Heart J*. 1997;18:208-225
2. Nicol ED, Fittall B, Roughton M, Cleland JGF, Dargie H, Cowie MR. Nhs heart failure survey: A survey of acute heart failure admissions in england, wales and northern ireland. *Heart*. 2008;94:172-177
3. Cowie MR, Wood DA, Coats AJS, Thompson SG, Suresh V, Poole-Wilson PA, Sutton GC. Survival of patients with a new diagnosis of heart failure: A population based study. *Heart*. 2000;83:505-510
4. Levy D, Kenchaiah S, Larson MG, Benjamin EJ, Kupka MJ, Ho KKL, Murabito JM, Vasan RS. Long-term trends in the incidence of and survival with heart failure. *N Engl J Med*. 2002;347:1397-1402
5. Cowie MR, Wood DA, Coats AJ, Thompson SG, Poole-Wilson PA, Suresh V, Sutton GC. Incidence and aetiology of heart failure; a population-based study. *Eur Heart J*. 1999;20:421-428
6. Packer M, Coats AJS, Fowler MB, Katus HA, Krum H, Mohacsi P, Rouleau JL, Tendera M, Castaigne A, Roecker EB, Schultz MK, Staiger C, Curtin EL, DeMets DL, the Carvedilol Prospective Randomized Cumulative Survival Study Group. Effect of carvedilol on survival in severe chronic heart failure. *N Engl J Med*. 2001;344:1651-1658
7. Packer M, Poole-Wilson PA, Armstrong PW, Cleland JGF, Horowitz JD, Massie BM, Ryden L, Thygesen K, Uretsky BF. Comparative effects of low and high doses of the angiotensin-converting enzyme inhibitor, lisinopril,

- on morbidity and mortality in chronic heart failure. *Circulation*. 1999;100:2312-2318
8. Cohn JN, Tognoni G, the Valsartan Heart Failure Trial Investigators. A randomized trial of the angiotensin-receptor blocker valsartan in chronic heart failure. *N Engl J Med*. 2001;345:1667-1675
  9. Pfeffer MA, Swedberg K, Granger CB, Held P, McMurray JJ, Michelson EL, Olofsson B, Ostergren J, Yusuf S, Pocock S, Investigators C, Committees. Effects of candesartan on mortality and morbidity in patients with chronic heart failure: The charm-overall programme. *Lancet*. 2003;362:759-766
  10. Pitt B, Zannad F, Remme WJ, Cody R, Castaigne A, Perez A, Palensky J, Wittes J, The Randomized Aldactone Evaluation Study Investigators. The effect of spironolactone on morbidity and mortality in patients with severe heart failure. *N Engl J Med*. 1999;341:709-717
  11. Grines CL, Bashore TM, Boudoulas H, Olson S, Shafer P, Wooley CF. Functional abnormalities in isolated left bundle branch block. The effect of interventricular asynchrony. *Circulation*. 1989;79:845-853
  12. Baldasseroni S, Opasich C, Gorini M, Lucci D, Marchionni N, Marini M, Campana C, Perini G, Deorsola A, Masotti G, Tavazzi L, Maggioni AP. Left bundle-branch block is associated with increased 1-year sudden and total mortality rate in 5517 outpatients with congestive heart failure: A report from the italian network on congestive heart failure. *Am Heart J*. 2002;143:398-405
  13. Rossillo A, Verma A, Saad EB, Corrado A, Gasparini G, Marrouche NF, Golshayan AR, Mccurdy R, Bhargava M, Khaykin Y, Burkhardt JD, Martin DO, Wilkoff BL, Saliba WI, Schweikert RA, Raviele A, Natale A. Impact of

- coronary sinus lead position on biventricular pacing. *J Cardio Electrophysiol.* 2004;15:1120-1125
14. Ypenburg C, van Bommel RJ, Delgado V, Mollema SA, Bleeker GB, Boersma E, Schalij MJ, Bax JJ. Optimal left ventricular lead position predicts reverse remodeling and survival after cardiac resynchronization therapy. *J Am Coll of Cardiol.* 2008;52:1402-1409
  15. Butter C, Auricchio A, Stellbrink C, Fleck E, Ding J, Yu Y, Huvelle E, Spinelli J. Effect of resynchronization therapy stimulation site on the systolic function of heart failure patients. *Circulation.* 2001;104:3026-3029
  16. Curry CW, Nelson GS, Wyman BT, Declerck J, Talbot M, Berger RD, McVeigh ER, Kass DA. Mechanical dyssynchrony in dilated cardiomyopathy with intraventricular conduction delay as depicted by 3d tagged magnetic resonance imaging. *Circulation.* 2000;101:e2-
  17. Marsan NA, Bleeker GB, Ypenburg C, Ghio S, Van De Veire NR, Holman ER, Van Der Wall EE, Tavazzi L, Schalij MJ, Bax JJ. Real-time three-dimensional echocardiography permits quantification of left ventricular mechanical dyssynchrony and predicts acute response to cardiac resynchronization therapy. *J Cardio Electrophysiol.* 2008;19:392-399
  18. Auricchio A, Stellbrink C, Block M, Sack S, Vogt J, Bakker P, Klein H, Kramer A, Ding J, Salo R, Tockman B, Pochet T, Spinelli J. Effect of pacing chamber and atrioventricular delay on acute systolic function of paced patients with congestive heart failure. *Circulation.* 1999;99:2993-3001
  19. van Campen CMC, Visser FC, de Cock CC, Vos HS, Kamp O, Visser CA. Comparison of the haemodynamics of different pacing sites in patients

- undergoing resynchronisation treatment: Need for individualisation of lead localisation. *Heart*. 2006;92:1795-1800
20. Higgins SL, Hummel JD, Niazi IK, Giudici MC, Worley SJ, Saxon LA, Boehmer JP, Higginbotham MB, De Marco T, Foster E, Yong PG. Cardiac resynchronization therapy for the treatment of heart failure in patients with intraventricular conduction delay and malignant ventricular tachyarrhythmias. *J Am Coll of Cardiol*. 2003;42:1454-1459
  21. Bax JJ, Abraham T, Barold SS, Breithardt OA, Fung JW, Garrigue S, Gorcsan J, Hayes DL, Kass DA, Knuuti J, Leclercq C, Linde C, Mark DB, Monaghan MJ, Nihoyannopoulos P, Schalij MJ, Stellbrink C, Yu CM. Cardiac resynchronization therapy: Part 1--issues before device implantation. *J Am Coll Cardiol*. 2005;46:2153-2167
  22. Cazeau S, Leclercq C, Lavergne T, Walker S, Varma C, Linde C, Garrigue S, Kappenberger L, Haywood GA, Santini M, Bailleul C, Daubert J-C, The Multisite Stimulation in Cardiomyopathies Study I. Effects of multisite biventricular pacing in patients with heart failure and intraventricular conduction delay. *N Engl J Med*. 2001;344:873-880
  23. Abraham WT, Hayes DL. Cardiac resynchronization therapy for heart failure. *Circulation*. 2003;108:2596-2603
  24. Young JB, Abraham WT, Smith AL, Leon AR, Lieberman R, Wilkoff B, Canby RC, Schroeder JS, Liem LB, Hall S, Wheelan K. Combined cardiac resynchronization and implantable cardioversion defibrillation in advanced chronic heart failure: The miracle icd trial. *JAMA*. 2003;289:2685-2694

25. Bristow MR, Saxon LA, Boehmer J, Krueger S, Kass DA, De Marco T, Carson P, DiCarlo L, DeMets D, White BG, DeVries DW, Feldman AM, the Comparison of Medical Therapy P, Defibrillation in Heart Failure I. Cardiac-resynchronization therapy with or without an implantable defibrillator in advanced chronic heart failure. *N Engl J Med.* 2004;350:2140-2150
26. Cleland JG, Daubert JC, Erdmann E, Freemantle N, Gras D, Kappenberger L, Tavazzi L, Investigators CR-HFC-HS. The effect of cardiac resynchronization on morbidity and mortality in heart failure. *N Engl J Med.* 2005;352:1539-1549
27. Auricchio A, Stellbrink C, Sack S, Block M, Vogt J, Bakker P, Mortensen P, Klein H. The pacing therapies for congestive heart failure (path-chf) study: Rationale, design, and endpoints of a prospective randomized multicenter study. *Am J Cardiol.* 1999;83:130D-135D
28. Abraham WT, Fisher WG, Smith AL, Delurgio DB, Leon AR, Loh E, Kocovic DZ, Packer M, Clavell AL, Hayes DL, Ellestad M, Trupp RJ, Underwood J, Pickering F, Truex C, McAtee P, Messenger J, the MSG. Cardiac resynchronization in chronic heart failure. *N Engl J Med.* 2002;346:1845-1853
29. Cleland JGF, Daubert J-C, Erdmann E, Freemantle N, Gras D, Kappenberger L, Tavazzi L, the Cardiac Resynchronization -- Heart Failure Study I. The effect of cardiac resynchronization on morbidity and mortality in heart failure. *N Engl J Med.* 2005;352:1539-1549

30. Stellbrink C, Auricchio A, Butter C, Sack S, Vogt J, Böcker D, Block M, Kirkels H, Ramdat-Misier A, Group P-CIS. Pacing therapies in congestive heart failure ii study. *Am J Cardiol.* 2000;86:138K-143K
31. Foley PWX, Leyva F, Frenneaux MP. What is treatment success in cardiac resynchronization therapy? *Eur Pacing Clin Electrophysiol.* 2009;11 Suppl 5:v58-65
32. Chalil S, Stegemann B, Muhyaldeem SA, Khadjooi K, Foley PW, Smith RE, Leyva F. Effect of posterolateral left ventricular scar on mortality and morbidity following cardiac resynchronization therapy. *Pacing Clin Electrophysiol.* 2007;30:1201-1209
33. Duckett SG, Ginks MR, Knowles BR, Ma Y, Shetty A, Bostock J, Cooklin M, Gill JS, Carr-White GS, Razavi R, Schaeffter T, Rhode KS, Rinaldi CA. Advanced image fusion to overlay coronary sinus anatomy with real-time fluoroscopy to facilitate left ventricular lead implantation in crt. *Pacing Clin Electrophysiol.* 2011;34:226-34
34. Derval N, Steendijk P, Gula LJ, Deplagne A, Laborderie J, Sacher F, Knecht S, Wright M, Nault I, Ploux S, Ritter P, Bordachar P, Lafitte S, Réant P, Klein GJ, Narayan SM, Garrigue S, Hocini M, Haissaguerre M, Clementy J, Jaïs P. Optimizing hemodynamics in heart failure patients by systematic screening of left ventricular pacing sites: The lateral left ventricular wall and the coronary sinus are rarely the best sites. *J Am Coll Cardiol.* 2010;55:566-575
35. Blanc JJ, Etienne Y, Gilard M, Mansourati J, Munier S, Bosch J, Benditt DG, Lurie KG. Evaluation of different ventricular pacing sites in patients with



- severe heart failure: Results of an acute hemodynamic study. *Circulation*. 1997;96:3273-3277
36. van Gelder BM, Meijer A, Bracke FA. Timing of the left ventricular electrogram and acute hemodynamic changes during implant of cardiac resynchronization therapy devices. *Pacing Clin Electrophysiol*. 2009;32 Suppl 1:S94-97
  37. van Gelder BM, Bracke FA, Meijer A, Pijls NHJ. The hemodynamic effect of intrinsic conduction during left ventricular pacing as compared to biventricular pacing. *J Am Coll Cardiol*. 2005;46:2305-2310
  38. van Gelder BM, Bracke FA, Meijer A, Lakerveld LJM, Pijls NHJ. Effect of optimizing the vv interval on left ventricular contractility in cardiac resynchronization therapy. *Am J Cardiol*. 2004;93:1500-1503
  39. Steendijk P, Tulner SA, Bax JJ, Oemrawsingh PV, Bleeker GB, van Erven L, Putter H, Verwey HF, Van Der Wall EE, Schalij MJ. Hemodynamic effects of long-term cardiac resynchronization therapy: Analysis by pressure-volume loops. *Circulation*. 2006;113:1295-1304
  40. Tournoux FB, Alabiad C, Fan D, Chen AA, Chaput M, Heist EK, Mela T, Mansour M, Reddy V, Ruskin JN, Picard MH, Singh JP. Echocardiographic measures of acute haemodynamic response after cardiac resynchronization therapy predict long-term clinical outcome. *Eur Heart J*. 2007;28:1143-1148
  41. Oguz E, Dagdeviren B, Bilsel T, Akdemir O, Erdinler I, Akyol A, Ulufer T, Tezel T, Gurkan K. Echocardiographic prediction of long-term response to biventricular pacemaker in severe heart failure. *Eur J Heart Fail*. 2002;4:83-90

42. Ansalone G, Giannantoni P, Ricci R, Trambaiolo P, Fedele F, Santini M. Doppler myocardial imaging to evaluate the effectiveness of pacing sites in patients receiving biventricular pacing. *J Am Coll Cardiol.* 2002;39:489-499
43. Berger R, Shankar A, Fruhwald F, Fahrleitner-Pammer A, Freemantle N, Tavazzi L, Cleland JGF, Pacher R. Relationships between cardiac resynchronization therapy and n-terminal pro-brain natriuretic peptide in patients with heart failure and markers of cardiac dyssynchrony: An analysis from the cardiac resynchronization in heart failure (care-hf) study. *Eur Heart J.* 2009;30:2109-2116
44. Bax JJ, Ansalone G, Breithardt OA, Derumeaux G, Leclercq C, Schalij MJ, Sogaard P, St John Sutton M, Nihoyannopoulos P. Echocardiographic evaluation of cardiac resynchronization therapy: Ready for routine clinical use? A critical appraisal. *J Am Coll Cardiol.* 2004;44:1-9
45. Yu C-M, Bleeker GB, Fung JW-H, Schalij MJ, Zhang Q, van der Wall EE, Chan Y-S, Kong S-L, Bax JJ. Left ventricular reverse remodeling but not clinical improvement predicts long-term survival after cardiac resynchronization therapy. *Circulation.* 2005;112:1580-1586
46. Auger D, van Bommel RJ, Bertini M, Delgado V, Ng ACT, Ewe SH, Shanks M, Marsan NA, Mooyaart EAQ, Witkowski T, Poldermans D, Schalij MJ, Bax JJ. Prevalence and characteristics of patients with clinical improvement but not significant left ventricular reverse remodeling after cardiac resynchronization therapy. *Am Heart J.* 2010;160:737-743

47. Bleeker G, Bax J, Fung J, van der Wall E, Zhang Q, Schalij M, Chan J, Yu C. Clinical versus echocardiographic parameters to assess response to cardiac resynchronization therapy. *Am J Cardiol.* 2006;97:260-263
48. Yu C-M, Chau E, Sanderson JE, Fan K, Tang M-O, Fung W-H, Lin H, Kong S-L, Lam Y-M, Hill MRS, Lau C-P. Tissue doppler echocardiographic evidence of reverse remodeling and improved synchronicity by simultaneously delaying regional contraction after biventricular pacing therapy in heart failure. *Circulation.* 2002;105:438-445
49. Bax JJ, Bleeker GB, Marwick TH, Molhoek SG, Boersma E, Steendijk P, van der Wall EE, Schalij MJ. Left ventricular dyssynchrony predicts response and prognosis after cardiac resynchronization therapy. *J Am Coll Cardiol.* 2004;44:1834-1840
50. Rector TS, Kubo SH, Cohn JN. Validity of the minnesota living with heart failure questionnaire as a measure of therapeutic response to enalapril or placebo. *Am J Cardiol.* 1993;71:1106-1107
51. van Campen CMC, Visser FC, de Cock CC, Vos HS, Kamp O, Visser CA. Comparison of the haemodynamics of different pacing sites in patients undergoing resynchronisation treatment: Need for individualisation of lead localisation. *Heart.* 2006;92:1795-1800
52. Bleeker GB, Schalij MJ, Molhoek SG, Verwey HF, Holman ER, Boersma E, Steendijk P, Van Der Wall EE, Bax JJ. Relationship between qrs duration and left ventricular dyssynchrony in patients with end-stage heart failure. *J Cardiovasc Electrophysiol.* 2004;15:544-549
53. Auricchio A, Fantoni C, Regoli F, Carbucicchio C, Goette A, Geller C, Kloss M, Klein H. Characterization of left ventricular activation in patients with

- heart failure and left bundle-branch block. *Circulation*. 2004;109:1133-1139
54. Rodriguez LM, Timmermans C, Nabar A, Beatty G, Wellens HJ. Variable patterns of septal activation in patients with left bundle branch block and heart failure. *J Cardiovasc Electrophysiol*. 2003;14:135-141
  55. Taccardi B, Arisi G, Macchi E, Baruffi S, Spaggiari S. A new intracavitary probe for detecting the site of origin of ectopic ventricular beats during one cardiac cycle. *Circulation*. 1987;75:272-281
  56. Lambiase PD, Rinaldi A, Hauck J, Mobb M, Elliott D, Mohammad S, Gill JS, Bucknall CA. Non-contact left ventricular endocardial mapping in cardiac resynchronisation therapy. *Heart*. 2004;90:44-51
  57. Fung JWH, Chan JYS, Yip GWK, Chan HCK, Chan WWL, Zhang Q, Yu C-M. Effect of left ventricular endocardial activation pattern on echocardiographic and clinical response to cardiac resynchronization therapy. *Heart*. 2007;93:432-437
  58. Nishimura RA, Hayes DL, Holmes DR, Tajik AJ. Mechanism of hemodynamic improvement by dual-chamber pacing for severe left ventricular dysfunction: An acute doppler and catheterization hemodynamic study. *J Am Coll Cardiol*. 1995;25:281-288
  59. Parsai C, Bijnsens B, Sutherland GR, Baltaeva A, Claus P, Marciniak M, Paul V, Scheffer M, Donal E, Derumeaux G, Anderson L. Toward understanding response to cardiac resynchronization therapy: Left ventricular dyssynchrony is only one of multiple mechanisms. *Eur Heart J*. 2009;30:940-949

60. Anderson RH, Smerup M, Sanchez-Quintana D, Loukas M, Lunkenheimer PP. The three-dimensional arrangement of the myocytes in the ventricular walls. *Clin Anat.* 2009;22:64-76
61. Coppola BA, Omens JH. Role of tissue structure on ventricular wall mechanics. *Mol Cell Biomech.* 2008;5:183-196
62. Mirsky I, Parmley WW. Assessment of passive elastic stiffness for isolated heart muscle and the intact heart. *Circ Res.* 1973;33:233-243
63. Abraham TP, Nishimura RA. Myocardial strain: Can we finally measure contractility? *J Am Coll Cardiol.* 2001;37:731-734
64. Streeter DD, Spotnitz HM, Patel DP, Ross J, Sonnenbl.Eh. Fiber orientation in canine left ventricle during diastole and systole. *Circulation Research.* 1969;24:339
65. Ashikaga H, Coppola BA, Hopenfeld B, Leifer ES, McVeigh ER, Omens JH. Transmural dispersion of myofiber mechanics: Implications for electrical heterogeneity in vivo. *J Am Coll Cardiol.* 2007;49:909-916
66. Zwanenburg JJM, Gotte MJW, Kuijter JPA, Heethaar RM, van Rossum AC, Marcus JT. Timing of cardiac contraction in humans mapped by high-temporal-resolution mri tagging: Early onset and late peak of shortening in lateral wall. *Am J Physiol Heart Circ Physiol.* 2004;286:H1872-1880
67. Sengupta PP, Khandheria BK, Korinek J, Wang J, Jahangir A, Seward JB, Belohlavek M. Apex-to-base dispersion in regional timing of left ventricular shortening and lengthening. *J Am Coll Cardiol.* 2006;47:163-172
68. Plotnikov AN, Sosunov EA, Qu J, Shlapakova IN, Anyukhovskiy EP, Liu L, Janse MJ, Brink PR, Cohen IS, Robinson RB, Danilo P, Jr, Rosen MR.

Biological pacemaker implanted in canine left bundle branch provides ventricular escape rhythms that have physiologically acceptable rates.

*Circulation*. 2004;109:506-512

69. Graybiel A, McFarland RA, Gates DC, Webster FA. Analysis of the electrocardiograms obtained from 1000 young healthy aviators. *Am Heart J*. 1944;27:524-549
70. Antzelevitch C. Cardiac repolarization. The long and short of it. *Eur Pacing Clin Electrophysiol*. 2005;7:S3-S9
71. Antzelevitch C, Sicouri S, Litovsky S, Lukas A, Krishnan S, Di Diego J, Gintant G, Liu D. Heterogeneity within the ventricular wall. Electrophysiology and pharmacology of epicardial, endocardial, and m cells. *Circ Res*. 1991;69:1427-1449
72. Durrer D, Van Dam RT, Freud GE, Janse MJ, Meijler FL, Arzbaecher RC. Total excitation of the isolated human heart. 1970;41:899-912
73. Greenbaum RA, Ho SY, Gibson DG, Becker AE, Anderson RH. Left ventricular fibre architecture in man. *Br Heart J*. 1981;45:248-263
74. Nielsen PM, Le Grice IJ, Smaill BH, Hunter PJ. Mathematical model of geometry and fibrous structure of the heart. *Am J Physiol Heart Circ Physiol*. 1991;260:H1365-1378
75. LeGrice IJ, Smaill BH, Chai LZ, Edgar SG, Gavin JB, Hunter PJ. Laminar structure of the heart: Ventricular myocyte arrangement and connective tissue architecture in the dog. *Am J Physiol*. 1995;269:571-582
76. Bogaert J, Rademakers FE. Regional nonuniformity of normal adult human left ventricle. *Am J Physiol Heart Circ Physiol*. 2001;280:H610-H620

77. Cordeiro JM, Greene L, Heilmann C, Antzelevitch D, Antzelevitch C. Transmural heterogeneity of calcium activity and mechanical function in the canine left ventricle. *Am J Physiol Heart Circ Physiol*. 2004;286:H1471-1479
78. Cazorla O, Le Guennec J-Y, White E. Length-tension relationships of sub-epicardial and sub-endocardial single ventricular myocytes from rat and ferret hearts. *J Molecul Cellul Cardiol*. 2000;32:735-744
79. Cazorla O, Szilagyi S, Le Guennec J-Y, Vassort G, Lacampagne A. Transmural stretch-dependent regulation of contractile properties in rat heart and its alteration after myocardial infarction. *FASEB J*. 2005;19:88-90
80. Delgado V, Ypenburg C, van Bommel RJ, Tops LF, Mollema SA, Marsan NA, Bleeker GB, Schalij MJ, Bax JJ. Assessment of left ventricular dyssynchrony by speckle tracking strain imaging: Comparison between longitudinal, circumferential, and radial strain in cardiac resynchronization therapy. *J Am Coll Cardiol*. 2008;51:1944-1952
81. Helm RH, Leclercq C, Faris OP, Ozturk C, McVeigh E, Lardo AC, Kass DA. Cardiac dyssynchrony analysis using circumferential versus longitudinal strain: Implications for assessing cardiac resynchronization. *Circulation*. 2005;111:2760-2767
82. Dumesnil JG, Shoucri RM. Quantitative relationships between left ventricular ejection and wall thickening and geometry. *J Applied Physiol*. 1991;70:48-54
83. Dodge HT, Frimer M, Stewart DK. Functional evaluation of the hypertrophied heart in man. *Circ Res*. 1974;35:suppl II:122-127

84. Gould KL, Kennedy JW, Frimer M, Pollack GH, Dodge HT. Analysis of wall dynamics and directional components of left ventricular contraction in man. *Am J Cardiol.* 1976;38:322-331
85. LeGrice IJ, Takayama Y, Covell JW. Transverse shear along myocardial cleavage planes provides a mechanism for normal systolic wall thickening. *Circ Res.* 1995;77:182-193
86. Chen J, Liu W, Zhang H, Lacy L, Yang X, Song S-K, Wickline SA, Yu X. Regional ventricular wall thickening reflects changes in cardiac fiber and sheet structure during contraction: Quantification with diffusion tensor mri. *Am J Physiol Heart Circ Physiol.* 2005;289:H1898-1907
87. Costa KD, Takayama Y, McCulloch AD, Covell JW. Laminar fiber architecture and three-dimensional systolic mechanics in canine ventricular myocardium. *Am J Physiol Heart Circ Physiol.* 1999;276:H595-607
88. Takayama Y, Costa KD, Covell JW. Contribution of laminar myofiber architecture to load-dependent changes in mechanics of lv myocardium. *Am J Physiol Heart Circ Physiol.* 2002;282:H1510-1520
89. Rademakers FE, Rogers WJ, Guier WH, Hutchins GM, Siu CO, Weisfeldt ML, Weiss JL, Shapiro EP. Relation of regional cross-fiber shortening to wall thickening in the intact heart. Three-dimensional strain analysis by nmr tagging. *Circulation.* 1994;89:1174-1182
90. Gallagher K, Gerren R, Stirling M, Choy M, Dysko R, McManimon S, Dunham W. The distribution of functional impairment across the lateral border of acutely ischemic myocardium. *Circ Res.* 1986;58:570-583



91. Perrone-Filardi P, Bacharach S, Dilsizian V, Maurea S, Frank J, Bonow R. Regional left ventricular wall thickening. Relation to regional uptake of <sup>18</sup>fluorodeoxyglucose and <sup>201</sup>Tl in patients with chronic coronary artery disease and left ventricular dysfunction. *Circulation*. 1992;86:1125-1137
92. Ukkonen H, Beanlands RSB, Burwash IG, de Kemp RA, Nahmias C, Fallen EH, Anthony MRS, Tang SL. Effect of cardiac resynchronization on myocardial efficiency and regional oxidative metabolism. *Circulation*. 2003;107:28-31
93. Galderisi M, Cattaneo F, Mondillo S. Doppler echocardiography and myocardial dyssynchrony: A practical update of old and new ultrasound technologies. *Cardiovasc Ultrasound*. 2007;5:28
94. Cazeau S, Bordachar P, Jauvert G, Lazarus A, Alonso C, Vandrell MC, Mugica J, Ritter P. Echocardiographic modeling of cardiac dyssynchrony before and during multisite stimulation: A prospective study. *Pacing Clin Electrophysiol*. 2003;26:137-143
95. Pitzalis MV, Iacoviello M, Romito R, Massari F, Rizzon B, Luzzi G, Guida P, Andriani A, Mastropasqua F, Rizzon P. Cardiac resynchronization therapy tailored by echocardiographic evaluation of ventricular asynchrony. *J Am Coll Cardiol*. 2002;40:1615-1622
96. Marcus GM, Rose E, Vioria EM, Schafer J, De Marco T, Saxon LA, Foster E, Investigators VCC-CBPS. Septal to posterior wall motion delay fails to predict reverse remodeling or clinical improvement in patients undergoing cardiac resynchronization therapy. *J Am Coll Cardiol*. 2005;46:2208-2214

97. Bleeker GB, Schalij MJ, Boersma E, Holman ER, Steendijk P, van der Wall EE, Bax JJ. Relative merits of m-mode echocardiography and tissue doppler imaging for prediction of response to cardiac resynchronization therapy in patients with heart failure secondary to ischemic or idiopathic dilated cardiomyopathy. *Am J Cardiol.* 2007;99:68-74
98. Bax JJ, Marwick TH, Molhoek SG, Bleeker GB, van Erven L, Boersma E, Steendijk P, van der Wall EE, Schalij MJ. Left ventricular dyssynchrony predicts benefit of cardiac resynchronization therapy in patients with end-stage heart failure before pacemaker implantation. *Am J Cardiol.* 2003;92:1238-1240
99. Yu CM, Fung WH, Lin H, Zhang Q, Sanderson JE, Lau CP. Predictors of left ventricular reverse remodeling after cardiac resynchronization therapy for heart failure secondary to idiopathic dilated or ischemic cardiomyopathy. *Am J Cardiol.* 2003;91:684-688
100. Yu CM, Gorcsan J, 3rd, Bleeker GB, Zhang Q, Schalij MJ, Suffoletto MS, Fung JW, Schwartzman D, Chan YS, Tanabe M, Bax JJ. Usefulness of tissue doppler velocity and strain dyssynchrony for predicting left ventricular reverse remodeling response after cardiac resynchronization therapy. *Am J Cardiol.* 2007;100:1263-1270
101. Suffoletto MS, Dohi K, Cannesson M, Saba S, Gorcsan J, III. Novel speckle-tracking radial strain from routine black-and-white echocardiographic images to quantify dyssynchrony and predict response to cardiac resynchronization therapy. *Circulation.* 2006;113:960-968
102. Kapetanakis S, Kearney MT, Siva A, Gall N, Cooklin M, Monaghan MJ. Real-time three-dimensional echocardiography: A novel technique to quantify

- global left ventricular mechanical dyssynchrony. *Circulation*. 2005;112:992-1000
103. Chung ES, Leon AR, Tavazzi L, Sun J-P, Nihoyannopoulos P, Merlino J, Abraham WT, Ghio S, Leclercq C, Bax JJ, Yu C-M, Gorcsan J, III, St John Sutton M, De Sutter J, Murillo J. Results of the predictors of response to crt (prospect) trial. *Circulation*. 2008;117:2608-2616
  104. Simonetti OP, Kim RJ, Fieno DS, Hillenbrand HB, Wu E, Bundy JM, Finn JP, Judd RM. An improved mr imaging technique for the visualization of myocardial infarction. *Radiology*. 2001;218:215-223
  105. Kim RJ, Wu E, Rafael A, Chen E-L, Parker MA, Simonetti O, Klocke FJ, Bonow RO, Judd RM. The use of contrast-enhanced magnetic resonance imaging to identify reversible myocardial dysfunction. *N Engl J Med*. 2000;343:1445-1453
  106. Kautzner J, Riedlbauchová L, Cihák R, Bytesník J, Vancura V. Technical aspects of implantation of lv lead for cardiac resynchronization therapy in chronic heart failure. *Pacing Clin Electrophysiol*. 2004;27:783-790
  107. Rasche V, Binner L, Cavagna F, Hombach V, Kunze M, Spiess J, Stuber M, Merkle N. Whole-heart coronary vein imaging: A comparison between non-contrast-agent- and contrast-agent-enhanced visualization of the coronary venous system. *Magnetic resonance in medicine*. 2007;57:1019-1026
  108. Chiribiri A, Kelle S, Götze S, Kriatselis C, Thouet T, Tangcharoen T, Paetsch I, Schnackenburg B, Fleck E, Nagel E. Visualization of the cardiac venous system using cardiac magnetic resonance. *Am J Cardiol*. 2008;101:407-412

109. Nezafat R, Han Y, Peters DC, Herzka DA, Wylie JV, Goddu B, Kissinger KK, Yeon SB, Zimetbaum PJ, Manning WJ. Coronary magnetic resonance vein imaging: Imaging contrast, sequence, and timing. *Magnetic resonance in medicine*. 2007;58:1196-1206
110. Younger JF, Plein S, Crean A, Ball SG, Greenwood JP. Visualization of coronary venous anatomy by cardiovascular magnetic resonance. *J Cardio Magn Reson*. 2009;11:26
111. Mischi M, van den Bosch HM, Jansen AM, Sieben M, Aarts RM, Korsten HM. Quantification of regional left ventricular dyssynchrony by magnetic resonance imaging. *IEEE Trans Biomed Eng*. 2008;55:985-995
112. Mischi M, v d Bosch HCM, Jansen AHM, Aarts RM, Korsten HHM. Assessment of ventricular mechanical dyssynchrony by short-axis mri. *ConfProc IEEE Eng Med Biol Soc*. 2007;2007:6012-6015
113. Ordas S, Frangi A. Automatic quantitative analysis of myocardial wall motion and thickening from long-and short-axis cine mri studies. *Conf Proc IEEE Eng Med Biol Soc*. 2005;7:7028-7031
114. Fornwalt BK, Gonzales PC, Delfino JG, Eisner R, León AR, Oshinski JN. Quantification of left ventricular internal flow from cardiac magnetic resonance images in patients with dyssynchronous heart failure. *J Magn Reson Imaging*. 2008;28:375-381
115. Uribe S, Tejos C, Razavi R, Schaeffter T. New respiratory gating technique for whole heart cine imaging: Integration of a navigator slice in steady state free precession sequences. *J Magn Reson Imaging*. 2011;34:211-219
116. Chalil S, Stegemann B, Muhyaldeem S, Khadjooi K, Smith RE, Jordan PJ, Leyva F. Intraventricular dyssynchrony predicts mortality and morbidity

- after cardiac resynchronization therapy: A study using cardiovascular magnetic resonance tissue synchronization imaging. *J Am Coll Cardiol.* 2007;50:243-252
117. Zerhouni EA, Parish DM, Rogers WJ, Yang A, Shapiro EP. Human heart: Tagging with mr imaging--a method for noninvasive assessment of myocardial motion. *Radiology.* 1988;169:59-63
  118. Ibrahim el SH, Stuber M, Schar M, Osman NF. Improved myocardial tagging contrast in cine balanced ssfp images. *J Magn Reson Imaging.* 2006;24:1159-1167
  119. Shehata ML, Cheng S, Osman NF, Bluemke DA, Lima JAC. Myocardial tissue tagging with cardiovascular magnetic resonance. *J Cardio Magn Reson.* 2009;11:55
  120. Lardo AC, Abraham TP, Kass DA. Magnetic resonance imaging assessment of ventricular dyssynchrony: Current and emerging concepts. *J Am Coll Cardiol.* 2005;46:2223-2228
  121. Prinzen FW, Hunter WC, Wyman BT, McVeigh ER. Mapping of regional myocardial strain and work during ventricular pacing: Experimental study using magnetic resonance imaging tagging. *J Am Coll Cardiol.* 1999;33:1735-1742
  122. Osman NF, Kerwin WS, McVeigh ER, Prince JL. Cardiac motion tracking using cine harmonic phase (harp) magnetic resonance imaging. *Magn Reson Med.* 1999;42:1048-1060
  123. Garot J, Bluemke DA, Osman NF, Rochitte CE, McVeigh ER, Zerhouni EA, Prince JL, Lima JAC. Fast determination of regional myocardial strain

- fields from tagged cardiac images using harmonic phase mri. *Circulation*. 2000;101:981-988
124. Bilchick KC, Dimaano V, Wu KC, Helm RH, Weiss RG, Lima JA, Berger RD, Tomaselli GF, Bluemke DA, Halperin HR, Abraham T, Kass DA, Lardo AC. Cardiac magnetic resonance assessment of dyssynchrony and myocardial scar predicts function class improvement following cardiac resynchronization therapy. *JACC Cardiovasc Imaging*. 2008;1:561-568
  125. Xu C, Pilla JJ, Isaac G, Gorman JH, Blom AS, Gorman RC, Ling Z, Dougherty L. Deformation analysis of 3d tagged cardiac images using an optical flow method. *J Cardio Magn Reson*. 2010;12:19
  126. Ghio S, Constantin C, Klersy C, Serio A, Fontana A, Campana C, Tavazzi L. Interventricular and intraventricular dyssynchrony are common in heart failure patients, regardless of qrs duration. *Eur Heart J*. 2004;25:571-578
  127. Yu C-M, Fung W-H, Lin H, Zhang Q, Sanderson JE, Lau C-P. Predictors of left ventricular reverse remodeling after cardiac resynchronization therapy for heart failure secondary to idiopathic dilated or ischemic cardiomyopathy. *Am J Cardiol*. 2003;91:684-688
  128. Rutz AK, Ryf S, Plein S, Boesiger P, Kozerke S. Accelerated whole-heart 3d cspamm for myocardial motion quantification. *Magn Reson med*. 2008;59:755-763
  129. Lima JA, Judd RM, Bazille A, Schulman SP, Atalar E, Zerhouni EA. Regional heterogeneity of human myocardial infarcts demonstrated by contrast-enhanced mri. Potential mechanisms. *Circulation*. 1995;92:1117-1125

130. Zhuang X, Rhode KS, Razavi RS, Hawkes DJ, Ourselin S. A registration-based propagation framework for automatic whole heart segmentation of cardiac mri. *IEEE transactions on medical imaging*. 2010;29:1612-1625
131. Gersh BJ, Hahn CE, Prys-Roberts C. Physical criteria for measurement of left ventricular pressure and its first derivative. *Cardiovasc Res*. 1971;5:32-40
132. van Gelder BM, Meijer A, Bracke FA. Stimulation rate and the optimal interventricular interval during cardiac resynchronization therapy in patients with chronic atrial fibrillation. *Pacing Clin Electrophysiol*. 2008;31:569-574
133. Bland JM, Altman DG. Statistical methods for assessing agreement between two methods of clinical measurement. *Lancet*. 1986;1:307-310
134. Chalil S, Foley PWX, Muyhaldeen SA, Patel KCR, Yousef ZR, Smith REA, Frenneaux MP, Leyva F. Late gadolinium enhancement-cardiovascular magnetic resonance as a predictor of response to cardiac resynchronization therapy in patients with ischaemic cardiomyopathy. *Eur Pacing Clin Electrophysiol*. 2007;9:1031-1037
135. Chung ES, Leon AR, Tavazzi L, Sun JP, Nihoyannopoulos P, Merlino J, Abraham WT, Ghio S, Leclercq C, Bax JJ, Yu CM, Gorcsan J, St John Sutton M, De Sutter J, Murillo J. Results of the predictors of response to crt (prospect) trial. *Circulation*. 2008;117:2608-2616
136. Foley PWX, Chalil S, Khadjooi K, Irwin N, Smith RE, Leyva F. Left ventricular reverse remodelling, long-term clinical outcome, and mode of death after cardiac resynchronization therapy. *Eur J Heart Fail*. 2010

137. Nelson GS, Berger RD, Fetters BJ, Talbot M, Spinelli JC, Hare JM, Kass DA. Left ventricular or biventricular pacing improves cardiac function at diminished energy cost in patients with dilated cardiomyopathy and left bundle-branch block. *Circulation*. 2000;102:3053-3059
138. Garrigue S, Bordachar P, Reuter S, Jaïs P, Kobeissi A, Gaggini G, Haïssaguerre M, Clementy J. Comparison of permanent left ventricular and biventricular pacing in patients with heart failure and chronic atrial fibrillation: Prospective haemodynamic study. *Heart*. 2002;87:529-534
139. De Boeck BW, Teske AJ, Meine M, Leenders GE, Cramer MJ, Prinzen FW, Doevendans PA. Septal rebound stretch reflects the functional substrate to cardiac resynchronization therapy and predicts volumetric and neurohormonal response. *Eur J Heart Fail*. 2009;11:863-871
140. Kirn B, Jansen A, Bracke F, van Gelder B, Arts T, Prinzen FW. Mechanical discoordination rather than dyssynchrony predicts reverse remodeling upon cardiac resynchronization. *Am J Physiol Heart Circ Physiol*. 2008;295:H640-646
141. Cikes M, Bijnsens B, Durić Z, Bencic ML, Gosev I, Velagić V, Gasparović H, Milčić D, Biocina B. Detecting volume responders prior to implantation of a cardiac resynchronization therapy device via minithoracotomy: The septal flash as a predictor of immediate left ventricular reverse remodeling. *Heart Surg Forum*. 2009;12:E362-367
142. Voigt JU, Schneider TM, Korder S, Szulik M, Gürel E, Daniel WG, Rademakers F, Flachskampf FA. Apical transverse motion as surrogate parameter to determine regional left ventricular function



- inhomogeneities: A new, integrative approach to left ventricular asynchrony assessment. *Eur Heart J*. 2009;30:959-968
143. Kerckhoffs RC, Faris OP, Bovendeerd PH, Prinzen FW, Smits K, McVeigh ER, Arts T. Electromechanics of paced left ventricle simulated by straightforward mathematical model: Comparison with experiments. *Am J Physiol Heart Circ Physiol*. 2005;289:H1889-1897
  144. Gornick CC, Adler SW, Pederson B, Hauck J, Budd J, Schweitzer J. Validation of a new noncontact catheter system for electroanatomic mapping of left ventricular endocardium. *Circulation*. 1999;99:829-835
  145. Fung JW, Chan JY, Yip GW, Chan HC, Chan WW, Zhang Q, Yu CM. Effect of left ventricular endocardial activation pattern on echocardiographic and clinical response to cardiac resynchronization therapy. *Heart*. 2007;93:432-437
  146. Lab MJ. Mechanosensitive-mediated interaction, integration, and cardiac control. *Ann N Y Acad Sci*. 2006;1080:282-300
  147. Kuijpers NH, ten Eikelder HM, Bovendeerd PH, Verheule S, Arts T, Hilbers PA. Mechanoelectric feedback leads to conduction slowing and block in acutely dilated atria: A modeling study of cardiac electromechanics. *Am J Physiol Heart Circ Physiol*. 2007;292:H2832-2853
  148. Kerckhoffs RC, Lumens J, Vernooy K, Omens JH, Mulligan LJ, Delhaas T, Arts T, McCulloch AD, Prinzen FW. Cardiac resynchronization: Insight from experimental and computational models. *Prog Biophys Mol Biol*. 2008;97:543-561

149. Lima JAC, Judd RM, Bazille A, Schulman SP, Atalar E, Zerhouni EA. Regional heterogeneity of human myocardial infarcts demonstrated by contrast-enhanced mri : Potential mechanisms. *Circulation*. 1995;92:1117-1125
150. Schilling RJ, Peters NS, Davies DW. Simultaneous endocardial mapping in the human left ventricle using a noncontact catheter : Comparison of contact and reconstructed electrograms during sinus rhythm. *Circulation*. 1998;98:887-898
151. Bleeker GB, Kaandorp TA, Lamb HJ, Boersma E, Steendijk P, de Roos A, Van Der Wall EE, Schalij MJ, Bax JJ. Effect of posterolateral scar tissue on clinical and echocardiographic improvement after cardiac resynchronization therapy. *Circulation*. 2006;113:969-976
152. Ypenburg C, Schalij MJ, Bleeker GB, Steendijk P, Boersma E, Dibbets-Schneider P, Stokkel MP, van der Wall EE, Bax JJ. Impact of viability and scar tissue on response to cardiac resynchronization therapy in ischaemic heart failure patients. *Eur Heart J*. 2007;28:33-41
153. Rovner A, de Las Fuentes L, Faddis MN, Gleva MJ, Dávila-Román VG, Waggoner AD. Relation of left ventricular lead placement in cardiac resynchronization therapy to left ventricular reverse remodeling and to diastolic dyssynchrony. *Am J Cardiol*. 2007;99:239-241
154. Jongbloed MR, Lamb HJ, Bax JJ, Schuijf JD, de Roos A, Van Der Wall EE, Schalij MJ. Noninvasive visualization of the cardiac venous system using multislice computed tomography. *J Am Coll Cardiol*. 2005;45:749-753
155. Chiribiri A, Kelle S, Köhler U, Tops LF, Schnackenburg B, Bonamini R, Bax JJ, Fleck E, Nagel E. Magnetic resonance cardiac vein imaging: Relation to

- mitral valve annulus and left circumflex coronary artery. *JACC Cardiovasc Imaging*. 2008;1:729-738
156. Gerber TC, Sheedy PF, Bell MR, Hayes DL, Rumberger JA, Behrenbeck T, Holmes DR, Schwartz RS. Evaluation of the coronary venous system using electron beam computed tomography. *International J Cardio imaging*. 2001;17:65-75
  157. Kim RJ, Wu E, Rafael A, Chen EL, Parker MA, Simonetti O, Klocke FJ, Bonow RO, Judd RM. The use of contrast-enhanced magnetic resonance imaging to identify reversible myocardial dysfunction. *N Engl J Med*. 2000;343:1445-1453
  158. Ørn S, Manhenke C, Anand IS, Squire I, Nagel E, Edvardsen T, Dickstein K. Effect of left ventricular scar size, location, and transmuralty on left ventricular remodeling with healed myocardial infarction. *Am J Cardio*. 2007;99:1109-1114
  159. Nagel E, Schneider U, Schalla S, Ibrahim T, Schnackenburg B, Bornstedt A, Klein C, Lehmkuhl HB, Fleck E. Magnetic resonance real-time imaging for the evaluation of left ventricular function. *J Cardio Magn Reson*. 2000;2:7-14
  160. Bi X, Carr JC, Li D. Whole-heart coronary magnetic resonance angiography at 3 tesla in 5 minutes with slow infusion of gd-bopta, a high-relaxivity clinical contrast agent. *Magne Reson Med*. 2007;58:1-7
  161. Andersen K, Hennersdorf M, Cohnen M, Blondin D, Mödder U, Poll LW. Myocardial delayed contrast enhancement in patients with arterial hypertension: Initial results of cardiac mri. *Eur J Radiol*. 2009;71:75-81

162. Sandstede JJ, Beer M, Lipke C, Pabst T, Kenn W, Harre K, Neubauer S, Hahn D. Time course of contrast enhancement patterns after gd-bopta in correlation to myocardial infarction and viability: A feasibility study. *J Magn Reson Imaging*. 2001;14:789-794
163. Schlosser T, Hunold P, Herborn CU, Lehmkuhl H, Lind A, Massing S, Barkhausen J. Myocardial infarct: Depiction with contrast-enhanced mr imaging--comparison of gadopentetate and gadobenate. *Radiology*. 2005;236:1041-1046
164. Ortale JR, Gabriel EA, Iost C, Márquez CQ. The anatomy of the coronary sinus and its tributaries. *Surg radio anatomy*. 2001;23:15-21
165. Rosset A, Spadola L, Ratib O. Osirix: An open-source software for navigating in multidimensional dicom images. *J digital imaging*. 2004;17:205-216
166. Yushkevich PA, Piven J, Hazlett HC, Smith RG, Ho S, Gee JC, Gerig G. User-guided 3d active contour segmentation of anatomical structures: Significantly improved efficiency and reliability. *Neuroimage*. 2006;31:1116-1128
167. McConnell MV, Khasgiwala VC, Savord BJ, Chen MH, Chuang ML, Edelman RR, Manning WJ. Comparison of respiratory suppression methods and navigator locations for mr coronary angiography. *Am J roentgenology*. 1997;168:1369-1375
168. Rhode KS, Hill DL, Edwards PJ, Hipwell J, Rueckert D, Sanchez-Ortiz G, Hegde S, Rahunathan V, Razavi R. Registration and tracking to integrate x-ray and mr images in an xmr facility. *IEEE transactions on medical imaging*. 2003;22:1369-1378

169. Auricchio A, Sorgente A, Soubelet E, Regoli F, Spinucci G, Vaillant R, Faletra FF, Klersy C, Moccetti T. Accuracy and usefulness of fusion imaging between three-dimensional coronary sinus and coronary veins computed tomographic images with projection images obtained using fluoroscopy. *Eur Pacing Clin Electrophysiol.* 2009;11:1483-1490
170. Knackstedt C, Mühlenbruch G, Mischke K, Schimpf T, Spüntrup E, Günther RW, Sanli B, Kelm M, Schauerte P, Mahnken AH. Imaging of the coronary venous system in patients with congestive heart failure: Comparison of 16 slice msct and retrograde coronary sinus venography: Comparative imaging of coronary venous system. *International J cardio imaging.* 2008;24:783-791
171. Duckett SG, Chiribiri A, Ginks MR, Sinclair S, Knowles BR, Botnar R, Carr-White GS, Rinaldi CA, Nagel E, Razavi R, Schaeffter T. Cardiac mri to investigate myocardial scar and coronary venous anatomy using a slow infusion of dimeglumine gadobenate in patients undergoing assessment for cardiac resynchronization therapy. *J Magn Reson Imaging.* 2011;33:87-95
172. Rhode KS, Hill DLG, Edwards PJ, Hipwell J, Rueckert D, Sanchez-Ortiz G, Hegde S, Rahunathan V, Razavi R. Registration and tracking to integrate x-ray and mr images in an xmr facility. *Medical Imaging, IEEE Transactions on.* 2003;22:1369-1378
173. Auricchio A, Sorgente A, Singh JP, Faletra F, Conca C, Pedrazzini GB, Pasotti E, Siclari F, Moccetti T. Role of multislice computed tomography for preprocedural evaluation before revision of a chronically implanted transvenous left ventricular lead. *Am J Cardiol.* 2007;100:1566-1570

174. Knecht S, Skali H, O'Neill MD, Wright M, Matsuo S, Chaudhry GM, Haffajee CI, Nault I, Gijssbers GH, Sacher F, Laurent F, Montaudon M, Corneloup O, Hocini M, Haïssaguerre M, Orlov MV, Jaïs P. Computed tomography-fluoroscopy overlay evaluation during catheter ablation of left atrial arrhythmia. *Eur Pacing Clin Electrophysiol.* 2008;10:931-938
175. Singh JP, Houser S, Heist EK, Ruskin JN. The coronary venous anatomy: A segmental approach to aid cardiac resynchronization therapy. *J Am Coll Cardiol.* 2005;46:68-74
176. Macías A, García-Bolao I, Díaz-Infante E, Tolosana JM, Vidal B, Gavira JJ, Berruezo A, Brugada J, Mont L. Cardiac resynchronization therapy: Predictive factors of unsuccessful left ventricular lead implant. *Eur Heart J.* 2007;28:450-456

## Appendix 1

### Publications from this Thesis

#### *Refereed Publications*

**Duckett SG**, Ginks M, Shetty AK, Bostock J, Gill JS, Hamid S, Kapetanakis S, Cunliffe E, Razavi R, Carr-White G, Rinaldi CA. Invasive acute hemodynamic response to guide left ventricular lead implantation predicts chronic remodeling in patients undergoing cardiac resynchronization therapy. *J Am Coll Cardiol.* 2011;58:1128-1136

**Duckett SG**, Ginks MR, Knowles BR, Ma Y, Shetty A, Bostock J, Cooklin M, Gill JS, Carr-White GS, Razavi R, Schaeffter T, Rhode KS, Rinaldi CA. Advanced image fusion to overlay coronary sinus anatomy with real-time fluoroscopy to facilitate left ventricular lead implantation in crt. *Pacing Clin Electrophysiol.* 2011;34:226-34

**Duckett SG**, Ginks M, Shetty AK, Knowles BR, Totman JJ, Chiribiri A, Ma Y-L, Razavi R, Schaeffter T, Carr-White G, Rhode K, Rinaldi CA. Realtime fusion of cardiac magnetic resonance imaging and computed tomography venography with x-ray fluoroscopy to aid cardiac resynchronisation therapy implantation in patients with persistent left superior vena cava. *Eur Pacing Clin Electrophysiol.* 2011;13:285-86

**Duckett SG**, Chiribiri A, Ginks MR, Sinclair S, Knowles BR, Botnar R, Carr-White GS, Rinaldi CA, Nagel E, Razavi R, Schaeffter T. Cardiac MRI to investigate

myocardial scar and coronary venous anatomy using a slow infusion of dimeglumine gadobenate in patients undergoing assessment for cardiac resynchronization therapy. *J Magn Reson Imaging*. 2011;33:87-95

**Duckett SG**, Camara O, Ginks MR, Bostock J, Chinchapatnam P, Sermesant M, Pashaei A, Lambiase PD, Gill JS, Carr-White GS, Frangi AF, Razavi R, Bijmens BH, Rinaldi CA. Relationship between endocardial activation sequences defined by high-density mapping to early septal contraction (septal flash) in patients with left bundle branch block undergoing cardiac resynchronization therapy. *Eur Pacing Clin Electrophysiol*. 2011 (In press)

**Duckett SG**, Ginks M, Knowles BR, Chiribiri A, Ma Y-L, Razavi R, Schaeffter T, Carr-White G, Rinaldi CA, Rhode K. A novel cardiac mri protocol to guide successful cardiac resynchronization therapy implantation. *Circ Heart Fail*. 2010;3:e18-21



### **Abstracts**

**Simon G Duckett** MRCP, Matthew Ginks MRCP, Anoop Shetty MRCP, Julian Bostock MSc, Jaswinder S Gill FRCP, Shoaib Hamid MD, Stam Kapetanakis FRCP/MD, Eliane Cunliffe BSc, Reza Razavi FRCP/MD, Gerry Carr-White FRCP/PhD, C Aldo Rinaldi FRCP/MD. Invasive acute hemodynamic response to guide LV lead implantation predicts chronic remodelling in patients undergoing cardiac resynchronisation therapy; *BCS Manchester UK 06/2011*

**SG Duckett** MRCP, Oscar Camara PhD, Matthew Ginks MRCP, Julian Bostock MSc, Phani Chinchapatnam PhD, Maxime Sermesant PhD, Ali Pashaei PhD, Jaswinder S Gill FRCP/ MD, Gerry Carr-White FRCP/PhD, Alejandro F. Frangi PhD, Reza Razavi FRCP/MD, Bart H Bijmens PhD, C Aldo Rinaldi FRCP/MD. Electromechanical interaction in patients undergoing cardiac resynchronisation therapy - comparison of intracardiac activation maps and early septal contraction in left bundle branch block *BCS Manchester UK 06/2011*

**SG Duckett** MRCP, MR Ginks MRCP, A Shetty MRCP, S Kapetanakis MRCP, CA Rinaldi MD/FRCP, Schaeffter PhD, GS Carr-White PhD/ FRCP Razavi MD/FRCP, Systolic Dyssynchrony Index derived from cardiac magnetic resonance imaging predicts left ventricular remodeling in heart failure patients undergoing CRT  
*SCMR USA 01/2011*

**SG Duckett** MRCP, MR Ginks MRCP, A Shetty MRCP, S Kapetanakis MRCP, CA Rinaldi MD/FRCP, Schaeffter PhD, GS Carr-White PhD/ FRCP Razavi MD/FRCP, Systolic Dyssynchrony Index derived from cardiac magnetic resonance imaging

predicts left ventricular remodeling in heart failure patients undergoing CRT  
*SCMR Nice France 02/2010*

**SG Duckett**, MBBS, Peter Koken, MSc, Anoop K. Shetty, MBBS, Christian Stehning, PhD, Reza Razavi, FRCP, MD, Tobias Schaeffter, PhD, Andrea J. Wiethoff, PhD, Assessment of the grey zone: a comparison of two methods in heart failure patients awaiting cardiac resynchronization therapy *SCMR Nice France 02/2010*

**SG Duckett** MRCP, MR Ginks MRCP, BR Knowles MPhys, A Shetty MRCP, S Kapetanakis MRCP, R Razavi MD/FRCP, T Schaeffter PhD, K Rhode PhD, GS Carr-White PhD/ FRCP, CA Rinaldi MD/FRCP, CMR & 3D echo derived systolic dyssynchrony index to predict acute haemodynamic response to LV and BIV pacing in patients awaiting CRT *Heart Rhythm Congress*. Birmingham, UK (October 2010)

**SG Duckett** MRCP, MR Ginks MRCP, BR Knowles MPhys, Y Ma PhD, A Shetty MRCP, J Bostock, M Cooklin MD/FRCP, J Gill MD/FRCP, R Razavi MD/FRCP, T Schaeffter PhD, K Rhode PhD, GS Carr-White PhD/ FRCP, CA Rinaldi MD/FRCP, Advanced image fusion to overlay coronary sinus anatomy and myocardial scar with real time fluoroscopy to aid left ventricular lead implantation during CRT *Heart Rhythm Congress*. Birmingham, UK (October 2010)

**SG Duckett**, Dr A Chiribiri MD, Dr MR Ginks MRCP, S Sinclair, BR Knowles Mphys, Professor R Botnar PhD, Dr GS Carr-White FRCP/PhD, Dr CA Rinaldi FRCP/MD, Professor E Nagel MD/PhD, Professor R Razavi MRCP/MD, Professor T Schaeffter PhD Whole-heart magnetic resonance imaging for the visualization of venous

anatomy and myocardial scar using slow infusion of Gd-BOPTA in single exam.

*SCMR Phoenix Arizona 22/01/2010*

**SG Duckett**, MRCP1, Matthew Ginks, MRCP1, Benjamin R. Knowles, Amedeo Chiribiri MD1, MPhys1, Stephen Sinclair, DCR1, Gerry Carr-White, MRCP/PhD2, C Aldo Rinaldi, MD/FRCP1, Rene Botnar, PhD1, Eike Nagel, MD/PhD1, Reza Razavi, MRCP/MD1, Tobias Schaeffter, PhD Imaging myocardial scar and coronary vein anatomy in patients awaiting cardiac resynchronisation therapy using a single CMR examination and a high-relaxivity contrast agent. *ISMRM Stockholm 05/05/2010*

**SG Duckett**, MRCP, Matthew Ginks, MRCP, Benjamin R. Knowles, MPhys, Amedeo Chiribiri MD, Anoop Shetty, MRCP, Stephen Sinclair, DCR, Gerry Carr-White, FRCP/PhD2, Eike Nage, MD/PhD, Reza Razavi, MRCP/MD, Tobias Schaeffter, PhD, C Aldo Rinaldi, MD/FRCP Coronary vein and myocardial scar imaging with a single cardiac mri examination using a high relaxivity contrast agent in patients with severe heart failure awaiting crt implantation. *BCS Manchester 08/06/2010*

**SG Duckett** MRCP, MR Ginks MRCP, BR Knowles MPhys, Y Ma PhD, A Shetty MRCP, GS Carr-White PhD/ FRCP, R Razavi MD/FRCP, T Schaeffter PhD, K Rhode PhD, CA Rinaldi MD/FRCP Real Time Overlay Of Coronary Vein Anatomy And Myocardial Scar To Guide Left Ventricular Lead Implantation In Cardiac Resynchronisation Therapy. *HRS Denver 12-15/05/2010*

**SG Duckett** MRCP, MR Ginks MRCP, BR Knowles MPhys, Y Ma PhD, A Shetty MRCP, GS Carr-White PhD/ FRCP, R Razavi MD/FRCP, T Schaeffter PhD, K Rhode PhD, CA Rinaldi MD/FRCP, Advanced Imaging And Overlay Technology To Guide Left Ventricular Lead Implantation In CRT Patients With Previous Failed Procedures. *HRS Denver 12-15/05/2010*

**SG Duckett** MRCP, MR Ginks MRCP, BR Knowles MPhys, Y Ma PhD, A Shetty MRCP, GS Carr-White PhD/ FRCP, R Razavi MD/FRCP, T Schaeffter PhD, K Rhode PhD, CA Rinaldi MD/FRCP Imaging fusion & overlay technology to guide LV lead implant in CRT, Cardiosostim, Nice 16-18/06/2010

**SG Duckett** MRCP, MR Ginks MRCP, BR Knowles MPhys, A Shetty MRCP, S Kapetanakis MRCP, R Razavi MD/FRCP, T Schaeffter PhD, K Rhode PhD1, GS Carr-White PhD/ FRCP, CA Rinaldi MD/FRCP, CMR & 3D Echo predictors of acute haemodynamic response to LV pacing. Cardiosostim, Nice 16-18/06/2010

**SG Duckett** MRCP, O. Camara PhD, P. Chinchapatnam PhD, M. Sermesant PhD, A. Pashaei PhD, M. Ginks MRCP, A.F. Frangi PhD, G. Carr-White FRCP/PhD, R. Razavi FRCP/MD, B.H. Bijnens PhD, CA. Rinaldi FRCP/MD. Electromechanical relationship with LBBB & a Septal Flash. Cardiosostim, Nice 16-18/06/2010

**SG Duckett** MRCP, MR Ginks MRCP, BR Knowles MPhys, Y Ma PhD, A Shetty MRCP, GS Carr-White PhD/ FRCP, R Razavi MD/FRCP, T Schaeffter PhD, K Rhode PhD, CA Rinaldi MD/FRCP Predicting haemodynamic response to LV pacing; A

comparison of Systolic Dyssynchrony Index derived from Cardiac magnetic resonance imaging and 3D echo. HRS *Denver 12-15/05/2010*

## Appendix 2

### Ethics sheets and patient information



St Thomas' Hospital Research Ethics Committee

#### PATIENT INFORMATION SHEET

**Title of Project: Predict response to CRT from echo and MRI data using biophysical model**

<b>Principal Investigator:</b> Prof. Reza Razavi	<b>Ethics Committee:</b> St. Thomas' Hospital
<b>Other Investigator/s enrolling patients:</b> Dr S Duckett, Dr M Ginks	<b>Code No:</b> 09/H0802/38

*You are being invited to take part in a research study. Before you decide it is important for you to understand why the research is being done and what it will involve. Please take time to read the following information carefully. Talk to others about the study if you wish.*

- *Part 1 tells you the purpose of this study and what will happen to you if you take part.*
- *Part 2 gives you more detailed information about the conduct of the study.*

*Ask us if there is anything that is not clear or if you would like more information.*

*Take time to decide whether or not you wish to take part.*

## **PART 1**

### **Outline explanation**

You have been recommended by your cardiologist to have cardiac resynchronisation therapy. This is a special kind of pacemaker usually consists of 3 electrical leads which are positioned in the heart to improve the efficiency of the heart. Although this treatment has been shown to be effective, up to 30% of patients do not improve with this new pacemaker in terms of their ability to exercise and quality of life.

### **What is the purpose of the study?**

At present it is not clear which patients will respond to having cardiac resynchronisation therapy. We have designed this study to evaluate the electrical and mechanical function of the heart to see if we can discover measurements that will help us predict the patients that will respond. The data that we acquire will then be used to make mathematical models of the function of the heart which will help us optimise the treatment of patients referred for cardiac resynchronisation therapy in the future.

### **Why have I been chosen?**

You have been chosen to take part as you are eligible for this new pacemaker on the basis of our current evidence from large clinical trials.

**Do I have to take part?**

No. It is up to you to decide whether or not to take part. If you do, you will be given this information sheet to keep and be asked to sign a consent form. You are still free to withdraw at any time and do not need to give a reason. A decision to withdraw at any time, or a decision not to take part, will not affect the standard of care you receive.

**What will happen to me if I take part?**

You will be given a consent form to sign.

As part of your routine care prior to having cardiac resynchronisation therapy you will be seen as an outpatient. You will have a questionnaire to fill in which takes 10 to 15 minutes, a walking test, an oxygen monitoring test and an ultrasound scan of your heart called an echocardiogram. These tests are routine and take 1 to 2 hrs to perform. They give us information on your functional status prior to your pacemaker.

On the same day you will also have a scan called a magnet resonance imaging scan (MRI), this looks at the heart giving us more information about its function and areas of localised scarring. The MRI scan involves lying still in a scanner for 60 to 90 minutes while images are taken. The MRI does not involve X rays and is part of the routine work-up for the type of pacemaker you are having.



This will all be done prior to your pacemaker procedure. Once your pacemaker is inserted we would like to follow you up at 3 and 6 months with a repeat of the questionnaire, walking and oxygen monitoring test and ultrasound of your heart (echocardiogram).

All the data we acquire will be used in the development of mathematical models that will be helpful in the future for predicting which patients will respond to cardiac resynchronisation therapy.

**How does this differ from “standard practice” i.e. routine care (if you were not to take part in the study)?**

The assessment with the questionnaire, walking test, oxygen monitoring and echocardiogram are all routine. Also the MRI is part of our routine assessment for the type of pacemaker you are receiving.

In addition to routine care, you would have:

2 extra outpatient hospital visits lasting 1 to 2 hrs

**What do I have to do?**

You would need to do the routine assessments, which include the questionnaire, walking test, oxygen monitoring, echocardiogram and MRI prior to your pacemaker. We would then need to see you at 3 and 6 months after your

pacemaker has been inserted to repeat the initial assessments. (Not including the MRI scan)

**What is the procedure that is being tested?**

We are assessing the electrical and mechanical function of the heart using MRI and echocardiography. This allows us to develop measures that will enable us to predict which patients are likely to respond to cardiac resynchronisation therapy. The data will be used to develop mathematical models of the heart helping us understand the function of the heart.

**What are the contraindications of taking part?**

If carried out according to accepted standards and guidelines, MRI is a harmless imaging technique. We have safety procedures and well-trained staff to minimise any possible risks associated with the procedure. Because MRI uses a strong magnet, it is not safe for some people to be scanned. This includes people who have a heart pacemaker or some other types of implanted device. You will be asked to fill in a screening form to make sure that you do not come into any of these categories. For the same reason, it is important that magnetic objects are not brought too close to the scanner.

**What are the possible disadvantages and risks of taking part?**

The MRI scan may be uncomfortable, as you need to lie flat for 60 to 90 minutes. Most people tolerate this procedure very well.

You will be required to have two extra out patient hospital visits after your pacemaker has been implanted. You will be reimbursed for the extra journeys.

**What are the possible benefits of taking part?**

The main benefit is that by doing the study we will be able to identify the best site for implantation of the extra lead into your heart and increase the chance of the pacemaker improving your symptoms. You will also have closer follow up with the two extra hospital visits after the pacemaker is implanted.

**What happens when the research study stops?**

You will still be routinely followed up in our clinic and monitored by your cardiologist. The results of the supplementary tests will not exclude you from any useful treatment approved for your condition.

**What if there is a problem?**

Any complaint about the way you have been dealt with during the study or any possible harm you might suffer will be addressed. The detailed information on this is given in Part 2.

**Will my taking part in the study be kept confidential?**

Yes. All the information about your participation in this study will be kept confidential. The details are included in Part 2.

**Contact Details:**

Prof. Reza Razavi. St Thomas' Hospital, 4<sup>th</sup> Floor Lambeth Wing.

Telephone 02071885440. Mobile phone: 07900240841

**This completes Part 1 of the Information Sheet.**

**If the information in Part 1 has interested you and you are considering participation, please continue to read the additional information in Part 2 before making any decision.**

<b>PART 2</b>
---------------

**What if relevant new information becomes available?**

Sometimes during the course of a research project, new information becomes available about the procedure that is being studied. If this happens, your research doctor will tell you about it and discuss whether you want to or should continue in the study.

**What will happen if I don't want to carry on with the study?**

If you withdraw from the study, we will need to use the data collected up to your withdrawal. We will ask you to keep in contact with us to let us know your progress.

**What if there is a problem?**

**Complaints:** If you have a concern about any aspect of this study, you should ask to speak with the researchers who will do their best to answer your questions (Prof. Reza Razavi 02071885440). Should you wish to complain formally, you can do this through the NHS Complaints Procedure. Details can be obtained from the hospital.

**Harm:** In the event that you are harmed during the research study there are no special compensation arrangements. If you are harmed and this is due to someone's negligence then you may have grounds for a legal action for compensation against Guy' & St. Thomas' NHS Trust but you may have to pay your legal costs. The normal National Health Service complaints mechanisms will still be available to you.

**Will my taking part in this study be kept confidential?**

Procedures for handling, processing, storage and destruction of your data are compliant with the Data Protection Act 1998.

All information which is collected about you during the course of the research will be kept strictly confidential. Any information about you which leaves the hospital will have your name and address removed so that you cannot be recognised from it.

Your data will be collected from the referral letter and patient notes, as well from your oral information; Data will be automatically stored securely, in an encrypted format; Authorised persons such as researchers, regulatory authorities and Research and Development (for monitoring of the quality of the research) will have access to these data; Data will be retained for 15 years.

Your own GP may be notified of your participation in the trial, after your consent.

**What will happen to the results of the research study?**

These will be published in a research paper with the aim of advancing the knowledge of MRI and heart failure. All patient identities are treated as strictly confidential and anonymous in any publication.

**Who is organising and funding the research?**

The research is organised by Prof Reza Razavi and will be partially funded by Kings College London. The study is being undertaken primarily for academic reasons.

**Who has reviewed the study?**

The study has been independently reviewed by the St Thomas' Hospital Ethics Committee.

**A copy of the information sheet and a signed consent form to keep will be given to you.**

***Thank you for considering taking part or taking time to read this sheet.***



Rayne Institute, KCL  
Guy's & St Thomas' NHS Trust  
St Thomas' Hospital  
Lambeth Palace Road  
London SE1 7EH  
  
Tel : 0207 188 1026  
Fax : 0207 188 1011

Study Number: **09/H0802/38**

Patient Identification Number for this trial:

## **CONSENT FORM**

**Title of Project:** Predicting response to cardiac resynchronisation therapy from echocardiographic and cardiac magnetic resonance imaging data using biophysical models

Name of Researcher: Professor Reza Razavi

**Please initial box**

1. I confirm that I have read and understand the information sheet dated 04/03/2009 (version 1) for the above study. I have had the opportunity to consider the information, ask questions and have had these answered satisfactorily.

☐

2. I understand that my participation is voluntary and that I am free to withdraw at any time, without giving any reason, without my medical care or legal rights being affected.

☐

3. I understand that relevant sections of any of my medical notes and data collected during the study may be looked at by responsible individuals from regulatory authorities or from the NHS Trust, where it is relevant to my taking part in this research. I give permission for these individuals to have access to my records.

☐

4. I agree to my GP being informed of my participation in the study.

☐

5. I agree to take part in the above study.

☐


---

Name of Patient

---

Date

---

Signature

---

Name of Person taking consent

---

Date

---

Signature



(if different from researcher)

\_\_\_\_\_  
Researcher

\_\_\_\_\_  
Date

\_\_\_\_\_  
Signature

When completed, 1 for patient; 1 for researcher site file; 1 (original) to be kept in medical notes



**St Thomas' Hospital Research Ethics Committee**

### PATIENT INFORMATION SHEET

**Title of Project: Biophysical modelling to guide selection and implantation of CRT**

<b>Principal Investigator:</b> Prof. Reza Razavi	<b>Ethics Committee:</b> St. Thomas' Hospital
<b>Other Investigator/s enrolling patients:</b> Dr S Duckett, Dr M Ginks	<b>Code No:</b> 09/H0802/37

*You are being invited to take part in a research study. Before you decide it is important for you to understand why the research is being done and what it will involve. Please take time to read the following information carefully. Talk to others about the study if you wish.*

**LV**

ke

part.

- *Part 2 gives you more detailed information about the conduct of the study.*

*Ask us if there is anything that is not clear or if you would like more information.*

*Take time to decide whether or not you wish to take part.*

## **PART 1**

### **Outline explanation**

You have been recommended by your cardiologist to have cardiac resynchronisation therapy. This involves a special pacemaker usually consists of 3 electrical leads which are positioned in the heart to improve the co-ordination of the contraction as the heart beats. Although this treatment has been shown to be effective, up to 30% of patients do not improve with this new pacemaker in terms of their ability to exercise and quality of life.

### **What is the purpose of the study?**

At present it is not clear which patients will respond to having this type of pacemaker. We have designed this study to evaluate the electrical and mechanical function of the heart to see if we can discover measurements that will help us predict the patients that will respond. The data that we acquire will then be used to make mathematical models of the function of the heart which will help us optimise the treatment of patients referred for cardiac resynchronisation therapy in the future.

### **Why have I been chosen?**

You have been chosen to take part since you are eligible for this new pacemaker on the basis of our current evidence from large clinical trials.

**Do I have to take part?**

No. It is up to you to decide whether or not to take part. If you do, you will be given this information sheet to keep and be asked to sign a consent form. You are still free to withdraw at any time and do not need to give a reason. A decision to withdraw at any time, or a decision not to take part, will not affect the standard of care you receive.

**What will happen to me if I take part?**

You will be given a consent form to sign.

As part of your routine care prior to having the cardiac resynchronisation therapy you will be seen as an outpatient. You will have a questionnaire to fill in which takes 10 to 15 minutes, a walking test, an oxygen monitoring test and a scan of your heart called an echocardiogram. These tests are routine and take 1 to 2hrs to perform. They give us information on your functional status prior to your pacemaker.

On the same day you will also have a scan called a magnet resonance imaging scan (MRI), this looks at the heart giving us more information about its function and areas of localised scarring. The MRI scan involves lying still in a tube for 60 to 90minutes while images are taken before an injection of a substance called gadolinium is given to see if there are any scars in the heart. The MRI does not

involve X rays and is part of the routine work-up for the type of pacemaker you are having.

We would like to do an additional test called an electrophysiological study. This involves you coming in as an inpatient for a day. This procedure would be done 3 to 7 days prior to your pacemaker. This study is done in a special cardiac catheterisation laboratory which allows us to do a further MRI scan which takes 30 minutes immediately before the electrophysiological study. The benefit of this is it allows us to directly compare the MRI scan data with the electrophysiological invasive study data.

You are required to lie flat for 3-4 hrs in a cardiac catheterisation lab. During this procedure we would use a special wire called a pressure wire, this passed either through the artery in your wrist or groin to your heart. It enables us to measure changes in your blood pressure. We also pass a tube called an electrical mapping catheter to your heart through the artery in your groin. The catheter and pressure wire are passed to your heart under X ray guidance. This allows us to map the electrical activity of the heart, also by using this catheter we can stimulate different areas of the heart and see how this affects your blood pressure. During this study we will also be performing another echocardiogram to gain more information about the function of the heart.

This will all be done prior to your pacemaker procedure. Once your pacemaker is inserted we would like to follow you up at 3 and 6 months with a repeat of the questionnaire, walking and oxygen monitoring test and echocardiogram.

All the data we acquire will be used in the development of mathematical models that will be helpful in the future for predicting which patients will respond to biventricular pacing.

**How does this differ from “standard practice” i.e. routine care (if you were not to take part in the study)?**

The assessment with the questionnaire, walking test, oxygen monitoring and echocardiogram are all routine. Also the MRI is part of our routine assessment for the type of pacemaker you are receiving.

In addition to routine care, you would have:

The electrophysiological studies (inpatient stay, takes 3 to 4hrs)

2 extra outpatient hospital visits lasting 1 to 2 hrs

**What do I have to do?**

You would need to do the routine assessments, which include the questionnaire, walking test, oxygen monitoring, echocardiogram and MRI prior to your pacemaker. You will need to come in for a day to have the electrophysiological studies. We would then need to see you at 3 and 6 months after your pacemaker has been put in to repeat the initial assessments. (Not including the MRI scan and electrophysiological studies)

**What is the procedure that is being tested?**

We are assessing the electrical and mechanical function of the heart to see how that compares with MRI and echocardiography. This allows us to develop measures that will enable us to predict which patients are likely to respond to biventricular pacing. This data will be used to develop mathematical models of the heart helping us understand the function of the heart.

**What are the side effects of taking part?**

Part of the study involves an invasive procedure called electrophysiological non-contact mapping. The electrophysiological study involves passing a tube called a catheter to your heart through the artery in your leg and also a wire again through the artery in your leg or wrist to your heart. There is the potential to develop bruising from the site that the pressure wire is inserted (wrist or groin) and also the site that the mapping catheter is inserted (groin).

The MRI scan can not be done under certain circumstances, such as if you suffer with claustrophobia or have previously had any operations on the brain.

You will be required to have two extra out patient hospital visits after your pacemaker has been implanted.

**What are the possible disadvantages and risks of taking part?**

As the electrophysiological study is an invasive procedure there are associated risks (see below)

- 1% chance of groin haematoma or false aneurysm as a result of arterial puncture,
- risk of stroke < 0.1%
- infection / pulmonary embolus (clot on the lung) < 1%

– pericardial tamponade (development of fluid around the heart) <1%

**What are the possible benefits of taking part?**

The main benefit is that by doing the study we will be able to identify the best site to implant the lead into your heart and increase the chance of the pacemaker improving your symptoms. You will also have closer follow up with the two extra hospital visits after the pacemaker is implanted.

**What happens when the research study stops?**

You will still be routinely followed up in our clinic and monitored by your cardiologist. The results of the supplementary tests will not exclude you from any useful treatment approved for your condition.

**What if there is a problem?**

Any complaint about the way you have been dealt with during the study or any possible harm you might suffer will be addressed. The detailed information on this is given in Part 2.

**Will my taking part in the study be kept confidential?**

Yes. All the information about your participation in this study will be kept confidential. The details are included in Part 2.

**Contact Details:**

Prof. Reza Razavi. St Thomas' Hospital, 4<sup>th</sup> Floor Lambeth Wing.

Telephone 02071885440. Mobile phone: 07900240841

**This completes Part 1 of the Information Sheet.**

**If the information in Part 1 has interested you and you are considering participation, please continue to read the additional information in Part 2 before making any decision.**



## PART 2

### **What if relevant new information becomes available?**

Sometimes during the course of a research project, new information becomes available about the procedure that is being studied. If this happens, your research doctor will tell you about it and discuss whether you want to or should continue in the study.

### **What will happen if I don't want to carry on with the study?**

If you withdraw from the study, we will need to use the data collected up to your withdrawal. We will ask you to keep in contact with us to let us know your progress.

### **What if there is a problem?**

**Complaints:** If you have a concern about any aspect of this study, you should ask to speak with the researchers who will do their best to answer your questions (Prof. Reza Razavi 02071885440). Should you wish to complain formally, you can do this through the NHS Complaints Procedure. Details can be obtained from the hospital.

**Harm:** In the event that you are harmed during the research study there are no special compensation arrangements. If you are harmed and this is due to someone's negligence then you may have grounds for a legal action for compensation against Guy' & St. Thomas' NHS Trust but you may have to pay your legal costs. The normal National Health Service complaints mechanisms will still be available to you.

**Will my taking part in this study be kept confidential?**

Procedures for handling, processing, storage and destruction of your data are compliant with the Data Protection Act 1998.

All information which is collected about you during the course of the research will be kept strictly confidential. Any information about you which leaves the hospital will have your name and address removed so that you cannot be recognised from it.

Your data will be collected from the referral letter and patient notes, as well from your oral information; Data will be automatically stored securely, in an encrypted format; Authorised persons such as researchers, regulatory authorities and Research and Development (for monitoring of the quality of the research) will have access to these data; Data will be retained for 15 years.

Your own GP may be notified of your participation in the trial, after your consent.

**What will happen to the results of the research study?**

These will be published in a research paper with the aim of advancing the knowledge of MRI and heart failure. All patient identities are treated as strictly confidential and anonymous in any publication.

**Who is organising and funding the research?**

The research is organised by Prof Reza Razavi and will be partially funded by Kings College London. The study is being undertaken primarily for academic reasons.

**Who has reviewed the study?**

The study has been independently reviewed by the St Thomas' Hospital Ethics Committee.

**A copy of the information sheet and a signed consent form to keep will be given to you.**

***Thank you for considering taking part or taking time to read this sheet.***



Rayne Institute, KCL  
Guy's & St Thomas' NHS Trust  
St Thomas' Hospital  
Lambeth Palace Road  
London SE1 7EH

Tel : 0207 188 1026

Fax : 0207 188 1011

Study Number: **09/H0802/37**

Patient Identification Number for this trial:

## **CONSENT FORM**

**Title of Project: Biophysical modelling to guide selection and implantation of CRT**

Name of Researcher: Professor Reza Razavi

**Please initial box**

1. I confirm that I have read and understand the information sheet dated ☐ 04/03/2009 (version 1) for the above study. I have had the opportunity to consider the information, ask questions and have had these answered satisfactorily.

2. I understand that my participation is voluntary and that I am free to ☐ withdraw at any time, without giving any reason, without my medical care or legal rights being affected.

3. I understand that relevant sections of any of my medical notes and data collected during the study may be looked at by responsible individuals from ☐ regulatory authorities or from the NHS Trust, where it is relevant to my taking part in this research. I give permission for these individuals to have access to my records.

4. I agree to my GP being informed of my participation in the study. ☐

5. I agree to take part in the above study. ☐

\_\_\_\_\_

Name of Patient

\_\_\_\_\_

Date

\_\_\_\_\_

Signature

\_\_\_\_\_

Name of Person taking consent

\_\_\_\_\_

Date

\_\_\_\_\_

Signature

(if different from researcher)

---

Researcher

---

Date

---

Signature

When completed, 1 for patient; 1 for researcher site file; 1 (original) to be kept in medical notes